Università
Ca'Foscari
Venezia

Corso di Laurea Magistrale
(*ordinamento ex D.M. 270/2004*) In
Scienze e Tecnologie dei
Bio e Nanomateriali

Ca' Foscari
Dorsoduro 3246
30123 Venezia

Tesi di Laurea

Self-diagnostic Coatings for Cultural Heritage: Fluorescent additives.

Characterization, Lightfastness and Influence on a Waterborne Coating's Yellowing and Plasma Removability of Commercial Pigments

Relatore
Prof. Alvise Benedetti

Laureando
Francesca Rossi
Matricola 820678

Anno Accademico
2013 / 2014

AIM OF THE WORK

Main purpose of this thesis is the identification of different types of photo-luminescent additives for the formulation of innovative waterborne self-diagnostic protective coatings which could serve in the field of cultural heritage conservation, enabling to monitor the coating's health status. The research focuses on the characterization of structure and photo-oxidative degradation of some commercial fluorescent products; specifically, dispersions of water-insoluble additives (pigments) have been formulated, after having selected and characterized four products. The selected emitting substances have been shown to be $BaMgA_{l1}0O_{17}:Mn^{2+}Eu^{2+}$ and $Y_2O_2S:Eu^{2+}$ as inorganic and $Eu^{3+}(TTA)_3(TPPO)_2$ (tris (2-thenoyltrifluoroacetonate)-(bis-triphenylphosphinoxide) europium chelate) and HPQ (2-2'hydroxyphenyl-4(3H)-quinazolinone) as organic pigments.

In order to assess their performances in relation to the particle size, the pigments have also been ground to nanometric sizes with the bead mill technique. In particular, the influence of external conditions on the emission response, such as the inclusion in an acrylic matrix and a prolonged ultraviolet irradiation, has been investigated for three different particle size distributions. Also the influence of the additives on the photo-oxidative degradation and plasma removability of an acrylic coating have been evaluated. The research is part of the European project PANNA (Plasma and Nano for New Age soft conservation), therefore the removability tests have been carried out by means of a portable atmospheric cold plasma torch developed within the project framework. The obtained results and their chemical and physical differences allow one to declare the two organic samples as complementary fluorescent additives, combinable and suitable for various applications in the field of conservation dedicated coatings.

INDEX

INTRODUCTION

The aim of this work is to evaluate various luminescent compounds to be used in the field of restoration as self-diagnostic additives, in order to define candidates that retain their activity even after exposure to strong ultraviolet light, and to examine the correlations between ageing and fluorescence activity. The outcome will therefore offer the restorers an innovative tool to solve ongoing issues regarding conservation practice and focus on concepts such as complete reversibility and ease of functionality monitoring in the protective coating technology. The possibility to impart self-diagnostic properties to a coating will allow an easy evaluation of presence, uniformity and functionality of the coating, all at the same time. As the coating erodes from a surface the amount of additive decreases; it is therefore also possible to use the spectroscopic response as a measure of coating thickness, which may be related to its specific features. Self-diagnostic coatings will provide a prompt knowledge of the coating's health status, thus preventing further form of degradation. Photo-luminescent molecules and additives active in the infrared region of the electromagnetic spectrum are good candidates to impart self-diagnostic properties to the coatings. They do not absorb in the visible range and so do not alter the aesthetic properties of the artefact and of the coating itself. While IR active additives require a portable FTIR device, for photo-luminescent additives, absorbing UV-light and emitting in the visible range, a hand-held UV-light source could be sufficient to detect and evaluate the coating status. Once the behaviour of each fluorescent coating in time is known in respect to its thickness and fluorophore concentration, the health status analysis could be performed.

The fluorescence excitation energy varies from substance to substance. In particular, the common UV-lamp excitation wavelength of 365nm can be safely used by restorers. It ensures invisibility of the additives under normal lighting conditions, while enabling to assess the quality of the coating and to determine the need for re-application of each specific coating without any risk for the operator.

The selection criteria for the best additive are based on the intensity of the response in both waterbased matrices and coatings. The response has to fulfil two main

features: be definite enough to be detectable using also a portable device, and allow its conversion into coating thickness by means of a calibration curve. Fluorescent additives will thus enable the restorer to effectively map the erosion of the coating, without the need for expensive monitoring devices, and also to avoid scaffolding that may hinders the artefact view. It is of course imperative that the additives do not impair the transparency of the coating nor its hydrophobicity, removability, water vapour permeability, and corrosion protection. These properties must remain unaltered or preferably be improved by the additives. In this thesis, the influence of four selected pigments on the colorimetric behaviour and on the plasma removability of a simple waterborne acrylic coating has been studied. The thesis is part of the FP7 EU-project 'Plasma And Nano for New Age soft conservation' (PANNA) focused on the development of a cultural heritage dedicated plasma jet for coating removal and deposition. The formulation of the removable coatings themselves is also included in the project.

The cleaning and preservation of cultural heritage assets must take into account a variety of substrates. These include stone, metal, mural paintings, and a variety of 'dirt' types such as soot, graffiti, corrosion products, oil paint and wax. Although a wide range of organic and inorganic protective coatings are commercially available, most of them cannot be removed with sustainable methods such as dissolution by means of organic solvents or laser ablation, without damages for the artefact. Thus, when they no longer serve their purpose, options for a continued preservation are limited. The plasma jet cleaning technique will allow for the removal of organic substances in a 'green' and non-contact way without any thermal, mechanical or chemical damage to the artefacts.

The objective of this thesis is the study of organic and inorganic photo-luminescent molecules to be applied as self-diagnostic additives in waterborne coatings. The study focuses on pigments dispersions, their ease of removability by means of cold plasma and their fluorescent behaviour. Subsequently, these properties will be evaluated also in respect to the presence in the coating of dyes instead of pigments. The reason for choosing pigments mainly lies on their lower interaction with the matrix and their higher resistance to light exposure compared to dyes. These are useful characteristics when speaking of coating removability and decay monitoring.

Fluorescent dyes within microspheres are very stable, losing less than 1% of their fluorescent signal in six months, however once the microspheres are dissolved in solvent, stability decreases. Exposure to sunlight has been shown to significantly degrade dyes in less than one week.

This study focuses on those commercialize products matching the basic conservation requirements (see chapter 2), given the vastness of existing fluorescent molecules. The choice of water-based formulations, instead of solvent-based, comes from a simple consideration: acqueous media are safer and easier to work with, avoiding solvent emission problems and reducing solvent-surface interactions. On the other hand, once selected the fluorescent additive, it would be challenging to formulate completely removable high performances waterborne coating for cultural heritage requirements. In fact, in order to impart the desired characteristics (e.g. hydropobicity), the formulation usually includes organic-inorganic hybrids matrices (e.g. acryl-silane/siloxane) (see chapter 5); introducing inorganic bonds, these may reduce the coating removability by means of atmospheric cold plasma torch (see chapter 6).

In function of its fluorescence evaluation it is imperative to perform a thorough study of the selected additive itself, its fluorescence mechanism and deterioration. The workflow can be divided in three parts, each one responding to key-questions:

- 1° Part (Chapter 2 and 3): screening, selection and analysis of the pigments:
  Is fluorescence affected by the matrix (e.g. solvatochromic behavior, etc.)?
  How does the luminescence mechanism works for the selected additives?
  In this part a screening of the available commercial colourless fluorescent additives' properties, in three matrices with different polarity, was performed. For the selection, the pigments were then divided in two categories: organic and inorganic. The properties tested were: dispersability/solubility, dispersion aspect, fluorescence colour/peaks and intensity (in powder and 1% mixture) and weather-fastness. For studying the latter, the additives were embedded in a hydrophobic coating developed for the PANNA project. The main criteria for the selection were the intensities of the characteristic emission peak after one month of exposure to atmospheric conditions. The number of the samples to be

embedded was reduced on the base of their IR spectra match, dividing as such the pigments in IR families and testing only one additive out of each family. Two pigments for each category (i.e. organic and inorganic) were selected, and several physical and chemical analyses performed in order to identify the fluorescent molecules. Another pigment was also subject of study owing to its singular fluorescent behaviour: a variation in its fluorescent output was observed as function of the sample's weathering. This opened up new scenarios, such as the possibility of using a mixture of different pigments with different aging behaviours as meter for coating health status or light exposure.

- 2° Part (Chapter 4 and 5): particles de-agglomeration and milling, coating formulation and application:

  Do the pigments' particles milling and/or the coating formulation influence the fluorescent output?

  Do the pigments presence and/or particle size influence the properties of a waterborne coating or vice versa?

  This part was focused on the determination of an optimal particle size-fluorescence response relation. Milling was carried out on the selected products; in this context other additives, such as dispersants, surfactants and thickeners, were evaluated in order to obtain a stable dispersion. Also a basic coating formulation was optimized.

- 3° Part (Chapter 6) : fluorescence, coating yellowing and plasma removability evaluation in relation to UV ageing:

  Do the pigments presence and/or particle size influence the properties of the aged coating?

  Does the exposure to UV light influence the pigments luminescence?

  Is there a correlation between thickness, concentration and fluorescence giving the chance to the restorer to easily acquire information on the coating health status?

  The coatings obtained in the second part, with different pigments particle size distributions, were artificially aged. 15years of natural UV exposure were simulated, and several coatings' properties tested. The main property concerning

the PANNA project being the plasma removability, before and after different aging periods the coatings removal has been evaluated.

The matrix behaviour in the presence of different sized pigment's particles is of great interest since the presence of additives could impart profound changes to the coating properties. At best, it could give multifunctional materials with predictable and tailored properties, raise the resistance to photo-oxidative oxidation and/or termal excursion or improve generally the chemical and mechanical properties.

Not only focuses this thesis on the characterization of useful commercial products, but also on the correlation of thickness and fluorescence, giving the chance to the restorer to easily acquire information on the coating health status (e.g. eroded %). The fluorescence being influenced by matrix effects (see chapter 6), all the investigated properties (fluorescence decay and influence on matrix stability, yellowing and removability) will need to be related to a particular coating formulation.

Chapter – 1 –

INTRODUCTION TO FLUORESCENCE

INTRODUCTION TO

FLUORESCENCE

1.1 - LUMINESCENCE THEORY

Fluorescence occurs when a molecule absorbs light photons from the u.v.-visible light spectrum, known as excitation, and then rapidly emits light photons as it returns to its ground state (10^{-9}-10^{-5} seconds, while phosphorescence emission are much longer). Fluorimetry characterizes the relationship between absorbed and emitted photons at specified wavelengths: it is a precise quantitative analytical technique, inexpensive and easily mastered.

All chemical compounds absorb energy which causes excitation of electrons bound in the molecule, such as increased vibrational energy or, under appropriate conditions, transitions between discrete electronic energy states. For a transition to occur, the absorbed energy must be equivalent to the difference between the initial electronic state and a high-energy state. This value is constant and characteristic of the molecular structure. This is termed excitation wavelength. If conditions permit, an excited molecule will return to ground state by emission of energy through heat and/or emission of energy quanta such as photons. The emission energies or wavelengths of these quanta are also equivalent to the difference between two discrete energy states and are characteristic of the molecular structure. Fluorescent compounds or fluorophors can be identified and quantified on the basis of their excitation and emission properties [1].

The so called “excitation spectrum” is obtained measuring the luminescent intensity at a fixed wavelength while varying the excitation energy, conversely the “emission spectrum” record the emission intensity as a function of wavelength using a fixed excitation energy [4].

The principal advantage of fluorescence over radioactivity and absorption spectroscopy is the ability to separate compounds on the basis of either their excitation or emission spectra, as opposed to a single spectrum. This advantage is further enhanced by commercial fluorescent dyes that have narrow and distinctly separated excitation and

emission spectra. Although, maximum emission occurs only for specific excitation and emission wavelength pairs, the magnitude of fluorescent intensity is dependent on both intrinsic properties of the compound and on readily controlled experimental parameters, including intensity of the absorbed light and concentration of the fluorophor in solution.

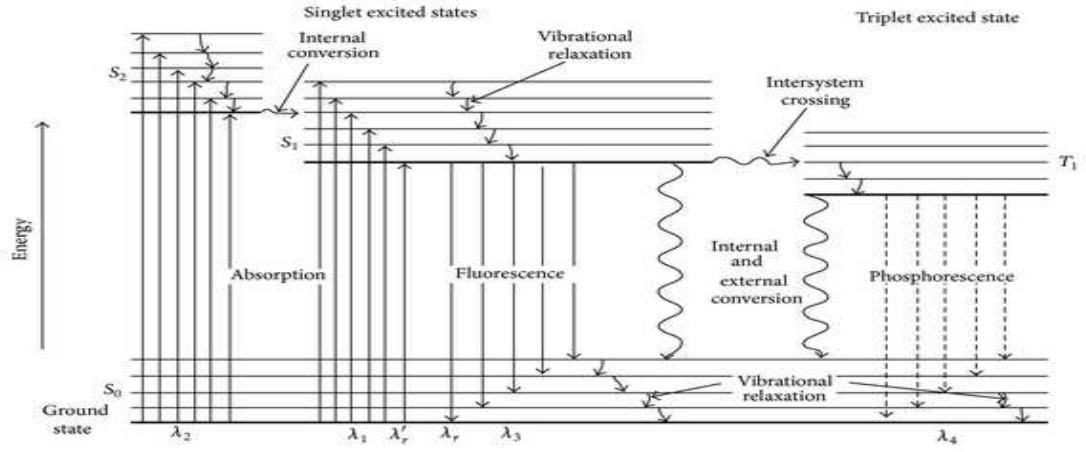

Figure 1.1 - Jablonsky diagram for a photoluminescent molecule

1.1.1 - PROCESS STAGES

As shown in Fig. 1.1 absorption transitions can occur from the ground singlet electronic state (S_0) to various vibrational levels of the excited singlet electronic states (S_1 and S_2). Molecules excited to electronic states S_1 and S_2, rapidly lose any excess vibrational energy and relax to the ground vibrational level of that electronic state. This non radiative process is termed 'vibrational relaxation'. Note that direct excitation to the triplet state is not shown because this transition involves a change in multiplicity, it has a very low probability of occurrence, hence is called a 'forbidden transition'.

The fluorescence process could be divided in three stages [2,3]:

- *Stage 1 : Excitation* A photon of energy $h\upsilon_{EX}$ is supplied by an external source such as an incandescent lamp or a laser and absorbed by the fluorophore, creating an excited electronic singlet state (S_2). The rate of photon absorption is very rapid and takes place in about 10^{-15} s.
- *Stage 2 : Excited-State Lifetime* The excited state exists for a finite time (typically 10^{-5} to 10^{-10} s). During this time, the fluorophore undergoes

conformational changes and is also subjected to a multitude of possible interactions with its molecular environment. These processes have two important consequences. First, the energy of S_2 is partially dissipated, yielding a relaxed singlet excited state (S_1) from which fluorescence emission originates. Second, not all the molecules initially excited by absorption (Stage 1) return to the ground state (S_0) by fluorescence emission. Other processes such as collisional quenching, fluorescence resonance energy transfer (FRET) and intersystem crossing may also de-populate S1. The fluorescence quantum yield, which is the ratio of the number of fluorescence photons emitted (Stage 3) to the number of photons absorbed (Stage 1), is a measure of the relative extent to which these processes occur.

- *Stage 3 : Fluorescence Emission* A photon of energy $h\upsilon_{EM}$ is emitted, returning the fluorophore to its ground state S_0. Due to energy dissipation during the excited-state lifetime, the energy of this photon is lower, and therefore of longer wavelength, than the excitation photon $h\upsilon_{EX}$. The difference in energy or wavelength represented by ($h\upsilon_{EX}$– $h\upsilon_{EM}$) is called the Stokes shift. The Stokes shift is fundamental to the sensitivity of fluorescence techniques because it allows emission photons to be detected against a low background, isolated from excitation photons. In contrast, absorption spectrophotometry requires measurement of transmitted light relative to high incident light levels at the same wavelength.

The entire fluorescence process is cyclical. Unless the fluorophore is irreversibly destroyed in the excited state (phenomenon known as photobleaching), it can be repeatedly excited and detected. The fact that a single fluorophore can generate many thousands of detectable photons is fundamental to the high sensitivity of fluorescence detection techniques. For polyatomic molecules in solution, the discrete electronic transitions represented by $h\upsilon_{EX}$ and $h\upsilon_{EM}$ are replaced by rather broad energy spectra called the fluorescence excitation spectrum and fluorescence emission spectrum, respectively. The bandwidths of these spectra are parameters of particular importance for applications in which two or more different fluorophores are simultaneously detected [2].

Photoluminescence is limited to systems incorporating structural and environmental features that cause the rate of radiationless relaxation or deactivation processes to be slowed to a point where the emission process can compete kinetically.

1.1.2 - DEACTIVATION PROCESSES

Vibrational Relaxation

Collisions between molecules of the excited species and those of the solvent lead to rapid energy transfer with a minuscule increase in temperature of the solvent. Vibrational relaxation is so efficient that the average lifetime of a *vibrationallv* excited molecule is 10^{-12}s or less, a period significantly shorter than the average lifetime of an *electronically* excited state. As a consequence, fluorescence from solution always involves a transition from the lowest vibrational level of an excited electronic state*; s*everal closely spaced emission lines are produced, however, and the transition can terminate in any of the vibrational levels of the ground state. A consequence of the efficiency of vibrational relaxation is that the fluorescence band for a given electronic transition is displaced toward lower frequencies or longer wavelengths from the absorption band (the Stokes shift). Overlap occurs only for the resonance peak involving transitions between the lowest vibrational level of the ground state and the corresponding level of an excited state. [3,4]

Internal Conversion

A molecule could pass to a lower energy electronic state, between two states of the same multiplicity, without emission of radiation with intramolecular processes. The transition is often highly efficient when there is an overlap in vibrational wave function. Internal conversion through overlapping vibrational levels is usually more probable than the loss of energy by fluorescence from a higher excited state. When the excited molecule proceeds from the higher electronic state to the lowest vibrational state of the lower electronic excited state via internal conversion and vibrational relaxations, the fluorescence occurs at a certain wavelength λ, regardless of whether radiation with λ_1 or λ_2 was responsible for the excitation. Quinine provides a classical example of this type of behaviour (Fig. 1.2).[4]

Internal conversion may also result in the phenomenon of *predissociation.* Here, the electron moves from a higher electronic state to an upper vibrational level of a lower electronic state in which the vibrational energy is great enough to cause rupture of a bond. Large molecules have an appreciable probability for the existence of bonds with strengths lower than the electronic excitation energy of the chromophores.

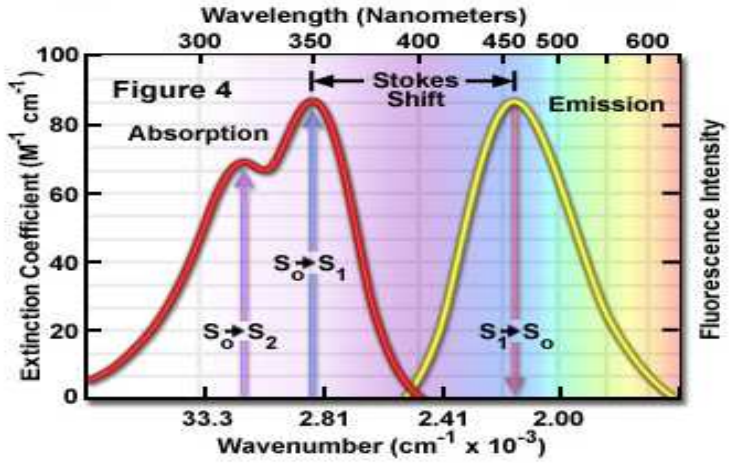

Figure 1.2 - Fluorescence absorption and emission spectra for a solution of quinine

Rupture of these bonds can occur as a consequence of absorption by the chromophore followed by internal conversion of the electronic energy to vibrational energy associated with the weak bond. Predissociation should be differentiated from dissociation, in which the absorbed radiation directly excites the electron of a chromophore to a sufficiently high vibrational level to cause rupture of its bonds. In this case, no internal conversion is involved. Dissociation processes also compete with the fluorescence process. Therefore fluorescence seldom results from absorption of ultraviolet radiation of wavelengths shorter than 250 nm, i.e. highly energetic.

External Conversion – Matrix effect

Deactivation of an excited electronic state may involve interaction and energy transfer between the excited molecule and the solvent or other solutes. This process is called *external conversion.* Evidence for external conversion includes a marked solvent effect on the fluorescence intensity of most species. Furthermore, those conditions that tend to reduce the number of collisions between particles (low temperature and high viscosity) generally lead to enhanced fluorescence. Unfortunately the details of external conversion processes are not well understood.[4]

1.1.3 - VARIABLES INFLUENCING FLUORESCENCE

Quantum Yield

The emission intensity is proportional to the amplitude of the fluorescence excitation spectrum at the excitation wavelength. Absorption and emission efficiencies are most usefully quantified in terms of the molar extinction coefficient (ε) for absorption and the quantum yield (QY) for fluorescence. Both are constants under specific environmental conditions. The value of ε is specified at a single wavelength (usually the absorption maximum), whereas QY is a measure of the total photon emission over the entire fluorescence spectral profile.. The *quantum yield* or efficiency, for fluorescence or phosphorescence is simply the ratio of the number of molecules that luminesce to the total number of excited molecules. For a highly fluorescent molecule, the quantum efficiency approaches unity under some conditions, while chemical species that do not fluoresce appreciably have efficiencies that approach zero.[3,4]

The fluorescence quantum yield for a compound is determined by the relative rate constants k, for the processes by which the lowest excited singlet state is deactivated. These processes are fluorescence (k_f), intersystem crossing (k_{is}). External conversion (k_{ec}), internal conversion (k_{ic}), predissociation (k_{pd}), and dissociation (k_d).

$$QY = \varphi = \frac{k_f}{k_f + k_{is} + k_{ec} + k_{ic} + k_{pd} + k_d}$$

Those variables that lead to high values for the fluorescence rate constant k_f, and low values for the other k_x terms enhance fluorescence. The magnitude of k_{pd} and k_d mainly depend on chemical structure, while the other constant are mainly influenced by the environment.

Fluorescence intensity "F" per molecule is proportional to the product of the molar absorptivity "ε" and QY

$$F = \varphi \; I_0 (1 - \varepsilon - \varepsilon bc)$$

where I_0 is the incident radiant power (dependent on the source type, wavelength and other instrument factors), b is the path length of the cell, and c is the molar concentration of the fluorescent compound.[1,4]

Transition types

Fluorescent emission is confined to the less energetic between $\pi^*-\pi$ and $\pi^*- n$ orbital transitions (both less energetic than the $\sigma*-\sigma$). Most commonly it is associated with π^* orbital state because such excited states exhibit relatively short average lifetimes *(k,* is larger) and the deactivation processes that compete with fluorescence are less likely to occur.[4]

Structure

The most intense and the most useful fluorescence is found in compounds containing aromatic functional groups. Most unsubstituted aromatic hydrocarbons fluoresce in solution, the quantum efficiency usually increasing with the number of rings and their degree of condensation. The simple heterocyclics, such as pyridine, furan, thiophene, and pyrrole, do not exhibit fluorescence. On the other hand, fused ring structures ordinarily do fluoresce. With nitrogen heterocyclics, the lowest-energy electronic transition is believed to involve an $n-\pi^*$ system that rapidly converts to the triplet state and prevents fluorescence. The fusion of benzene rings to a heterocyclic nucleus, however, results in an increase in the molar absorptivity of the absorption band. The lifetime of an excited state is shorter in such structures, and fluorescence is observed for compounds such as quinoline, isoquinoline, and indole. Substitution on the benzene ring causes shifts in the wavelength of absorption maxima and corresponding changes in the fluorescence emission. In addition, different substitutions frequently affect the quantum efficiency drastically changing the deactivation rate constants magnitude and the transitions energies.[3,4]

Structural rigidity

It is found empirically that fluorescence is particularly favoured in molecules with rigid structures, probably by a the internal conversion rate lowering. The influence of rigidity has also been invoked to account for the increase in fluorescence of certain organic chelating agents when complexed with a metal ion. One part of a non-rigid molecule can undergo low-frequency vibrations with respect to its other parts: such motions undoubtedly account for some energy loss.[4]

Temperature and Solvent Effects

All fluorophores are subjected to intensity variations as a function of temperature. In general fluorescence intensity decreases with increasing temperature due to increased molecular collisions that occur more frequently at higher temperatures. The increased frequency of collisions at elevated temperatures improves the probability for deactivation by external conversion. A decrease in solvent viscosity also increases the likelihood of external conversion and leads to the same result. The degree of response of an individual compound to temperature variations is unique to each compound.

The fluorescence of a molecule is decreased by solvents containing heavy atoms or other solutes with such atoms in their structure: carbon tetrabromide and ethyl iodide are examples. The effect is similar to that which occurs when heavy atoms are part of the fluorescing compounds: orbital spin interactions result in an increase in the rate of triplet formation and a corresponding decrease in fluorescence. Compounds containing heavy atoms are frequently incorporated into solvents when enhanced phosphorescence is desired. The dependence from the solvent is most often observed with fluorophores that have large excited-state dipole moments, resulting in fluorescence spectral shifts to longer wavelengths in polar solvents.

Moreover , the presence of dissolved oxygen often reduces the intensity of fluorescence in a solution. This effect may be the result of a photochemically induced oxidation of the fluorescing species. More commonly, however, the quenching takes place as a consequence of the paramagnetic properties of molecular oxygen, which promotes intersystem crossing and conversion of excited molecules to the triplet state. Other paramagnetic species also tend to quench fluorescence.[4]

Sample pH

The fluorescence of an aromatic compound with acidic or basic ring substituents is usually pH dependent and both the wavelength and the emission intensity are likely to be different for the protonated and unprotonated forms of the compound. The changes in the emission spectra mainly arise from the differing number of resonance species that are associated with the acidic and basic forms of the molecules. For example, aniline has several resonance forms but anilinium ion has only one. That is, the additional resonance forms lead to a more stable first excited state and fluorescence in the ultraviolet region is the consequence.[1,3,4]

The fluorescence of certain compounds as a function of pH has been used for the detection of end points in acid-base titrations: changes in acid or base dissociation constants with excitation are common and are occasionally as large as four or five orders of magnitude. These observations suggest that analytical procedures based on fluorescence frequently require close control of pH.

Fluorophore concentration

The power of fluorescence emission F is proportional to the radiant power of the excitation beam that is absorbed by the system. That is,

$$F = \varphi \, I_0(1 - \varepsilon - \varepsilon bc) = \varphi K''(I_0 - I) = K'(I_0 - I)$$

where I_0 is the power of the beam incident on the solution, I is its power after traversing a length b of the medium, φ is the quantum efficiency of the fluorescence process, and K" is a constant dependent on geometry and other factors. The quantum efficiency of fluorescence is a constant for a given system, and so the product $\varphi K''$ is lumped into a new constant K’ on the right side of the equation. To relate F to the concentration of the fluorescing species, we write Beer's law in the form

$$\frac{I}{I_0} = 10^{-\epsilon bc}$$

where 10 is the molar absorptivity of the fluorescing molecules and “bc” is the absorbance.

Expanding in McLaurin series, providing 2.303 εbc = A < 0.05, and having Io constant we have (with a maximum relative error 0,13% caused by the series approximation):

$$F = K' I_0(\, 2{,}303\varepsilon bc) = 2{,}303\varphi K'' \, I_0 \varepsilon bc \; = Kc$$

Thus, a plot of the fluorescence intensity of a solution versus concentration of the emitting species should be linear (at low concentrations).[4]

Fluorophore–Fluorophore Interactions

Fluorescence quenching can be defined as a bi-molecular process that reduces the fluorescence quantum yield without changing the fluorescence emission spectrum; it can result from transient excited-state interactions (collisional quenching) or from

formation of non-fluorescent ground-state species [2]. When c becomes great enough that the absorbance is larger than about 0.05, the higher-order terms for the McLaurin series becomes important and linearity is lost; F then lies below an extrapolation of the straight-line. This excessive absorption is known as primary absorption. Another factor responsible for negative departures from linearity at high concentration is secondary absorption, that occurs when the wavelength of emission overlaps an absorption band. Fluorescence is then decreased as the emission radiation traverses the solution and is reabsorbed by other molecules in solution. Secondary absorption can be absorption by the analyte species itself or absorption by other species in the solution. The effects of these phenomena are such that a plot of fluorescence versus concentration may exhibit a maximum. As the concentration of molecules in a solution increases, probability increases that excited molecules will interact with each other and lose energy through processes other than fluorescent emission. Absorption effects are often termed *inner filter effects* and any process that reduces the probability of fluorescent emission is known as *quenching*.

Photo-oxidative deterioration

In general, the displacement of the absorption band in the direction of longer wavelengths (UV to visible and then to IR) takes place in relation to the extension of the area within which the molecule is able to relocate the peripheral electrons of the atoms involved. Extended conjugated systems, with more than six conjugated double bonds, will therefore show an emission in the visible range (i.e. a colour) starting from the absorption in the violet portion of the spectra, thus showing a pale yellow color to the naked eye. When a fluorophore underwent photo-oxidative ageing, the oxidation of organic molecules generally leads to an extension of the unsaturation contained in the molecule; it may require several specific chemical reactions, with formation of various intermediates, or can lead to significative transformations (e.g. splitting into two sections, cyclizations, etc.) or it may be even blocked for many reasons, as particular conditions of stability.The chemical synthesis of pigments strongly depends from this type of evaluations.

As for the fluorescence, the UV light, that is the principal region of absorption, also breaks down the chemical bonds within a fluorophores itself, preventing the fluorescence process to take place. As it will be seen for the pigment and dye samples studied in this thesis, the excitation spectral curve shifts to lower wavelength (more

energetics) as a consequence of a prolonged UV exposure. The electronic delocalization is reduced and the difference between ground state and excited state increased. Thereafter the fluorophore progressively loses the ability to interact with the same relatively 'low energetic' photons that caused them to fluoresce in the first place, i.e. the fluorescent emission intensity will progressively decrease for a fixed excitation wavelength.

Sample preparation

Fluorescence is a very sensitive technique. However, it is extremely susceptible to interference by contamination of trace levels of organic chemicals: potential sources of contamination are ubiquitous since any aromatic organic compound can be a possible source of fluorescence signal. In addition, care must be taken to eliminate all forms of solid interference (suspended particulates such as dust and fibres) causing false signals due to light scattering [1].

1.2 – INSTRUMENTAL

A light source produces light photons over a broad energy spectrum, typically ranging from 200 to 900 nm. Photons impinge on the excitation monochromator, which selectively transmits light in a narrow range centred about the specified excitation wavelength. The transmitted light passes through adjustable slits that control magnitude and resolution by further limiting the range of transmitted light. The filtered light passes into the sample cell causing fluorescent emission by fluorophores within the sample. Emitted light enters the emission monochromator, which is positioned at a 90º angle from the excitation light path to eliminate background signal and minimize noise due to stray light. Again, emitted light is transmitted in a narrow range centered about the specified emission wavelength and exits through adjustable slits, finally entering the photomultiplier tube (PMT). The signal is amplified and creates a voltage that is proportional to the measured emitted intensity. Since source intensity may vary over time, most research grade fluorimeters are equipped with an additional "reference PMT" which measures a fraction of the source output just before it enters the excitation monochromator, and used to ratio the signal from the sample PMT [1].

Emission spectra collected on different instruments will vary because of different wavelength dependencies of the wavelength selectors and transducers. The shape of a properly corrected emission spectrum reflects only how the luminescence efficiency varies with excitation wavelength. To correct the emission spectrum, a calibrated light source is employed and calibration factors for the emission monochromator and transducer are determined. The uncorrected emission results are then multiplied by appropriate correction factors to give the corrected spectrum. There is substantial machine-to-machine variability between fluorimeters, even from the same manufacturer. When the same sample is analysed with two different fluorimeters the fluorescence signals will not necessarily be equivalent. It may be possible to correct for this variability using the internal controls run prior to and during a fluorimeter session. Obviously all samples for a given experiment should be analysed with the same fluorimeter, using identical experimental conditions [1].

The spectrofluorimeter used to perform the photoluminescence and lifetimes measurements is the Horiba Jobin Yvon Fluorolog®-3 (Fig.1.3), able to perform

measurements in emission and excitation, in both solid and liquid samples. The excitation of the sample occurs through a 450W Xenon lamp, which has an emission spectrum between 250nm and 850nm (selected through a double-grating monochromator), or through external laser or LED sources at specific frequencies. The optical emission of the sample is analyzed by a single grating monochromator coupled to a suitable detector: a Hamamatsu photomultiplier R928 operating between 185 and 900 nm.

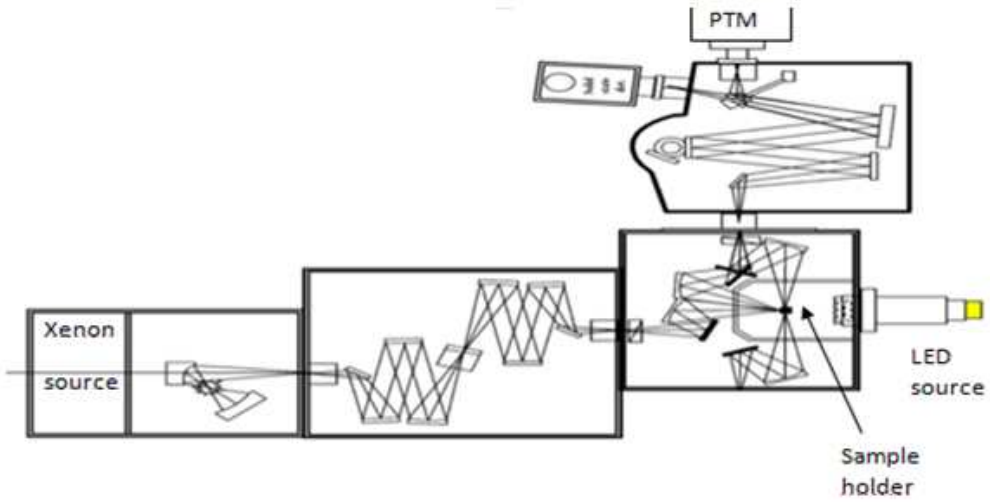

Figure 1.3 - Spectrofluorimeter scheme

Fluorescence lifetime

Lifetime measurements can give information about collisional deactivation processes, about energy transfer rates, and about excited-state reactions. Lifetime measurements can also be used analytically to provide additional selectivity in the analysis of mixtures containing luminescent species.

For the lifetimes analysis the fluorimeter can operate in Time Correlated Single Photon Counting (TCSPC) or Multi Channel Scaling (MCS) mode. In the first case a pulsed sources at high repetition frequency (1 MHz) is used, enabling to estimate lifetimes ranging from hundred picoseconds to a few microseconds, as a NANOLED-370 with emission at 373 nm and pulse duration of 1.3 ns. In the second case, continuous or pulsed sources are used at low repetition frequency (typically 10 Hz) to estimate lifetimes ranging from a few microseconds to tens of milliseconds, as a pulsed laser Nd:YAG at 1064 nm included in a system incorporating a non-linear crystal for the generation of photons at different energies: the NT 342/3 / GRAPE / AW of Ekspla, with selectable emission from 210 nm to 2300nm. The pulse duration is about 6ns with

a repetition frequency of 10Hz. The maximum energy of the pulse is about 3mJ in the UV, visible and 30mJ 10mj in the near IR. As an alternative, pulsed laser diodes with a specific wavelength have been used. Among these, for example, SpectraLED-370 with emission at 377 nm and a bandwidth of 12 nm has been used, in which the duration of excitation can be freely selected and activated intermittently.

Portable spectrometer

Fiber optics are also employed for "surface readers", to transmit light from the excitation monochromators to the sample surface and then transport emitted light to the emission monochromators. This setup has the advantage of speed, but has the disadvantages of the inline geometry and smaller path length which increase the probability of quenching. Fluorescence and reflectance probes work in a similar manner: the central bundle carries the excitation radiation to a sample and the outer core collects and delivers the fluorescence or reflectance from the sample, to a monochromator or spectrograph. The collection leg is terminated with a quick connect 11 mm ferrule and the 6 individual 200 or 400 µm fibers are arranged in a single line, for best coupling efficiency to a slit. On this setup is based the Ocean Optics Jaz - Portable Wireless Spectrometer, meant to be used by the restorer for in-situ measurement, that has been used for the screening tests with a 365nm LED excitation.

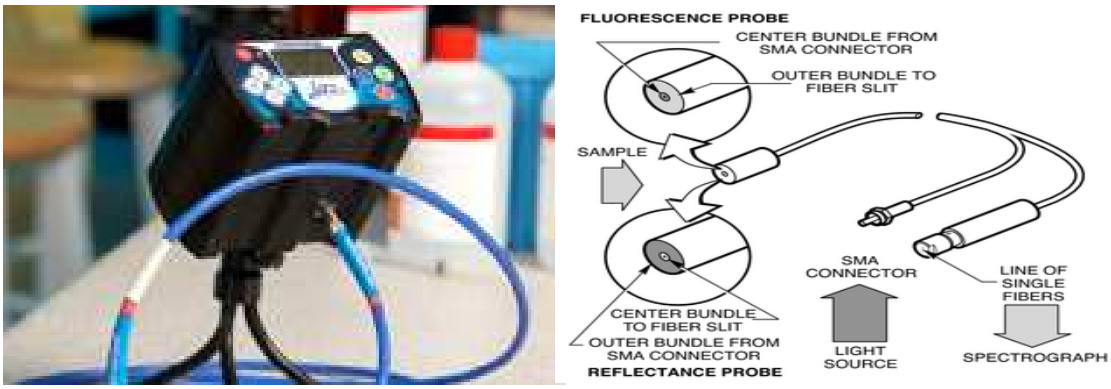

Fig. 1.4 Portable spectrometer with fluorescence inspection probes

1.3 – COMMERCIAL PRODUCTS

1.3.1 – DYES, PIGMENTS AND LIGHTFASTNESS

Colour-giving substances can be divided into two types: dyes and pigments. Pigments are inorganic or organic, coloured, white or black materials which are practically insoluble in the medium in which they are incorporated. Dyes, unlike pigments, do dissolve during their application and in the process lose their crystal or particulate structure. It is thus by physical characteristics rather than by chemical composition that pigments are differentiated from dyes. The necessary insolubility for pigments can be achieved by avoiding solubilizing groups in the molecule or by forming insoluble organic structures .

For the ender-user, an important difference between the two is their lightfastness. The degree of lightfastness indicates the degree to which a colour-giving substance is affected by ultraviolet light, a constituent of both natural daylight and artificial light. Blended with paint or ink all dyes have poor to moderate lightfastness, while the lightfastness of pigments varies from poor to excellent. Moreover fluorescent pigments can be used without losing their fluorescence (unlike dyes), for short dwell times in applications with processing temperatures up to 180°C (e.g. plasticized PVC formulations) without affecting the colour properties.

Fluorescent pigments are still more lightfast than conventional pigments, the degree fading depending on the following factors: 1) Colour of the pigment; 2) Pigment loading and thickness of the end product. The higher the pigment loading and the coating thickness, the better the lightfastness; 3) Type of binder polymer; 4) Intensity and angle of the incident light.[5]

Pigments can be distinguished not only by their degree of lightfastness but also by other properties such as opacity, transparency and tinting strength. Their quality could be measured by the particle size distribution, thermal stability, solvent resistance, compatibility towards the substrate, brilliancy, etc.. In particular, slight variation in the particle size affects the physical appearance of the pigment and compatibility towards the application. A fine particle size provides good coverage and good hiding power

compared against bigger particles. Generally small particles with low strength give better results than bigger particles with higher strength.

When mixing two or more compounds, the lightfastness of each compound plays its independent role, thus the total emission's colour (that is the additive sum of the emitters) will change along the exposure time. The lightfastness may be improved by including UV-absorbers in the formulation and/or by making use of clear overcoats containing UV-absorbers.[6]

1.3.2 - PHOTOLUMINESCENT MATERIALS

In this section, only a general outlook will be given to the emission/excitation properties of different photoluminescent materials, considering the hugeness of this topic both in physics (explanation of the phenomena) and chemistry field (syntesis of new materials).

Rare Earth

In the case of the lanthanides, the emission is due to transitions inside the 4f shell, thus intra-configurational f-f transitions. The incomplete 4f shell is shielded from the surroundings by the filled $5s^2$ and $5p^6$ orbitals therefore the effect of the host lattice or of the surrounding organic ligands on the intra 4f transition is small but, in any case, essential. Giving the very small crystal field splitting for this ions the emission curve presents sharp peaks. Although photoluminescence of rare earths ions can be an efficient process, only a very low amount of radiation is absorbed by direct excitation in the 4f levels due to a molar absorption coefficient smaller than 10 L mol^{-1} cm^{-1}.

Rare earth ions presents two differents emission behaviour. Those with 4f electrons well shielded from the surroundigs presents sharp emission lines, with a long (ms) lifetime of the excited state: this is the case for Gd^{3+} (emission in the UV range), Eu^{3+} (lines in the red spectral area), Tb^{3+}(main emission in the green area, but often there is a strong contribution from high energy levels in the blue area), Dy^{3+}(transition at 470 nm and 570 nm) and Pr^{3+}(emission dependent from the host lattice). Other ions emits broad band, due to the return from 5d orbital into the 4f orbital when 4f→5d transition occurs in the excitation, as Ce^{3+}; in this case lifetime is shorter if compared with the other rare earths (ns).

Since the luminescence intensity is not only proportional to the luminescence quantum yield but also to the amount of radiation absorbed, low light absorption lead to weak luminescence. However, dispersing in host lattices or bonding the ions with organic ligand, this problem can be overcome by the so-called *antenna effect* (or *sensitization*). Because of the intense absorption bands of the inorganic matrices or organic chromophores, much more light can be absorbed and, subsequently, the excitation energy is transferred from the organic ligands to the lanthanide ion by intramolecular energy transfer. There are two possible interconfigurational transitions: charge-transfer transition ($4f^n \rightarrow 4f^{n+1}L^{-1}$, where L is a ligand) and $4f^n \rightarrow 4f^n\text{-}5d^1$ transitions. Both transitions appear as broad absorption bands. Tetravalent ions (Ce^{4+}, Pr^{4+}, Tb^{4+}) exhibit charge-transfer band as well as trivalents ions that have the tendency to become divalent (Sm^{3+}, Eu^{3+}, Yb^{3+}). On the other hand, divalent ions (Sm^{2+}, Eu^{2+}, Yb^{2+}) and trivalent ions (Ce^{3+}, Pr^{3+},Tm^{3+}) that have the tendecy to become tetravalent show 4f-5d transition. Considering the divalent ions the most applied is Eu^{2+} that shows a 5d→4f decay, whose emission could vary from violet to yellow. Usually decay time for this ion is around 1 μs. Lattice, as observed for Sm^{2+} (that usually emits in the red region) Yb^{2+} (emission in the ultraviolet/blue region) and Ce^{3+}, strongly influence the wavelength of emission.[7]

Regarding the organic compounds containg rare earths, the most diffused are lanthanide diketonates complexes of *β*-diketone ligands (1, 3-diketones) with lanthanide ions. These complexes are the most popular and the most intensively investigated on one side because many different *β*–diketones are commercially available and the synthesis of the lanthanide complexes is relatively easy, and on the other side because of their excellent luminescence properties. Finally they are even easy dispersible in organic matrix or utilized to functionalize nanoparticles.

Transition metals

Transition metal ions are extensively used as photoluminescence active centres both in inorganic lattice and with organic complex, representing the most important class of luminescent centre. They have an incompletely filled d shell so their electronic configuration is d^n(0> n > 10). For example, many d^{10} metal such as Cu(I), Ag(I), Au(I), Zn(II) and Cd(II) complexes were synthesized and extensively studied showing peculiar properties.

Quantum Dots

Quantum-dots (QDs) are semiconductor nanocrystals generally composed by atoms from II-IV groups (e.g. CdSe, CdS, ZnS and ZnSe) or III-V groups (e.g. InP and InAs) defined as particle with a dimension smaller or comparable to the exciton Bohr radius, usually between 2 and 20 nm. The photoluminescent properties of the QDs arise from interaction between free electrons. When the energy of the exciting radiation overcome the band-gap of the materials, light is absorbed; in this process, electrons are promoted from the valence band to the conduction band. Light emission (said "excitonic fluorescence") arise from the recombination of free or trapped charge carriers (electrons or holes), and is observed as a sharp peak. In bulk measurements, the excited-state decay rates are slightly slower than those of organic dyes (1–5 ns), but much faster than those of lanthanide phosphors (1 μs–1 ms). Moreover, by changing the dimension of the QDs the emitted light can be tuned from the in all the visible range up to the Near-InfraRed (NIR) due to the particles size induced quantum effect.[7]

Figure 1.5 Light emission of 2(left) to 6 (right) nm CdSe dots ZnS capped excited in the UV range.

Finally it's possible to functionalize the surface of QDs with organic ligands in order to modify the luminescence properties and, at the same time avoid cluster aggregation. Those peculiar properties make the QDs particularly interesting for applications in many fields such as biodiagnostics, bioimaging, photonics, optoelectronics, and sensors.[8]

Organic molecules

Photoluminescence behavior of organic molecule is the basis of many application, as sensor and biosensors, displays, laser, OLED and labels. In general, photoluminescent

compounds are aromatic molecule or, at least, highly unsaturated aliphatic compounds. In aromatic compounds the lowest-lying transition is a $\pi \rightarrow \pi^*$ type that is characterized from a high molecular absorption and high photoluminescent quantum yield. Modifying the structure with substituent or hetero atoms the luminescence behaviour of the molecule is strongly affected. Characteristics of the substituents, effects of the environment (presence of oxygen, nature of the solvent pH, concentration of species, etc), and many other factors strongly influence the photoluminescence properties of organic compounds.

Photoluminescent polymers

Regarding the polymers field there are two main directions for obtaining luminescent materials: firstly the use of intrinsically fluorescent polymers having conjugated fluorescent groups. The second route is the synthesis of material with a polymeric host material in which the luminescence behaviour is given by either organic or inorganic fillers.[7]

Various methods of design and synthesis have been developed: fluorescent polymers can be synthesized by polymerization of fluorescent functional monomers, using fluorescent compounds as initiator, or using fluorescent compounds as chain transfer agents. The potential use of light-emitting polymer is ultimately limited by their low quantum efficiency as well as by their poor stability to molecular oxygen. Moreover even workability is not so easy, nearly always involving use of solvents. For these reasons in many applications the use of a polymeric composite is favoured. Dispersing luminescent fillers in a hosting polymeric matrix it is possible to apply standard techniques of polymer processing to the development of photoactive material. Moreover standard polymers present improved thermo-mechanical properties and a greater resistance towards ageing compared to intrinsic photoluminescent polymers. On the other hand, obtaining uniform properties, both optical and mechanical, is a challenge as for all the composite materials. Lately many polymeric matrices were used as hosting materials for rare earth nanoparticles: PS, PMMA , polyethylene glycol, PEO, PVA, Polycarbonate, PDMS and many more. Some materials are even synthesized by mean UV-curing both in radical and cationic systems.

1.3.3 - ORGANIC AND INORGANIC PIGMENTS

Typically, two types of molecules display fluorescence: organic compounds with a high degree of conjugated unsaturation and extended π cloud structure, or inorganic compounds where it is relatively easy to promote an electron to a higher vacant energy level (usually a d- or f- level), and the molecule may be excited to a higher vibrational and rotational energy state.[9]

A comparison of the respective application properties of inorganic versus organic pigments shows some fundamentally important differences between the two families. In some application areas, inorganic pigments are used to an appreciable extent, frequently in combination with organic pigments.[10,11]

Organic pigments

Organic fluorescent pigments are 0,08-8% dye materials in colourless polar resin carriers. Only a few commercially available fluorescent dyes can be made into pigments. Typically, a polymer is coloured with a fluorescent dye preferably during the condensation/polymerization process. The resulting coloured resin is usually clear, brittle and friable: it is pulverised into a fine powder (0,5-20 µm), which is the final fluorescent pigment. In the manufacture of polyester alkyd resins or of amide (urea, melamine, and similar)-formaldehyde condensates of low molecular weight, to each type of said resins the colorant is fixed by absorption, therefore the applications of such pigments are in practice limited to inks and paints.

Suitable polycondensation resins are, for example, those wherein the reactants for the formation of said resins are [12,13]:

- at least one component “A” chosen from aromatic sulfonamides containing 2 hydrogens bonded to the nitrogen of the sulfonamide group, like benzenesulfonamide derivatives
- at least one component “B” chosen from substances containing 2 or more NH_2 groups, each of the said NH_2 groups being bonded to a carbon, the said carbon being bonded by a double bond to an O, S or N atom.
- at least one aldehyde component “C”.

A monocarboxylic acid may be added as such or may be formed in situ by reacting a monoamine and a dicarboxylic acid in sufficient quantity to form the desired corresponding monocarboxylic co-condensate to function as terminator and control the molecular weight of the resin formed.

There are different types of carrier resins for fluorescent pigments[14]:

- Thermoplastic and thermoset (Melamine Formaldehyde type) used in printing inks: the oldest types of carrier resins, based on para-toluene sulfonamide (PTSA)-melamine-formaldehyden fully condensed and melt at a range of about 115-135C°. In the thermoset resins, through post curing and some chemical modification of the PTSA-MF resins, solvent resistance was increased and softening temperature was raised to 175 C°. Melamine-formaldehyde resins, of high transparency and also light-fast and free from yellowing, are suitable as carrier resins for organic and inorganic dyes and pigments, particularly for organic fluorescent pigments. For the preparation of these products soluble or insoluble organic or inorganic dyes and/or pigments are mixed with the starting material prior to the condensation, optionally in combination with the modifying agents. It is also possible to add the dyes and pigments to the chemicals used for preparing the starting materials.
- Thermoset (Benzoguanamine Formaldehyde type) used in printing inks: here the melamine component of the PTSA-MF is replaced by benzoguanamine. This results in a spherical particle size rather than ragged edges, specifically developed for plastics to minimize the plating tendency. They are especially recommended for applications demanding improved resistance to polar solvents, plasticizers, heat, pressure and migration. Typical applications are in the solvent based paper coating field, textile field, or that of solvent based silk screen inks, paints and aerosol coatings, crying manufacturing or water base paper coatings.
- Thermoplastic (Polyamide type) developed for use in plastics: they are based on aliphatic diamines and isophthalic acid with melting points from 110-150°C, or on polyfunctional glycols and phthalic anhydride with a melting point around 90°C, depending on the intended application.
- Thermoplastic (Vinyl or Acrylic type): they do not contain any formaldehyde and display very high colour strength.

- Aqueous dispersions (Acrylic type), a newer development in fluorescent pigment manufacture, are specifically designed for printing and writing inks: they are manufactured by adding fluorescent dyes into acrylic monomer and then polymerizing, thus creating coloured latex particles (globules). They are formaldehyde free and have a fine particle size (sub micron), which is very suitable for ink manufacture.

Inorganic pigments

Most inorganic pigments are extremely weather fast and many exhibit excellent hiding power. Their physical properties is usually an advantage, being superior to that of most organic pigments under comparable conditions, although they not only exhibit coloristic limitations but also frequently present application problems (e.g. sensitivity to acids and light). There are stabilized versions of such pigments, which claim improved lightfastness and acid resistance; these products also claim to be chemically fast to hydrogen sulphide, which affects the brightness of a coating through sulphide formation. However, if the particle surfaces of such types are damaged in the course of the dispersion process, the above-mentioned deficiencies are apparent at the damaged site.[10]

Most inorganic fluorescent pigments (IFP) are either colourless or have very pale colours under daylight, but when excited by UV radiation, they fluoresce in relatively bright colours. The visible colour of these inorganic pigments is due entirely to emitted radiation and they are additive colours. Thus, a blend of equal parts of a green glowing and a red glowing pigment results in a yellow glowing pigment.[14]

Instead of being caused by localized electronic systems within the organic molecules, in the inorganic compounds the luminescence is determined by lattice's structure and thus their luminescence is altered or disappears completely when their crystal structure is altered in any way (melting, decomposing or breaking). The average particle size of inorganic commercial pigments is larger than organic pigments, around 2-4 microns, although nowadays nanocrystals are commonly synthesized obviating the need of grind large particles.

The classical IFPs have been based on the zinc sulphide and zinc cadmium sulphide (e.g. [Zn, Cd]S doped (activated) with silver, copper, or manganese). The activator used, an intentionally added impurity atom distributed in the host crystal, its type and

amount, determine the colour of the fluorescence: for example, when silver is used, the fluorescence colour ranges from deep blue to deep red. Common matrices are aluminates of alkali earth metals or oxides, sulphides and oxysulphides of rare earth elements.[14]

An important use of fluorescent inorganic pigments is in document security applications, hence they should possess excellent lightfastness and superior rub (dry & wet) fastness other to the fastness to various solvents and chemicals (ethyl acetate, ethanol, acetone, trichloroethylene, benzene, xylene, bleaching solutions, caustic soda, acetic acid, hydrochloric acid, perspiration, soap, detergent, etc.) must be excellent.[10]

1.4 - COMMON APPLICATIONS

Lightning

In common fluorescent lamps an electric discharge in the tube causes mercury atoms to emit ultraviolet light at 254 nm. The tube is lined with a coating of a fluorescent materials which absorb the ultraviolet radiation and re-emits visible light at 436 nm (blue), 546 nm (green) and 579 nm (yellow-orange) in modern trichromatic phosphor systems emitting white light.

Tracing – Biochemistry and Medicine

Expecially in the life-sciences fluorescence is used generally as a non-destructive way of tracking or analyse biological molecules by means of the fluorescent emission at a specific frequency where there is no background from the excitation light. For example a protein or other component can be "labelled" with an extrinsic fluorophore, a fluorescent dye that can be a small molecule, protein, or quantum dot. Fluorescent probes find a large use in many biological applications owing their sensitivity to physical and chemical conditions.

Tagging/Visualization - Forensic

Notwithstanding its intrinsically very high sensitivity, molecular fluorescence spectroscopy is not utilized as a general technique of forensic analysis, because spectra

tend to be broad and featureless. Fluorescence-based approaches currently applies to the authentication of currency and passports, identification of valuables, origin specification of gun powders and explosives, surveillance, etc. The photoluminescence phenomenon is also useful in criminalistics, for ultrasensitive latent fingerprint and body fluids detection, visualization of fibers, ink discrimination, and so on.
Fluorescence spectral examination may occasionally be used in areas such as document examination, specifically for ink differentiation in instances of document alteration, but fluorescence spectra as such tend to pertain primarily to the area of research.

With this thesis we aim to exploit the visualization potentiality of fluorescent compounds linking the spectral emission of a coating containing a specific commercially available fluorophore to practical in-situ evaluation immediately useful to the restorer, in the case of protective coatings formulation for cultural heritage.

REFERENCES

[1] *FMRC Manual*, Fluorescent microsphere resource center - University of Washington, 1999

[2] *Handbook of Fluorescent probes*, Y. Kileg, 2012

[3] *Practical Fluorescence*, G.Guilbaut, 1990

[4] *Chimica Analitica Strumentale*, Skoog and Leary, Edises ed., 2001

[5] *www.talens.com* – Royal Talens Fine Art Products

[6] *www.dayglo.com* – Day Glo Color Corporation

[7] *UV-cured Photoluminescent Coatings: Acrylic and Epoxy Systems*, PhD thesis, I. Roppolo, Politecnico di Torino, 2012

[8] *Semiconductor Clusters, Nanocrystals, and Quantum Dots*, A. P. Alivisatos, Science Vol. 271, 1996

[9] *Paints and varnishes–Vocabulary*, Part 1, Farbmittel and Begriff, ISO 4618-1, 1984

[10] *Industrial Organic Pigments*, Third Edition. W. Herbst and K. Hunger, Wiley ed., 2004

[11] *Introduction to measurement of color fluorescent materials*, A.Springsteen, Analytica Chimica Acta Vol.380, Elsevier ed., 1999

[12] *Exploring Chemical Analysis*, D.C. Harris, Macmillan ed., 2004

[13] *Process for the Preparation of Fluorescent and Non Fluorescent Pigments*, European patent EP1606353B1, 2008

[14] *Raw Materials & Additives for Specialty Inks & Coatings*, A. Nurhan Becidyan, 2001

[15] *Melamine Resin and Dye Mixtures*, U.S. patent USP4116918, 1978

[16] *www.kremer-pigmente.com* - Kremer Pigmente GmbH & Co. KG

[17] *www.dyes-pigments.com* - Kolorjet Chemicals

Chapter – 2 –

COMMERCIAL PRODUCTS SCREENING

COMMERCIAL PRODUCTS
SCREENING

The objective of this section is the selection of additives able to impart self-diagnostic properties to a waterborne protective coating: their presence will allow an instant evaluation of presence, uniformity and functionality of the protective film, hence a prompt restoration intervention. Since the coating is developed to ensure a simpler and more effective restoration of art pieces, it is vital for those additives not to impair the coating's properties. A protective coating for restoration purposes has defined characteristics, starting with its aesthetic performance (e.g. transparency) and including removability as much as physical, chemical and mechanical resistance.

Good candidates for this purpose are therefore compounds that do not absorb in the visible range while active in other regions of the electromagnetic spectrum, as IR-active and colourless photoluminescent molecules. While the formers need a potable FTIR devices to be detected, for the visualization of the latter a simple hand-held UV-light source is sufficient; for further characterizations, then, a simple portable spectrometer can be used. Photoluminescent molecules can exist in the form of dyes or pigments, hence giving solutions or dispersions. This study focuses on pigments dispersions, owing their lightfastness and the dependence of their fluorescent emission on a number of factors, as seen in Chapter 1.1. Nevertheless the presence of dyes instead of pigments has been evaluated in course of work.

The additives were selected for waterbased formulations, none the less, in order to characterize the additives, the available commercial pigments were screened in three solvents with different polarity: water, ethanol and ethyl-acetate. The screening of the colourless fluorescent additives evaluates their general properties: dispersability/solubility, dispersion aspect, fluorescent output in 1% mixture and/or in solution. For some of the additives these properties are shown to be matrix dependent. Of course, since the needs of restoration is aging-linked, also the fluorescent output of the additives in a coating held indoor and exposed to atmospheric conditions were evaluated. In this case the pigments were incorporated as powder in a special

waterborne coating formulation previously tested within the PANNA project, which was then applied in order to obtain a 20µm dry thickness on glass slides.

The primary criterion for the selection was the intensity of the main fluorescent emission peak after weathering, as recovered with a portable spectrometer. As a matter of fact, the incorporation of photoluminescent moleculesinto a protective coating and the correlation between a long-period aging and fluorescence output of the coating is one of the main goals of the European project PANNA. For this reason it is essential for the fluorescence intensity decay to be a slow and controllable phenomenon.

For the selection, the pigments were then divided into two categories: organic and inorganic. Two additives with emission in different visible spectral regions were selected out of each category, basing on the fluorescent intensity after one month of exposure and the decrease percentage in relation to the un-weathered sample. The chosen ones were then taken to the next stages in order to obtain a stable dispersion within a water matrix. As discussed in the previous chapter (Sect.1.3), organic and inorganic compounds show different chemical properties including a different response to UV-light exposure, therefore a specific aging behaviour . For example inorganic pigments present lower quantum efficiencies but at the same time higher resistance to UV rays and heat stability than organic pigments.

Note that giving the backscattering of the incident light in the portable spectrometer (which covers also the visible blue-violet region until 470nm), blue emitting pigments would hardly be useful for visualization and correlation purposes, while green to red emitting phosphors, possibly with sharp band, would be matter of interest.

2.1 – EXPERIMENTAL

A stock of fluorescent colourless ("invisible") powders, sold as "fluorescent pigments" with low excitation energy (i.e. 365nm wavelength, in the so called long-UV region) and different emission peaks, were purchased from RiskReactor manufacturer: 18 inorganic pigments ("P.F.L.I.") and 11 organic ("P.F.L.O.").
The available commercial pigments were screened in three matrices from high to low degree of polarity: water, ethanol and ethyl-acetate. The following properties were evaluated starting from commercial powder mixture in solvent (10g/l): solubility, aspect, fluorescent emission wavelength and intensity.

Figure 2.1 – Commercial powder mixtures in various solvents illuminated with a black-lamp

The wavelength chosen for illuminating the samples was 365nm, both with uv-lamp (Herolab 15W 60Hz), portable spectrometer (Jaz, OceanOptics, LED light EOS A1217995-1, dedicated paraxial setup) and subsequentely spectrofluorimeter (Fluorolog®-3, Horiba Jobin Yvon, Xenon lamp). The following specifications were used in the case of Jaz spectrometer measurements: A) on vials mixtures: 1,5cm distance from the probe,1sec integration, 1 scan to average; B) on coating (applied on glass slide): 30° incidence angle, 1cm distance from probe, 2 sec integration, 1 scan to average. The portable spectrometer was used in the first place for a fast testing of the on-field detectability of the pigments (owing to the fast sedimentation phenomenon occurring due to the large size of the pigments particles).

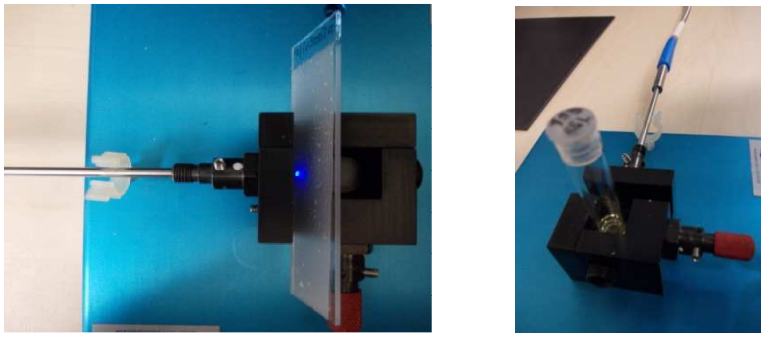

Figure 2.2 – Portable spectrometer fiber probe fixed to a sample holder and pointed on a formulation applied on glass slide and on a pigment's mixture in solvent.

For a more precise evaluation of the fluorescence properties, the Fluorolog spectrofluorimeter was instead exploited in the coatings testing (in particular the percentage of fluorescent intensity loss, regarding this section). This professional instrument is also equipped with a correction for the incident light fluctuations. Other than the possibility to obtain accurate photoluminescence (PL) and photoluminescence excitation (PLE) specra, removing the high signal from the reflection of the incident light, it also presents a 1,5nm shift in the PL curve detection in respect to the spectra obtained with the portable instrument, showing how the instrumental setup could influence the analyses evaluation.

Though 29 was the total starting number of additives tested, for what concerns the evaluation of the waterborne coatings the samples' number was reduced to 19 (10 inorganic and 9 organic). This reduction was made dividing them in families, basing on 99% matching of the infrared spectra (obtained with a Bruker Alpha ECO-ATR) and testing only one additive out of each family. The tested coatings, made from a 2,5% pigment in matrix formulation, had been previously applied with a bar coater in order to obtain a 20µm dry thickness (TQC VF spiral applicator) on microscope glass slide and oven dried for two hours at 70°C. The chosen concentration was fixed for all the samples, in this way it was possible to compare both the percentage of intensity loss and the final magnitude of fluorescent emission after weathering.

2.2 – RESULTS AND DISCUSSION

Upon 29 pigments 23 gave fluorescent mixture in water, 14 of them among the coated ones (Table 2.2). Only 8 of these remained visibly fluorescent after one month of exposure to atmospheric weathering (Fig 2.3), all of them appearing in their 10g/l water mixture as precipitate plus suspension. All the screening results, dividing inorganic and organic pigments, are shown in Table 2.1, 2.2 and 2.3.

Commercial name	**Colour** **visible / UV light**	**Solubility (1% w/w)** **Et-Ac./ W/ EtOH**	**Nominal emission (nm)**	**Eemission wavelength (nm)** **in PANNA waterbased coating**
INORGANIC PIGMENTS				
PF-00 Invisible Blue	white/ **blue**	part	450	456, 433
PF-01 Invisible Green	white green/ **bright white-green**	part/no/no	450	537, 462
PF-02 Invisible Yellow	white/ **clear green**	part	545	*545, 588, 611
PF-03 Invisible Orange	white/ **pink**	part		*587, 611
PF-07 Invisible Blue-White	white green/ **white**	part	500	456, 534, 516
PF-09 Invisible Violet	white/ **blue**	part/no/no		*545, 583, 610
PF-0B Bright White	white/ **blue**	part		446, 420, 536
PF-R7 Invisible Red	white/ **red**	part		626, 706, 616, 595, 687
PFLI-R UV Red	white/ **magenta**	part/no/part		625.5, 616, 705.5, 594, 630, 686, 586, 5, 696, 582
PFLI-P Purple	white/ **blue**	no/part/part		419, 524
PFLI-YG Yellow Green	green white/ **green**	part		515, 626
PFLI-B Blue	creme white/ **blue**	no/part/part	445	*440,483
PFLI-G Green	white green/ **green**	part	515	515, 458
PFLI-W White	white/ **blue**	no/part/part	515	*516, 626, 616, 594, 706
PFLI-BG Blue Green	white grey/ **blue**	part	616	
PFLI-O Orange	white/ **yellow pink**	no/no/part	625	*626, 616, 706, 594, 540, 583, 586
PFLI-Y Yellow	yellow green white/ **yellow-green**	part/no/part	576	626, 539, 706, 616, 595
PFLI-O Invisible Orange	pink white/ **pink yellow**	no	520	*520, 585
ORGANIC PIGMENTS				
DFSB-C0 Clear Blue	green white / **blue**	part/no/part	450	*450, 483, 519
DFSB-C7 Clear Red	cream yellow/ **orange-pink**	yes/part/yes		611-616, 592, 650, 687-705

DFSB-C0 Clear Blue, BBOT	green white / **blue**	part/no/part (recrystallization)	450	*447, 483
PFLO-R Red	cream white/ **orange-red**	yes/part/part	615	616, 595, 692-705, 651
PFLO-YG Yellow Green	white/ **bright green**	yes/no/part	495	500-545, 613.5, 616.5
PFLO-G Green	cream white/ **green**	no	545	497 ,530
PFLO-B Blue	green white / **blue**	part/no/part	460	451, 407
PFLO-Y Yellow	white/ **yellow-green**	part	595	543, 420, 685
PFSO-R Short UV Red	white/ **magenta**	part	610	458, 433, 408, 589-591, 544, 612-619, 697-701
PFSOB Organic Shortwave Blue	white/ **blue violet**	part	560	430, 458
DFPD-C2 Invisible Yellow	cream white/ **green-yellow**	no/part/part	540	535

* Emission wavelength in water 1% suspension (the pigment was not applied in coating)

Table 2.1 - Pigments' initial screening

Commercial name	**Probable composition** **(from SEM, IR and PL data)**	**IR family** **(99% match)**	**Aging test**
INORGANIC PIGMENTS			
PF-00 Invisible Blue	Mixture with PF-02	A	✓
PF-01 Invisible Green	Similarity with PF-00 and PFLI-R	B	✓
PF-02 Invisible Yellow	Pure (ZnS)	A	✗
PF-03 Invisible Orange	Similiarity with PF-02	A	✗
PF-07 Invisible Blue-White	Mixture with PF-00,PF-01,PFLI-R	B	✓
PF-09 Invisible Violet	Similiarity with PF-02	A	✗
PF-0B Bright White	Mixture	C	✓
PF-R7 Invisible Red	Aged PFLI-R	D	✓
PFLI-R UV Red	Pure (YOS:Eu)	E	✓
PFLI-P Purple	Mixture	F	✓
PFLI-YG Yellow Green	Mixture with PF-R7, PFLI-G	G	✓
PFLI-B Blue	Similarity with PF-R7	G	✗
PFLI-G Green	Pure (BaMgAlO:Mn,Eu)	G	✓
PFLI-W White	Similarity with PF-R7, PFLI-G	G	✗
PFLI-BG Blue Green	Similarity with PF-R7, PFLI-G	G	✗
PFLI-O Orange	Mixture with PFLI-Y	E	✗
PFLI-Y Yellow	Mixture ZnCdS,PF-R7	H	✓
PFLI-O Invisible Orange		A	✗
ORGANIC PIGMENTS			
DFSB-C0 Clear Blue		A	✗
DFSB-C7 Clear Red		B	✓

DFSB-C0 Clear Blue, BBOT	Aged PFLO-B	C	✗
PFLO-R Red	Pure (Eu(TTa)3(TPPo)2)	D	✓
PFLO-YG Yellow Green	Mixture with DFSB-C7	E	✓
PFLO-G Green	Pure (HPQ)	F	✓
PFLO-B Blue		C	✓
PFLO-Y Yellow		G	✓
PFSO-R Short UV Red	Mixture with DFSB-C0,DFSB-C7	H	✓
PFSOB Organic Shortwave Blue		H	✓
DFPD-C2 Invisible Yellow		G	✓

Table 2.2 – Pigments' families association and aged samples.

Commercial name (and glowing colour)	**Emission in PANNA waterbased matrix (365nm excitation)**			
	Main peak wavelength (nm)	**Maximun intensity (A.U.)**	**Loss (%) after 1 month natural weathering**	**Peak shift (nm) after 1 month natural weathering**
INORGANIC PIGMENTS				
PF-R7	626	99,8 ± 68,1	-12,7 ± 83,4	-
PFLI-R UV	625.5	194,2	-34,6	-
PFLI-P	419	15,1	3,5	-
PFLI-Y	626	72,9 ± 61,7	16,7 ± 16,7	Second peak disappearance
PFLI-YG	515	21,4 ± 15,4	-15,1 ± 15,5	-
PF-01	537	9,7	82,7	-17
PFLI-G	515	42,2 ± 36,2	-29,6 ± 28,5	-
PF-00	456	36,1	91,8	-
PF-07	456	27,6	87,6	-
PF-0B	446	57,9	71,1	-3
ORGANIC PIGMENTS				
DFSB-C7	611-616	165,1	29,9	-
PFSO-R	458	6,6	26,2	-3
PFLO-R	616	3055,3 ± 1398,2	86,8 ± 7,6	-
PFLO-Y	543	78,7± 54,4	11,2 ± 6,5	-
DFPD-C2	535	62,5 ± 24,1	8,1 ± 9,5	+8
PFLO-YG	500-545	40,8	64,7	-
PFLO-G	497-500	116,8 ± 51,01	11,8 ± 3,9	-
PFLO-B	451	270,5	74,5	+3
PFSOB	430,458	23,5	50,5	-1

Table 2.3 – Change in the main fluorescence peak emission for the coated samples after 1 month natural weathering. The glowing colour of the pigments is also shown.

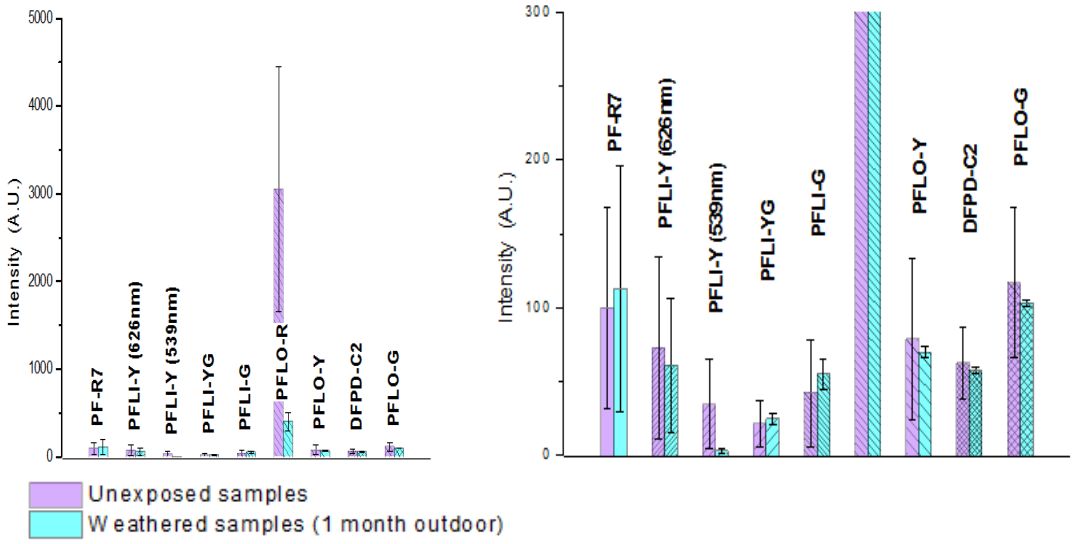

Figure 2.3 – Samples intensities before and after weathering (1 month outdoor).

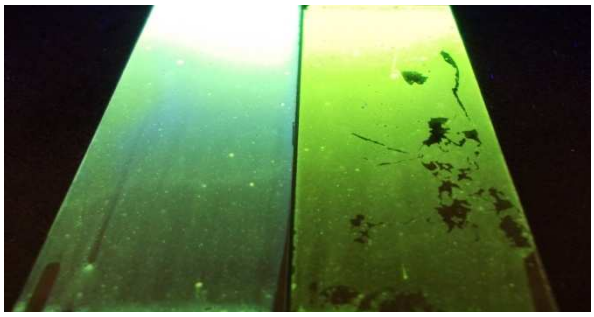

Figure 2.4 – PFLO-YG, 365nm excited coating before (left) and after (right) weathering

As shown in Table 2.3, not only the aging process influences the intensity of the photoluminescenct emission but also there could be a shift in the main emission wavelength or, as can be seen in Fig 2.4, an overall intensities redistribution in the PL curve, giving a change in the glowing perceived colour.

The pigments that still show an eye-visible fluorescence after the aging process are 4 (one red, two green and one yellow glowing) inorganic pigments and 4 (one red, one green and two yellow glowing) organic pigments. For the inorganic pigments (all in the right side of the plot in Fig.2.3) a slight increase in fluorescence was noted in the outdoor sample and ascribed to a probable matrix effect. This could be a change in the matrix polarity or acidity due to the exposure to humidity and UV light, but more probably a deterioration of the superficial layer, with a consequent un-covering of the fluorescent crystals. As can be seen in the left part of the plot (Fig.2.3), the lower

quantum efficiency (i.e. fluorescence intensity) of these pigments compared to that of the organic ones, has been reported.

Some observations on the samples composition are also presented in Table 2.2: many of the inorganic samples and some organic, appear to be composed by mixture of two or more separately sold fluorophore. Pigment PFLI-Y has been reported two times on the plot in Fig. 2.3 as its colour changes when exposed to UV-light for a month. As reported afterwards (see Chapter 3 and 4), this pigment is a mixture of two pigments, one of them giving the green part of the emission spectra (and the initial colour to the powder owing the additivity of colours in fluorescence) and less UV-resistant. The red glowing pigment that is light-resistant has the same fluorescent emission spectra of some other inorganic pigment tested, like PF-R7 and PFLI-R. The spectra reported in Fig. 2.5 shows the peaks obtained from both the weathered (blu line) and un-weathered sample (red line).

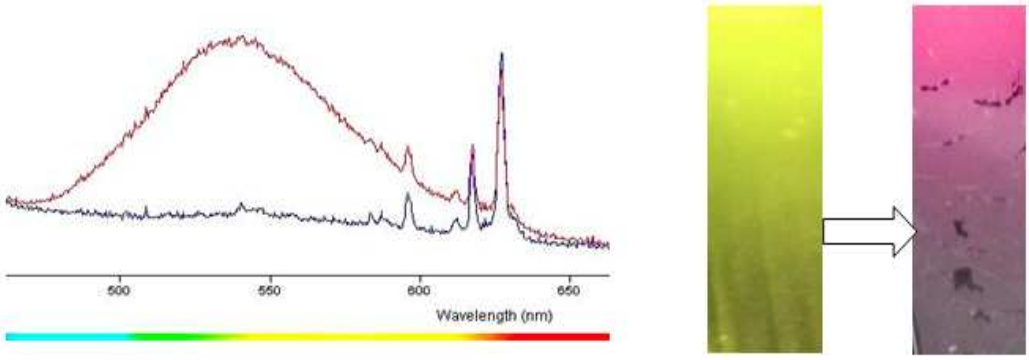

Figure 2.5 – 365nm-excited PL spectra and coating's photograp of PFLI-Y before (red line, green image) and after (blue line, red image) 1 month natural weathering.

The selection was based on a compromise between the lowest percentage of intensity loss due to the ageing process and the highest "final" fluorescent emission intensity.

2.3 – CONCLUSIONS

After an initial screening of their main properties, as solubility and fluorescence output in three different solvents, the 29 available fluorescent and colourless pigments were divided in two categories: organic and inorganic. The employment of these additives qualitatively selected in aqueous systems was the focus of the screening's subsequent part.

The ones showing the best fluorescent performance in a water-based matrix after UV and humidity exposure (one month outdoor weathering) have been chosen for each category. Namely these are PFLO-G for the organic pigments and PFLI-G for the inorganic pigments, both fluorescent in the green portion of the visible light spectra.

Although the fluorescence yield was not comparable to the previous two, considering the peculiar fluorescent behaviour of another additive, namely PFLI-Y (yellow glowing inorganic pigment), it was decided to proceed also with this one to the identification and grinding steps. Due to the UV-exposure the additive presents the disappearance of a fluorescence peak, thus a change in fluorescent emission (veering from green to red glow) that could be proved useful for restoration purposes. This pigment opened up new scenarios, as the possibility of using a mixture of different pigments with different aging behaviours as a meter of coating health status or light exposition. For this reason it was decided to consider also two other additives, PFLO-R (red glowing organic) and PF-R7 (red glowing inorganic), as complementary pigment for an eventual mixture with the two previously chosen. These are also the only red fluorescent samples that still fluoresce visibly after weathering thanks to their high starting emission intensity.

Further analyses were then conducted on these five commercial additives in order to identify the composing phosphors and characterize their photo-oxidative deterioration.

Chapter – 3 –

PRODUCTS

IDENTIFICATION

PRODUCTS
IDENTIFICATION

Once selected the commercial additives presenting light fatness properties from all the samples a deeper investigation is needed. This will allow to avoid interactions with other additives, to identify dedicated coating formulations and to define the pigments chemical and physical behaviour through ages. For this reasons analytical characterization of the chosen organic (PFLO-G and PFLO-R) and inorganic (PFLI-Y, PFLI-G and PF-R7) pigments was performed using different techniques accordingly to the needs of each one of them for an unambiguous identification: photoluminescence and photoluminescence excitation spectroscopy (PL/PLE), X-ray diffraction (XRD), scanning electron microscopy coupled to an energy-dispersive X-ray spectrometer (SEM-EDS), Fuorier Transformed Infrared Spectroscopy (FT-IR), Raman spectroscopy, mass spectrometry performed either with gas-chromatography and electrospray ionization (GC-MS and ESI-TOF-MS), nuclear magnetic resonance (1H-NMR), CHN elemental analyses.
According to the manufacturer, the pigments are a new type of dyeing matter supposed to have improved fluorescence and being excellently applicable in synthetic resins. As far as this research is concerned, the exact composition of the fluorescent materials is not accurately known and still a commercial secret. The material safety data sheets, (given only for the organic pigments) declare the powders to be composed by "*a pigmented melamine-formaldehyde copolymer, flushed as a sub-micron dispersion into a high quality printing ink varnish*"; an approximate lists of the resin ingredients is also given for each sample.

An exhaustive treatment of each characterization technique is beyond the aim of this thesis, hence in this context only a general overview on the above mentioned techniques [1] will be given to explain the reason for their employment:

Photoluminescence

PL/PLE are photoluminescence spectroscopic measurements, usually performed using a fluorimeter: the so called "excitation curve" (PLE) is obtained measuring the

luminescent intensity at a fixed wavelength while varying the excitation energy, conversely the “emission curve” (PL) records the emission intensity in function of wavelength using a fixed excitation energy.

Energy dispersive spectroscopy

EDS is an analytical technique used for the elemental analysis or chemical characterization of a sample. The high-energy electron beam (10-30 eV) that interacts with the sample surface generates a series of signals that are recognized by the detector. In particular, for each point scanned secondary electrons with an energy between 0 and 50 eV emitted from the surface , backscattered electron with energy ranging from 50 eV to that of incidence, and X-rays are produced. As X-rays energies are characteristic of the energetic difference between two shells and of the atomic structure of the emitting element, X-ray microanalysis gives specific information about the elemental composition of the sample, in terms of quantity (the intensity of this characteristic radiation is proportional to the concentration of the element in the sample) and distribution.

X-ray diffraction

XRD is a non-destructive analytical technique which can yield the unique fingerprint of Bragg reflections associated with a crystal structure. Since most materials have unique diffraction patterns, compounds and their purity can be identified easily by using a database. The particle size of the powder can also be determined by using the Scherrer formula, which relates the particle size to the peak width. The databases at our disposal make this type of analysis mainly useful for the inorganic pigments characterization.

Infrared spectroscopy

In FT-IR, a beam of infrared light passing through the sample records its infrared spectrum: when the excitation frequency is the same as the vibrational frequency of a particular bond, absorption occurs. FTIR spectroscopy is an analytical technique that allows infrared spectra recording: infrared light is guided through an interferometer and then through the sample (or vice versa), recorded as an interferogram and processed with the Fourier transform technique. Analysis of the position, shape and intensity of peaks in this spectrum reveals details about the molecular structure of the sample.

Raman spectroscopy

Raman spectroscopy is used to observe vibrational, rotational, and other low-frequency modes in a system and relies on inelastic scattering, or Raman scattering, of monochromatic light. A laser light interacts with molecular vibrations, phonons or other excitations in the system, resulting in the energy of the laser photons being shifted (to lower energies in the case of Stokes phenomenon). Infrared spectroscopy yields similar, but complementary, information. As a result, a Raman spectrum is information rich, and contains data relating to the specific chemical structure of the material being analysed, allowing the detection of weak IR frequencies. Raman spectroscopy is a non-destructive technique: it is non-contact, non-destructive, and requires no sample preparation. The identification of unknown materials is possible with the use of extensive Raman spectral databases. Databases were not available, thus Raman spectra have been mainly useful, together with infrared spectra, for a correct functional groups' interpretation.

Mass spectrometry – (Gas-chromatography and Electrospray ionization)

In GC-MS gas-liquid chromatography separates the components of a mixture while mass spectrometry works by ionizing chemical compounds to generate charged molecules or molecule fragments and measuring their mass-to-charge ratios. The molecules in the sample can be identified by correlating known masses to the identified masses or through a characteristic fragmentation pattern. Electrospray ionization (ESI) is a technique used in mass spectrometry to produce ions using an electrospray in which a high voltage is applied to a liquid to create an aerosol. It is especially useful in producing ions from macromolecules because it overcomes the propensity of these molecules to fragment when ionized. ESI is a so-called 'soft ionization' technique, since there is very little fragmentation. This can be advantageous in the sense that the molecular ion (or more accurately a pseudo molecular ion) is always observed, however very little structural information can be gained from the simple mass spectrum obtained.

Nuclear magnetic resonance

NMR can provide detailed information about the structure, dynamics, reaction state, and chemical environment of molecules. When placed in a magnetic field, NMR active nuclei (such as ^{1}H or ^{13}C) absorb electromagnetic radiation at a frequency characteristic of the isotope. Since electron distribution of the same type of nucleus varies according

to the local geometry and with it the local magnetic field at each nucleus, the intramolecular magnetic field around an atom in a molecule changes the resonance frequency. Chemical shift is the resonant frequency of a nucleus relative to a standard, thus position and number of chemical shift are diagnostic of the structure of a molecule.

Elemental analysis

CHN analysis is the most common elemental analysis and is accomplished by combustion. In this technique, a sample is burned in an excess of oxygen and various traps collect the combustion products like carbon dioxide, water, and nitric oxide. The masses of these combustion products can be used to calculate the composition of the unknown sample.

Fluorescence lifetime

FLT is a measure of the time a fluorophore spends in the excited states before returning to the ground state by emitting a photon. Whereas the luminescence quantum yield gives an idea of the luminescence quenching in the whole system, the luminescence decay time indicates the extent of quenching at the emitting site only. Although influenced by solvent effects, the lifetime is one of the most robust fluorescence parameters (mostly unaffected by inner filter effects, static quenching and concentration's variations), useful to discriminate between and among organic molecules and organo-metallic complexes owing to the different de-excitation probabilities.

3.1 – EXPERIMENTAL

The analyses were performed on PFLO-G, PFLO-R (organic samples), PFLI-G and PF-R7 (inorganic samples) powders, pursued from RiskReactor manufacturer.

In PL/PLE and lifetimes measurements the instrument used was a Horiba Jobin Yvon Fluorolog®-3 (see Fig.1.3); the emission curve was monitored in the 400-700nm range with an excitation wavelength of 365nm while the excitation curve was monitored between 260 and 500nm exciting each sample with its characteristic emission wavelength, basing on the PL results. For all the measurements, front face (FF) geometry, 1nm slits and 0,5nm increments were used. Attenuation filters (optical density filters OD1 and/or OD2) had to be introduced because of the high signal coming from the samples exceeding the linearity limit of the detector; also absorptive band pass filters (F390 for the green glowing and F500 for the red glowing samples) were introduced after the samples to avoid scattering phenomena, cutting out the reflected excitation radiation and its harmonics.

For the lifetimes, a NANOLED-370 with emission at 373 nm and pulse duration of 1.3 ns was used (in TCSPC mode) and a SpectraLED-370 with emission at 377 nm and a bandwidth of 12 nm was used (in MCS mode) (see Chapter 1.2). A 30° incidence angle with a 110° collecting angle was employed to reduce scattering phenomena. As in the case of PL and PLE, optical density filters and absorptive band pass filters were introduced.

EDS elemental analyses were performed using a Brucker Nano GmbH instrument, with primary energy of 20 (or 30) eV, coupled to a scanning electron microscope.

A Philips powder diffractometer equipped with PW100/70 goniometer was used for the XRD analyses with a Bragg Berentano reflection geometry. The radiation used was CuKα (λ = 1,542Å) Ni filtered, selected by a monochromator and a proportional counter PW1711/10, with a 0,5mm collimation and 0,2mm reception slit.

A Spectrum One from PelkinElmer was used for FT-IR measurements, ranging from 450 to 4000cm^{-1}, on samples in the form of KBr pellets.

Raman spectra were recorded for the organic samples using a Horiba Jobin Yvon Raman spectrometer equipped with a near infrared excitation line at 785,19nm of a diode laser source. A Horiba XploRa Raman-Microscope with a 50x magnification objective and a 1800line/mm grating was used. The induced fluorescence background

has led to the preferential use of the diode laser instead of the Argon laser source at 514nm, also present in the equipment.

^{1}H NMR at 289K was performed on the organic samples, dissolved in $(CD_3)_2SO$ with a Brucker AC200 instrument working at 200,13MHz.

Mass spectra were obtained only for PFLO-G sample and performed both with gas chromatography and electrospray ionization. The first instrument used was a Trace GC-MS equipped with a quadrupole Thermo Finnigan mass spectrometer and a HP5-MS 0,25µm column . The sample was dissolved and injected in column with a temperature ramp of 1 degree/min from 80 to 300°C and a solvent delay of 4 minutes. Various solvents were tested, here are presented the spectra for benzene (with which the optimal resolution was obtained). In the case of electrospray ionization, the instrument used was a Mariner ESI-TOF spectrometer from PerseptiveBiosystems equipped with reflectron. The sample was dissolved to a concentration 10^{-4}M in 1% formic acid water-MeCN, then 1µl of solution was injected and transported into the spray with a 20µl/min flux by a rheodyne valve. The spray is constituted by a stainless steel capillary positively charged at 4500 Volts. Once charged, the sample's mass is revealed by a time of flight analyser.

Also a CHN elemental analysis was performed only on PFLO-G, with a Perkin-Elmer 2400 elemental analyser. The compound is firstly oxidized at 950°C and then passes through a reduction line at 650°C, converting the elements of the sample into simple gases (CO_2, H_2O, N_2). The combustion products are separated by a chromatographic column and detected by thermal conductivity (TCD) which gives an output signal proportional to the concentration of the individual components of the mixture (the standard utilized was acetanilide).

3.2 – RESULTS AND DISCUSSION

3.2.1 – PFLO-G

3.2.1a – PFLO-G: RESULTS

The sample appears as a whitish crystalline powder, emitting in the blue-green region of the spectrum when excited with a 365nm light and only soluble in DMSO.
What is known about the pigment is the presence (as resin components [2], see section 3.3, of 2p-anilinesulfonamide (25-35%) and 4hydroxy-bensonitrile (45-55%).
The obtained information on the composition led to the identification of the fluorophore as 2-2' hydroxyphenyl-4(3H)quinazolinone, also called "HPQ".

Photoluminescence

As can be seen in Fig.3.1, with a 365nm excitation, the emission curve (red line) shows a broad band with two main peaks at 498 and 525nm, while the excitation curve (blue line) for the emission at 525nm covers the spectra from 260 to 385nm with a maximum at 365nm, decreasing until approximately 450nm. The fluorescence intensity is shown to be higher for dispersions in water than in other solvents.

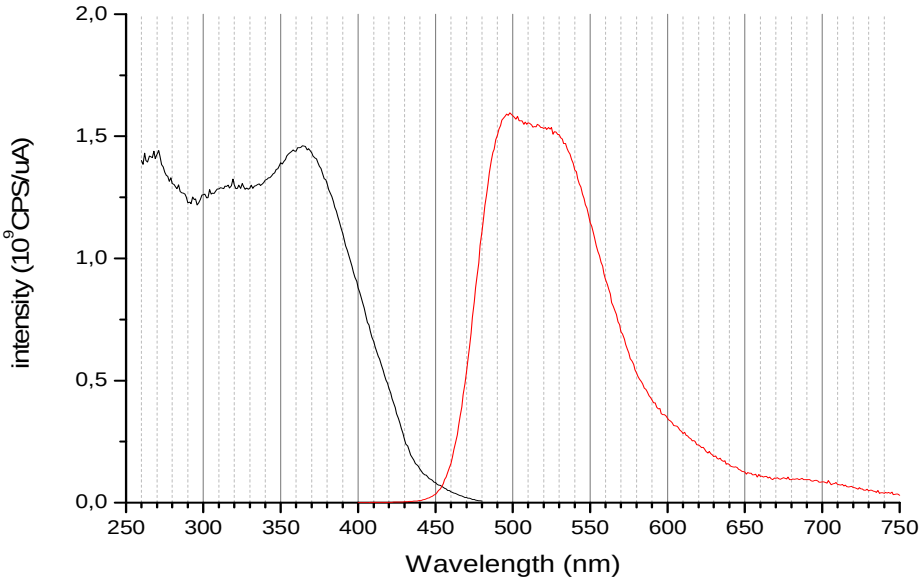

Figure 3.1 – PL/PLE spectra for PFLO-G powder

X-ray diffraction

Due to the lack of a comprehensive database no match has been found for the diffraction pattern.

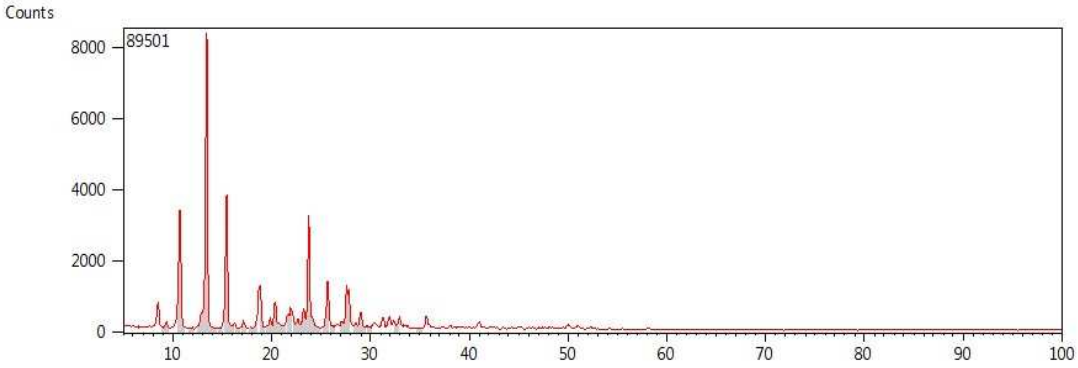

Figure 3.2 – XRD pattern

EDS elemental analysis

EDS analysis reveal the presence of Carbon, Oxygen, Nitrogen and trace of Sodium that may be considered to be reagent residues.

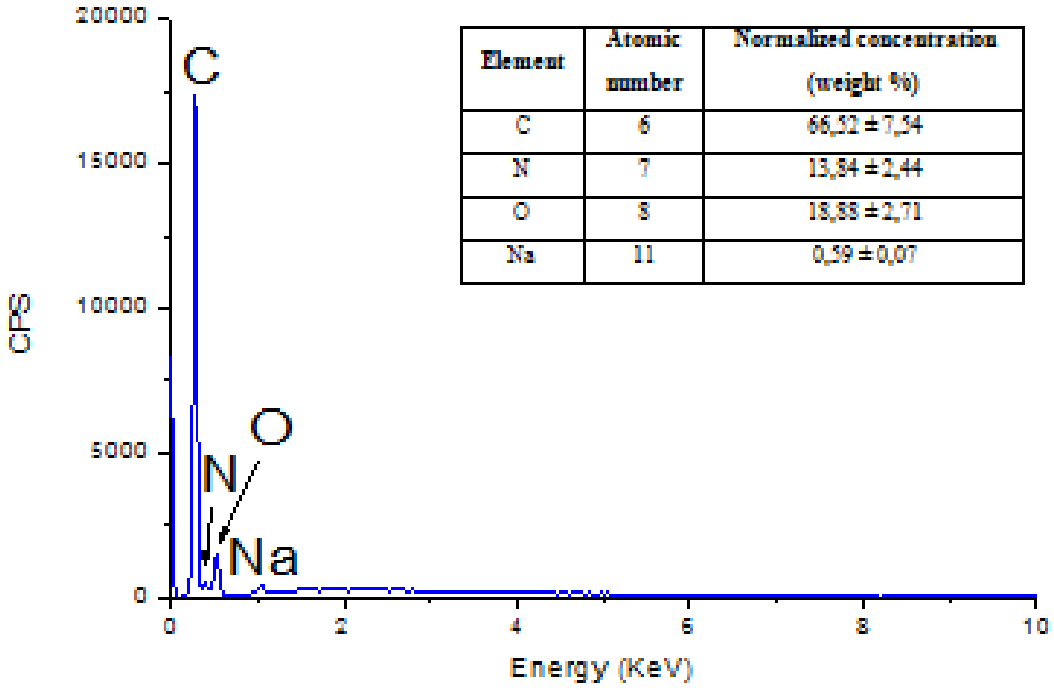

Element	Atomic number	Normalized concentration (weight %)
C	6	66,52 ± 7,54
N	7	13,84 ± 2,44
O	8	18,88 ± 2,71
Na	11	0,59 ± 0,07

Figure3.3 EDS spectra and quantitative results

CHN elemental analysis

For a three times repeated measurement, with a 0,1% of maximum error, the obtained percentages of elements were: 69,43%w Carbon, 4,04%w Hydrogen, 11,07%w Nitrogen and 15,46%w of other atoms. These information had obviously to be united with the mass spectrometry results to restrain the field of research. The obtained elemental relative percentage is in accord with the EDS results; assuming the molecule to have a mass below 500 m/z, it corresponds to the presence of maximum three Nitrogen atoms and three Oxygen atoms.

Mass spectrometry

The GC-MS spectrometry of the sample dissolved in benzene gives retention times of 12.50, 13.61 and 14.38 minutes respectively with an individuated molecular mass of 239.2, 207.3 and 294,2 (Fig. 3.4). The difficult interpretation of a spectra obtained with chromatographic separation (chemical “hard” ionization) of complex molecules led us to the employment of a “softer” ionization method, as electrospray ionization. This way it is possible to most certainly reveal the molecular ion. In this case (using as internal standards 7-hydroxy-metil-cumarine and triptophane-dansil-glicine) the exact mass for the protonated molecule is shown to be 239.0813 with a 10ppm maximum error (Fig.3.5), thus the molecule has a ~238 m/z.

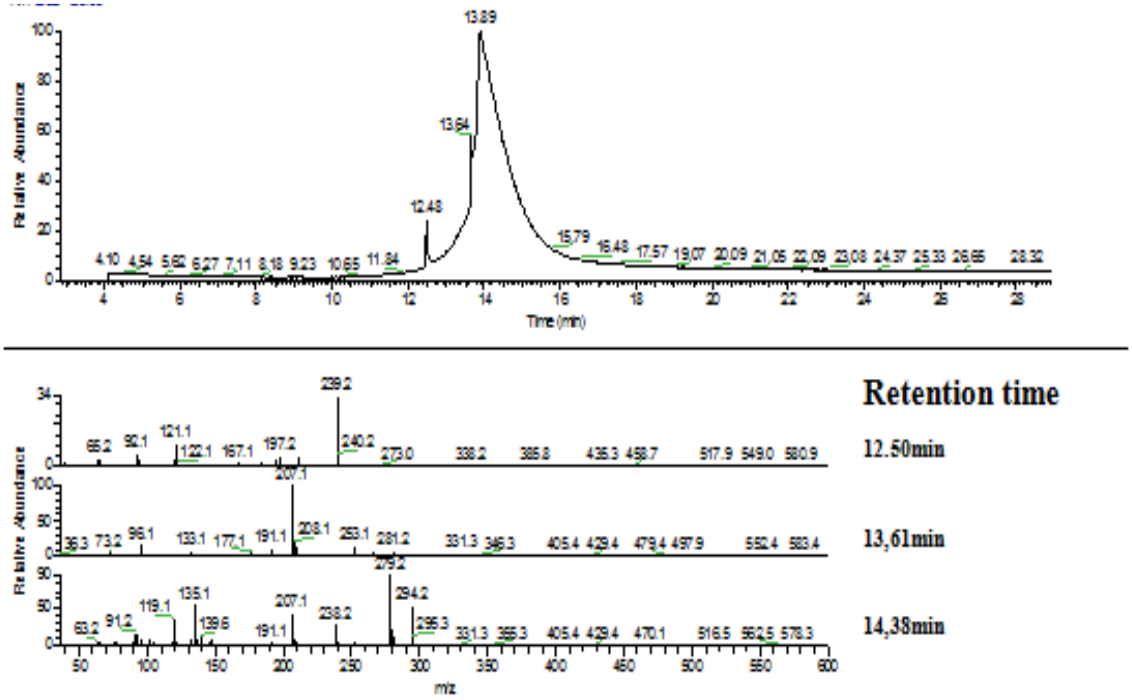

Figure 3.4 – GC-MS Chromatogram and mass specra for the different retention time of the sample dissolved in benzene

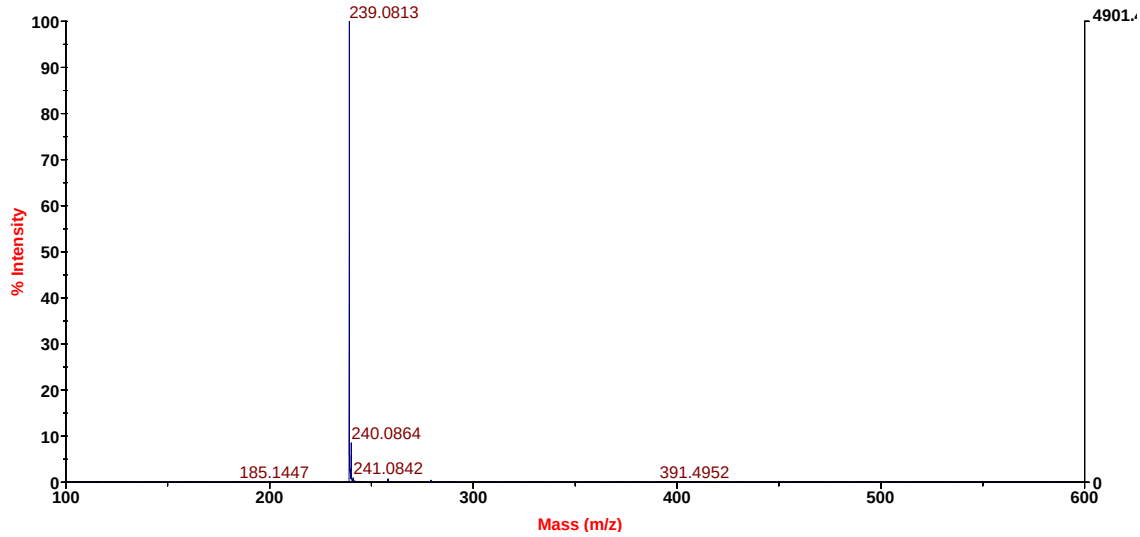

Figure 3.5 – ESI-MS mass spectra

The molecular formula search for the presence of C, H, N and O atoms performed with the mass spectrometer software for the exact mass 239.0813 gives only one output: $C_{14}H_{11}N_2O_2$. The molecular formula of the compound being $C_{14}H_{10}N_2O_2$ is completely in accord with the elemental analyses results.

Nuclear magnetic resonance

NMR spectroscopy on the sample solubilized in DMSO show the presence of 8 aromatic protons (6,8-8,8 ppm) from 6-membered rings, a double peaked broad band due to two acidic OH or/and NH (13,2ppm) and aromatic impurities (8 e 8,5ppm). No chemical shifts due to other types of protons seems to be present, excluding as such any CH_3, CH_2 or non-aromatic CH.

Figure 3.6 - ^{1}H NMR spectra showing the chemical shifts (ppm) for the powder solubilized in DMSO

Infrared and Raman spectroscopy

In FT-IR and Raman spectroscopy, peaks cover the spectra from 487 until 1674cm^{-1} (1683cm^{-1} in the Raman spectra, Fig 3.8) showing seven principal intense absorption: four at 1513(not Raman active), 1562, 1607, 1674 cm^{-1} and two at 761(not Raman active) and 828cm^{-1}; two strong peaks at 1329 and 1343 are also present in the Raman spectra. As for the latter, the intensity of peaks with Raman shifts below 487 cm^{-1} may be altered by the inner fluorescence of the sample. From the IR spectra absorption (Fig.3.7) it is possible to exclude the presence of triple bonds tertiary amines, esters and nitrogen dioxide. It is instead possible the presence of phenols, Ketones, amides and carboxylic acids.

Once identified the phosphor as HPQ, thanks to the combination of information from the various analyses performed, a more specific interpretation of the absorption bands has been possible (Table 3.1).

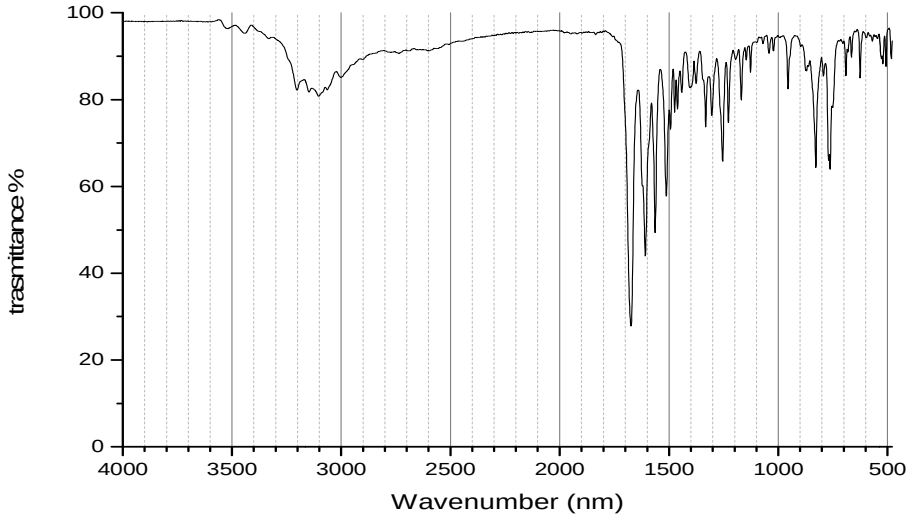

Figure 3.7 –Trasmittance infrared spectra (FTIR) of the pigment dispersed in KBr pellet

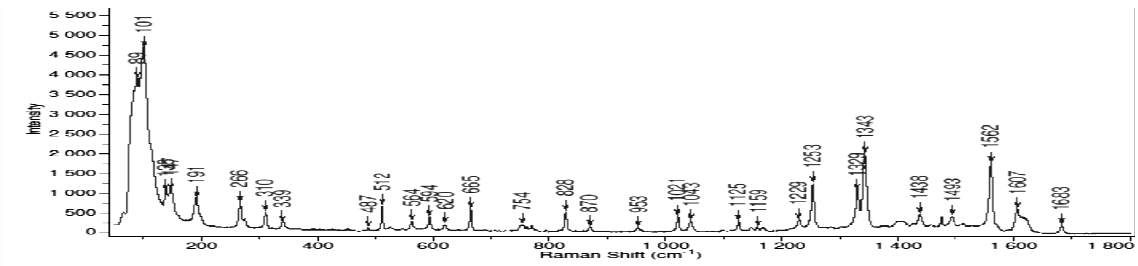

Figure 3.8 – Raman spectra with 785nm LED excitation

PFLO-G					
Peak(cm^{-1})	**Assignation**	**Peak(cm^{-1})**	**Assignation**	**Peak(cm^{-1})**	**Assignation**
704-897and 3331-3444 regions	primary amine N-H δ	1069-1254and 1376-1397 regions	Quinazoline C-H υ	1304, 1318	C-O υ or O-H δ
625-690 region	Amidic δ	828, 3148, 3204	Ring's C-H δ	3449-3520	O-H υ
1674	C=O υ	1608	C=C υ		

Table 3.1 – Combined IR-Raman spectra interpretation (for HPQ molecule) [3]

Lifetimes measurement

If a population of fluorophores is excited, the lifetime is the time it takes for the number of excited molecules to decay to 1/e or 36.8% of the original population according to:

$\frac{n^*(t)}{n^*(0)} = e^{-t/\tau}$ being the decay statistically exponential.

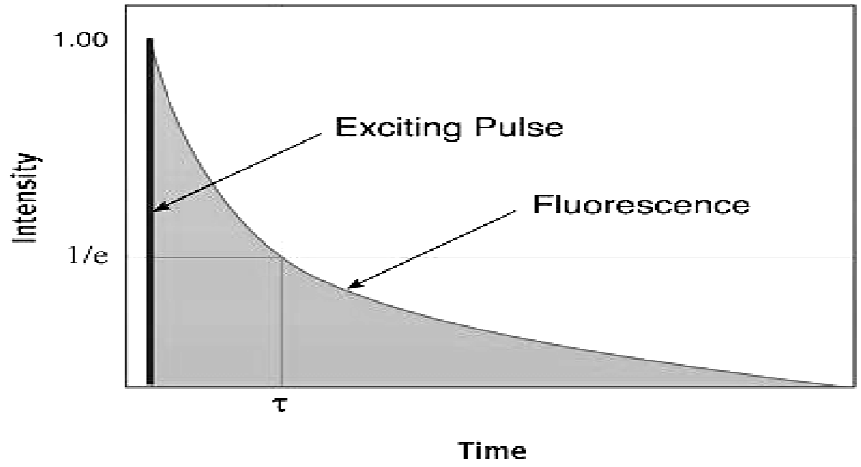

Figure 3.9 – Lifetime plot

The decay of the intensity as a function of time is given by:

$$I_{(t)} = \alpha \ e^{-\frac{t}{\tau}}$$

Where I is the intensity at time t, α is a normalization term (the pre-exponential factor) and τ is the lifetime.

The lifetime observed for PFLO-G was 6.29 nanoseconds, compatible with an organic molecule lifetime. Giving the nature of the molecule, TCSPC (time correlated single

photon counting) method was employed, which can measure events happening in the 1-100ns range with high repetition frequency (1-10MHz), using a NanoLED 373nm excitation. This method involves the following steps: firstly the time difference between the photon event and the corresponding excitation pulse (1,3ns) is measured converting the optical events into electronic pulses, then the digital timing result is used to address the histogram memory, so that each possible timing value corresponds to one memory cell; finally the addressed histogram cell is incremented until sufficient counts have been collected.

The lifetime is a measure of the probability of the excited state de-excitation, thus in the case of organic samples this probability will be the same within all the emission range independently from the excitation energy, since the electronic states do not correspond to discrete values but rather to continuous bands. Therefore the excitation wavelength chosen was 525nm and not the one corresponding to the maximum fluorescence intensity (498nm). In the next chapters this lifetime has been compared to the lifetime of the sample embedded in a matrix before and after UV-aging, since the decay kinetics can be influenced by chemical environment (see Fig.5.8).

3.2.1b – PFLO-G: DISCUSSION

The molecular formula $C_{14}H_{10}N_2O_2$ obtained by mass spectroscopy, the presence of one NH and one OH bond and the absence of other non-aromatic protons revealed by NMR[4] and of triple bonds revealed by IR spectroscopy, led to the identification of the compound as 2-(2'-hydroxyphenyl)-4(3H)-quinazolinone (HPQ).

HPQ is applied in the preparation of fluorescent compositions of inks and enamels, as well as fluorescent precipitating substrates for various enzymes [5]. After selectively binding with some metal ions, ESIPT reactions of HPQ might be blocked and its fluorescence quenched [6]: HPQ is used as selective ion sensor with tuneable solid state fluorescence in the selective detection of Zn^{2+} and Cd^{2+} ions, which cause a blue shifting of the emission curve; also an optode based on HPQ as a fluoroionophore shows fluorescent response toward Fe^{3+} with a wide linear concentration range, high selectivity and fast response time [5]. It is also employed in the design of watersoluble non-fluorescent probe for the assay and imaging of particular peptidases without diffusion-related signal dilution[7] and its derivatives are used for the in situ detection of

phosphatases activity for applications of sensitive fluorescence histochemistry and cytochemistry [8].

Fluorescence mechanism

HPQ is an organic fluorescent material that exhibits fluorescence by the excited-state intramolecular proton transfer (ESIPT) mechanism as shown in Fig. 3.26. Fluorescent dyes that exhibit ESIPT reactions have attracted great interest for several decades because such compounds show good photophysical properties such as intense luminescence, large Stokes shifts and significant photostability [9]. Many molecules with an intramolecular hydrogen bond possess two tautomeric forms, one of which is stable in the ground state, whereas the other is more stable in the first excited singlet state. When the interconversion of both forms merely involves movement of a proton along the hydrogen bond, proton transfer can be a very rapid process. After electronic excitation of the normal form (S_0) to the first excited state (S_1) the excited state (S_1') of the tautomer is rapidly formed. Fluorescence S_1'—> S_0' from the tautomer displays a large Stokes shift relatively to the absorption S_0 —> S_1 of the normal form; this fact leads to the first observation of this effect, later called excited state intramolecular proton transfer (ESIPT), by Weller in 1956.

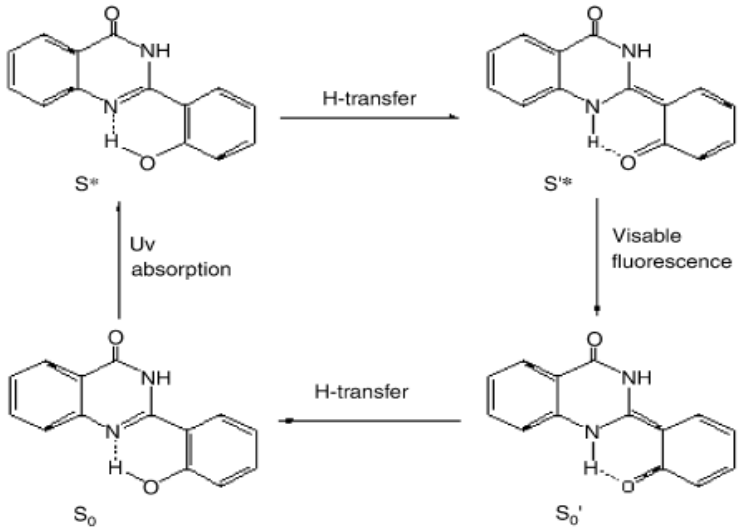

Figure 3.26 – Basic mechanism for ESIPT reaction of HPQ

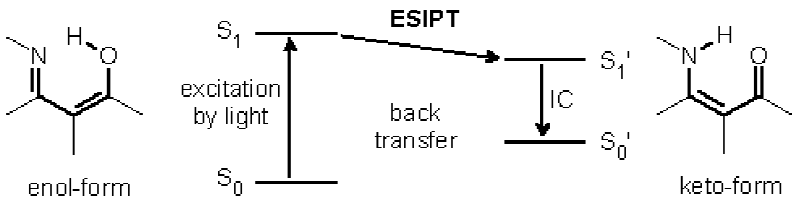

Figure 3.26b – ESIPT mechanism

Fluorescence influencing factors

The conformational twist between the phenyl and quinazolinone rings of HPQ leads to different molecular packing in the solid state, giving structures that show solid state fluorescence around 500 and 515nm[10]. The fluorescence and precipitation of HPQ depend on the concentration of its neutral phenolic form and therefore are pH related (the protonation of the acid-labile site, i.e. the quinoline nitrogen atom, blocks the ESIPT reaction) [8], thus the fluorescent emission in time is not only tied to the photo-oxidation but also to a possible acidification of the matrix. The limited alkalinity of HPQ, resulting from intramolecular H-bonding, kinetically limits the process of protonation in acidic-deficient conditions and offers readout stability via photochemically gated protonation by the light. Moreover, ESIPT becomes much more efficient in film than in solution because the torsional motion is virtually frozen far below the glass transition temperature, so that the H-bonded conformer is preferred energetically[11].The peak positions are also solvent related: for example, HPQ forms two different polymorphs in THF (tetrahydrofuran) giving specific emission wavelengths[5]. As the molecular packing in the solid state assumes a great importance, also does the solid-particle size and prcessing.

In summary, when formulating a coating comprising HPQ fluorophore, the pigment processing (e.g. particle size) and the matrix polarity, pH and viscosity have to be considered.

3.2.2 – PFLO-R

3.2.2a – PFLO-R: RESULTS

The sample appears as a yellowish white crystalline powder fluorescent under long UV excitation (365nm) emitting in the red region of the spectrum. The powder is well soluble in ethyl acetate and partially soluble in ethanol, in water it gives precipitate.
What is known about the pigment is the presence (as resin components) of m-toluic acid (30-60%) and 1,10-phenantroline (30-40%). It is also notified the presence of Eu_2O_3 and a heavy metal content minor to 10mg/Kg is specified.
The obtained information on the composition led to the identification of the fluorophore as the organo-metallic chelate $Eu^{3+}(TTA)_3(TPPO)_2$.

Photoluminescence

The emission curve for a 365nm excitation shows two sharp bands with two main peaks at 616nm and 698nm. The excitation curve, for the 616nm emission, covers the spectra from 260nm to 390nm with a maximum at 365nm, decreasing until approximately 470nm; a sharp peak of low intensity is also present at 465nm. The fluorescence intensity is shown to be higher for water dispersions than for solutions. When in a matrix, the PL peaks are splitted and change slightly.

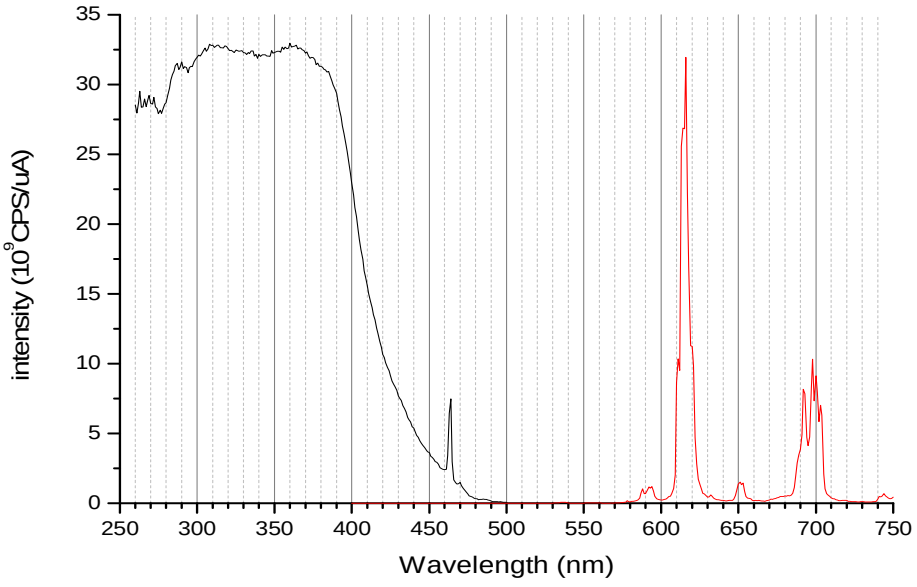

Figure 3.10 – PL/PLE spectra for PFLO-R

X-ray diffraction

Due to the lack of a comprehensive database no match has been found for the diffraction pattern.

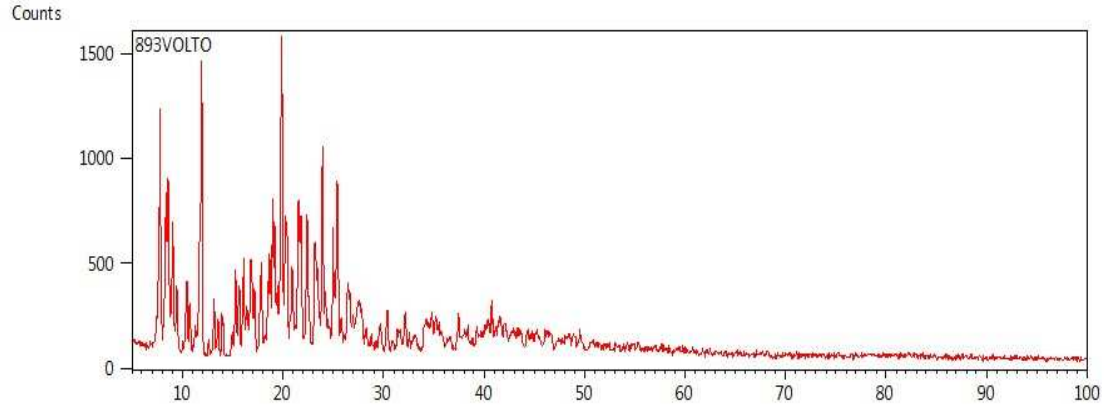

Figure 3.11 – XRD pattern

EDS elemental analysis

EDS analysis revealed the presence of Carbon, Phosphorus, Sulphur, Fluorine, Oxygen and Europium. Traces Chlorine may be considered to be reagent residues.

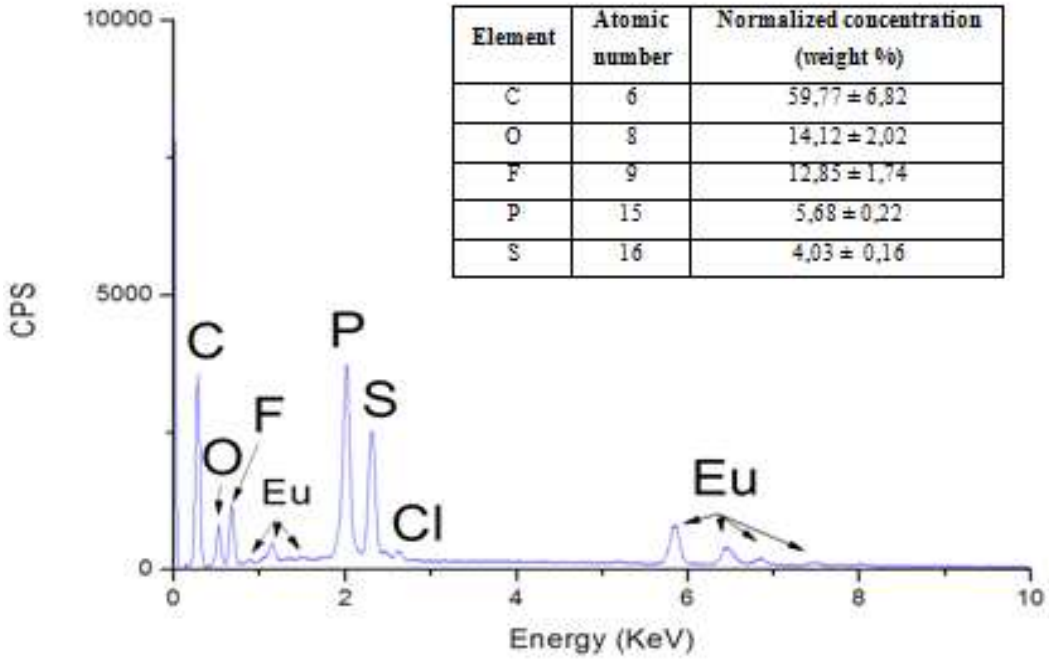

Element	Atomic number	Normalized concentration (weight %)
C	6	59,77 ± 6,82
O	8	14,12 ± 2,02
F	9	12,85 ± 1,74
P	15	5,68 ± 0,22
S	16	4,03 ± 0,16

Figure 3.12 – EDS spectra and quantitative results for PFLO-R

The simultaneous presence of these atoms and their approximate proportion, narrows the field of research to a few organo-metallic Europium coordination complexes which give red fluorescence, all of them with as first ligand 2-thenoyltrifluoroacetonate (TTA):

$Eu(TTA)_3(TPPO)_2$ with ligand triphenylphosphine oxide (a),

$Eu(TTA)_3(NaPO)$ with ligand 1,8-bis(diphenylphosphino)naphthalene oxide (b),

$Eu(TTA)_3(DPEPO)$ with bis(2-diphenylphosphino phenyl)ether oxide (c).

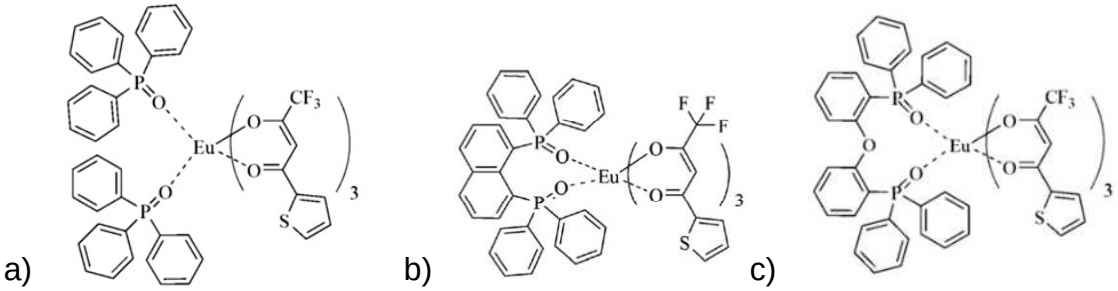

Figure 3.13 – Proposed $Eu(TTA)_3$ phosphinoxide ligands [5]

In this context the main PL peaks in the emission spectra of our powder corresponds to the five transitions $^5D_0$ -> ^7F_J (J=0-4) energy states of Europium.

To identify the compound, several spectroscopy methods were used for characterizing the functional groups present in the compound, comparing the results with reference spectra of the proposed Eu ligands.

Nuclear magnetic resonance

From NMR spectra (Fig. 3.14) it is possible to recognize several phenyl (8,8ppm and 7,4-7,7 ppm) and thiophene protons (6-6,7 ppm) and the peak at 3,2 is attributable to the hydrogen in the C=O-CH-C=O bond of TTA ligand. No match exists for $Eu(TTA)_3(NaPO)$ and $Eu(TTA)_3(DPEPO)$ ^{1}H-NMR spectral data [12,9], therefore it was possible to discard both ligands.

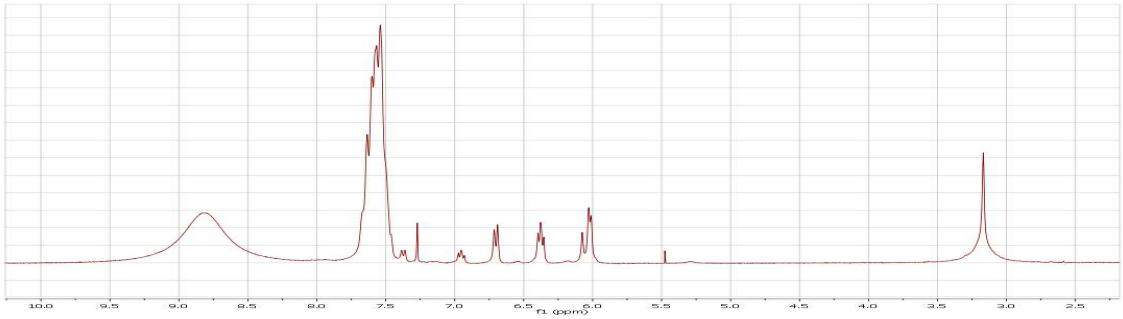

Figure 3.14 – ^{1}H NMR of the powder dissolved in $CDCl_3$

Infrared and Raman spectroscopy

From the FTIR spectra we can see that the finger print region (1300-1900cm^{-1}) is characteristic of a monosubstituted aromatic ring and together with the peaks at 2991, 3037, 3057, 3075 cm^{-1} is typical of the absorption of C-H stretching and from TPPO and DPEPO ligand. Other typical bands from the tri-phenil-phosphine-oxide are those of the groups C-H at 506, 540, 618, 766, 847, 859, 932, 996 cm^{-1}, C-C at 1438 cm^{-1}, P=O at 1028, 1072 and 1183 cm^{-1} and P-Phenyl at 696, 722, 749,1095 and 1122 cm^{-1}. Other absorption bands, and in particular the shape of the absorption in the regions 1028-1355cm^{-1} and 1434-1569cm^{-1}, could be ascribed to the ligand thenoyl-trifluoro-acetone (TTA) : thiophenic C=C at 467, 1231,1353, 1416,1522 cm^{-1} and C-H at 683 cm^{-1}, ethanol form of the betadiketonate at 1592cm^{-1}, and C-F_3 stretching at 506, 605, 683, 1161, 1189, 1231, 1248, 1294cm^{-1}.

Once identified the phosphor, thanks to the combination of information from the various analyses performed, a more specific interpretation of the absorption bands was possible (Table 3.2, Figure 3.16b).

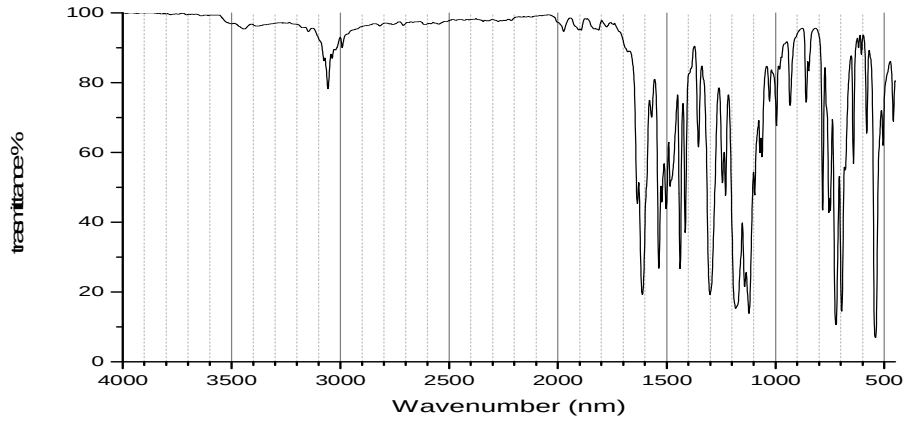

Figure 3.15 – Trasmission infrered spectra (FTIR) of the pigment dispersed in KBr pellet

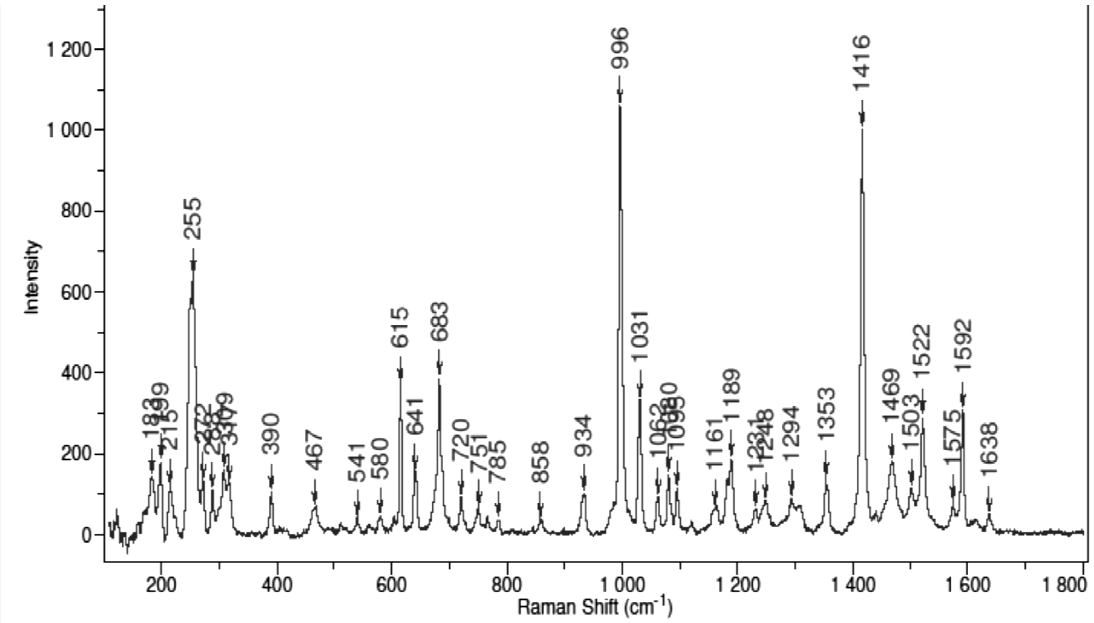

Figure 3.16 – Raman spectra with 785nm LED excitation

PFLO-R					
Peak(cm^{-1})	**Assignation**	**Peak(cm^{-1})**	**Assignation**	**Peak(cm^{-1})**	**Assignation**
473	Eu-O	1142-1415 region	TTA typical assorbption	1503-1378 region	TTA typical assorbption
2991,3037, 3057,3075	TPPO C-H ring δ	642,932 1301,1355	C-F υ	1522-1612	C=C b-diketonate υ
1438,1484	P=O	1415	C=S υ	1569,1635	C=O υ
506, 541, 618, 695, 749, 766, 847, 859, 996, 1028, 1072,1095, 1122	other TPPO tipycal assorbption	722,783	Thienyl C-H δ		

Table 3.2 - Combined IR-Raman spectra interpretation (for $Eu(TTA)_3(TPPO)_2$ molecule) [13]

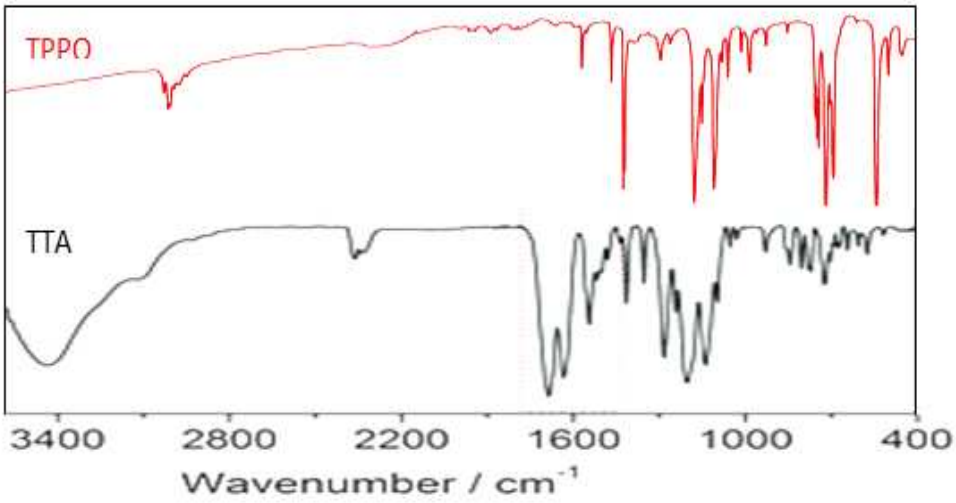

Figure 3.16b – IR spectra of TPPO and TTA lignads for Eu^{3+} [14]

Our compound was unambiguously identified by a simple melting temperature analysis since, as found in literature [14] the molecule with TPPO ligand has significantly lower T_m compared to the one with DPEPO. The complex's T_m with pure TPPO is reported to be 167°C and with DPEPO 253 °C; PFLO-R powder reaches the melting point around 150 degrees, thus the compound has been identified as $Eu(TTA)_3(TPPO)_2$.

Lifetime measurement

The lifetime obtained for this complex in the form of powder is 0,72 ms, in accord with the average lifetimes measured for Eu(TTA)-based complexes [15]. As it will be seen also in Chapter 5, this parameter widely changes when the complex is embedded in a polymeric matrix owing to quenching phenomena. The lifetime was monitored at 616nm, that is the maximum emission peak corresponding to the $^5D_0 -> ^7F_2$ transition, owing the discrete energy levels of the rare earths. The de-excitation probability of the rare earth is much lower than the organic's one, since the transitions are mostly intra-orbitalic and photon-radiationless, thus lifetimes of the excited states are much longer (up to tens of milliseconds). This led to the choice of a continuous source instead of a fast-pulsed one, having a 500ns pulse discrimination minor limit. Taking into account the phosphor nature as lanthanide complex, the method used for the lifetime analysis was the MCS (Multi channel scaling) and the measurement performed with a SpectraLED 377nm excitation.

3.2.2b – PFLO-R: DISCUSSION

The presence of Europium(III) in the sample was already declared by the manufacturer's technical data-sheet and further confirmed by the PL spectra in the form of Eu^{3+}.

Upper levels	Lower levels	λ(nm)
$^5D_1$	$^7F_1$, $^7F_2$, $^7F_3$, $^7F_5$, $^7F_6$	538, 554, 583, 655, 701
$^5D_0$	$^7F_0$, $^7F_1$, $^7F_2$, $^7F_3$, $^7F_4$	580, 596, 614, 651, 694

Table 3.3 -Energy levels and luminescence transitions for europium[16]

The phosphor falls within the organo-metallic complexes category, what still to be characterized is the type of ligand used. The EDS results widely narrowed the field of research, leading to the identification of one of the ligands as thenoyl-trifluoro-acetonate (TTA) owing to the presence and amounts of F and S atoms. The elemental analysis showed also the presence of Phosphorus, therefore the other ligand could be a phosphine oxide. Only three Eu^{3+}(TTA) additional ligands found in literature contain phosphine oxides: DPEPO, NaPO and TPPO, which discrimination is not possible by means of the substance's IR spectra. The NMR pattern, compared with the literature data, already excluded the presence of DPEPO and NaPO. The identification as $Eu^{3+}(TTA)_3(TPPO)_2$ is then confirmed by the melting point determination [17].

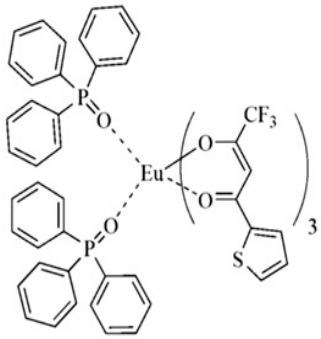

$Eu(TTA)_3(TPPO)_2$

Trivalent lanthanide ions can form, with a variety of organic ligands, stable coordination complexes or chelates exhibiting high stability and strong luminescence. In such complexes, the energy absorbed by the organic chromophore is first transferred to a triplet state of the molecule through the intersystem crossing and is then intra-molecularly transferred to a resonance level of the lanthanide ion which finally emits luminescence [13].

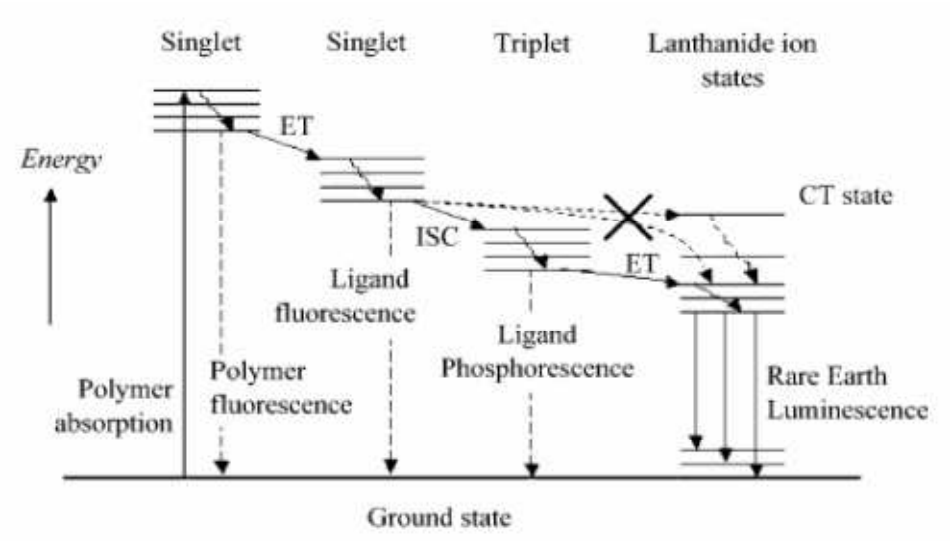

Figure 3.16c – Jablonski energetic diagram for rare earth luminescence in a polymeric matrix.

The so-called antenna effect is based on the sensitization of the lanthanide ions by suitable organic chromophore characterized by high extinction coefficient and intersystem crossing efficiency [14]; among the most studied ligands, β-diketones (as TTA in our sample) has emerged as one of the important antennas. Because the coordination sphere of the rare-earth ion is unsaturated in these six-coordinate complexes, the rare-earth ion can expand its coordination sphere by oligomer formation (with bridging β-diketonates ligands), but also by adduct formation with Lewis bases, such as water, 1,10-phenanthroline, 2,2-bipyridine or tri-n-octylphosphine oxide. In our sample the P=O function operate as a vulnerable anchoring function for lanthanide cations [18], while the TTA chromophoric ligands absorb and transfer energy efficiently to the central metal but also encapsulate and protect the central ion from the solvent molecules[19].The luminescence observed for a specific lanthanide complex is therefore a sensitive function of the energy of the lowest triplet level of the complex relative to a resonance level of the lanthanide ion. Because the position of the triplet level depends on the type of ligand, it is therefore possible to control the luminescence intensity observed for a given lanthanide ion by variation of the ligand[20].

Because of their excellent luminescent properties such as narrow emission bands or long lifetimes [24], lanthanide ions complexes are suitable for a wide range of applications: chemical sensors, probes and labels in a variety of biological and chemical devices, tuneable lasers, amplifiers for optical communications, luminescent probes for analyses, components of the emitting materials in multilayer organic light emitting

diodes or efficient light conversion molecular devices, among others [21]. Specifically, tri-phenyl-phosphine oxide (TPPO) was often used as neutral ligand in Ln^{3+} complexes [13].

The emission bands at 580 and 652 nm are very weak since their corresponding transitions ($^5D_0 \rightarrow ^7F_{0,3}$) are forbidden by the selection rules of forced dipole transitions. The emission band at 593 nm corresponds instead to the $^5D_0 \rightarrow ^7F_1$ magnetic transition; due to the independency of this transition with the ligand field it can be used as an internal standard to account for ligand differences. On the contrary, the $^5D_0 \rightarrow ^7F_2$ transition at 613-614 nm, that is the strongest emission (electric dipole) responsible for the luminescent colour of the complex, is a typical electric dipole transition is called "hypersensitive" : when the interactions of the rare earth complex with local chemical environment are stronger, the complex becomes more non-symmetrical, and the intensity of the electric dipolar transitions becomes more intense[22].

For what concerns the sample composition, the presence of 1,10-phenanthroline could come as pendant ligand in the resin polymer, for the formation of adducts with tris β-diketonate complexes, for the suppression of the complex dissociation in solution[23].

Fluorescence influencing factors

The two main drawbacks of lanthanide ions are: (a) the low absorption coefficients because of the Laporte-forbidden 4f–4f transition which prevent direct excitation of the luminescent of the Ln^{3+} ions and (b) the efficient non-radiative deactivation (e.g. back-transfer) of their excited states by high energy oscillators such as N-H or O-H (also C-H) bonds coming from solvent molecules [24]. For this reason it is rare to observe photoluminescence of complexes in aqueous solution, unless the ligands are able outdistance the Eu^{3+} ion from the molecules of H_2O and show low vibrational quenching. The presence of O-H groups, which extensively reduces the luminescence emission intensity, has therefore to be considered both when selecting the support for the luminescent material and when testing its performances (e.g. avoiding humidity changes).

The matrix could confer chemical and thermal stability as well as mechanical resistance to the complex and improve the photoluminescence properties of the complexes, since the luminescence intensity is very sensitive to the coordination environment of the metal ions[25]. The efficiency of the intermolecular energy transfer is also strongly dependent on the distance between the donor and acceptor because a better energy

transfer could take place from ligand to Eu^{3+} ion. However, the strength of the complex-polymer interaction plays a key role in the energy transfer process efficiency: strong interactions permit a more efficient absorption of light with channeling to the Eu^{3+} ions giving rise to a change in the electronic state, hence in the energy transfer probabilities, i.e. the photo-luminescent properties[26, 27, 28].

3.2.3 – PFLI-G

3.2.3a - PFLI-G: RESULTS

The sample appears as a whitish green powder emitting in the green region of the spectrum when excited with a long UV radiation (365nm). The powder is not soluble in either water, ethanol or ethyl acetate.

After a literature search, the powder was easily unambiguously identified as $BaMgAl_{10}O_{17}:Mn^{2+},Eu^{2+}$.

Photoluminescence

The emission curve for a 365nm excitation (red line) shows a sharp peak at 515nm and a weak broad band centred at 465nm. The excitation curve for a 525nm emission covers the spectra from 260nm to 390nm, showing two relative maxima at 260-270nm and 305-330nm, decreasing until approximately 450nm.

The fluorescence intensity is greatly affected by the presence of a matrix but not by its chemical composition, as it is shown in Chapter 5. Destroying the lattice structure, the application of mechanical stresses on the sample (e.g. pressing the powder with a spatula) causes a progressive blackening and a reduction of the fluorescent emission.

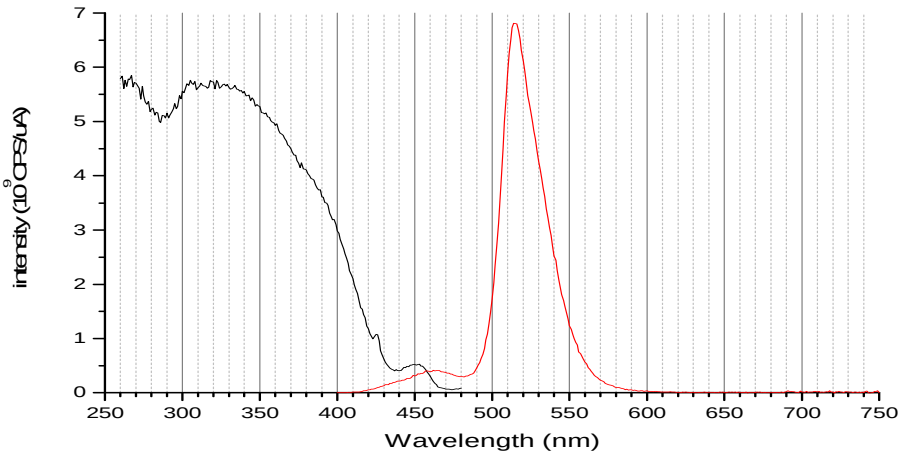

Figure 3.17 – PL/PLE spectra of PFLI-G

X-ray diffraction

The diffraction pattern gives a 84% match for a Barium Magnesium Aluminium Oxide with chemical formula $Ba_{0.956}$ ($Mg_{0.912}Al_{10.088}$) O_{17}

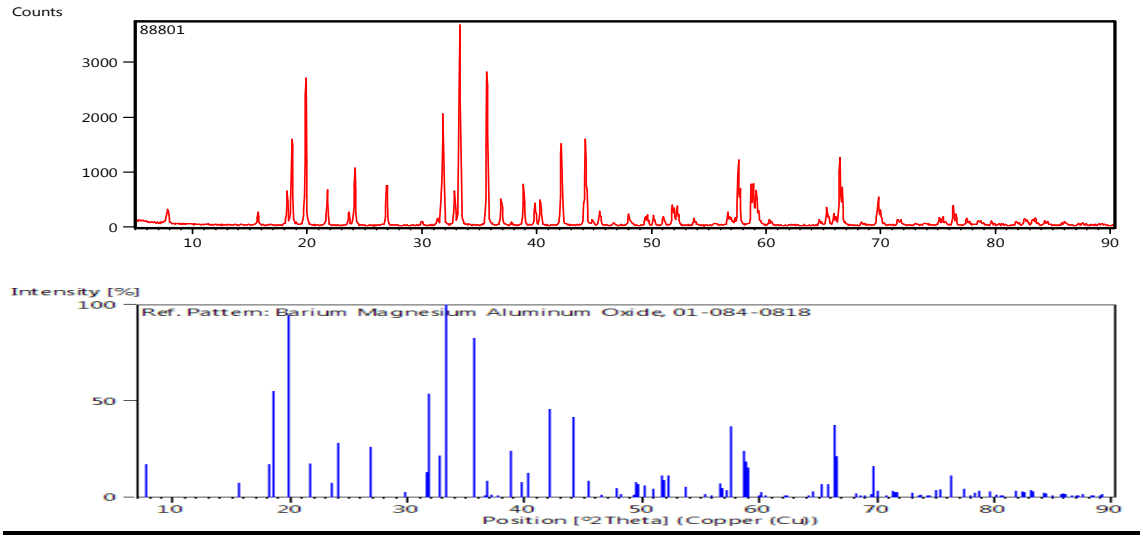

Figure 3.18 – XRD pattern of the sample and reference pattern for $BaMgAl_{10}O_{17}$

EDS elemental analysis

This analysis confirms the XRD data, showing the presence of Aluminum, Oxygen, Barium and Magnesium, but also reveals the presence of Manganese and/or Europium. Mn^{2+} and Eu^{2+} are indeed common dopants conferring luminescence properties to hexagonal aluminates.

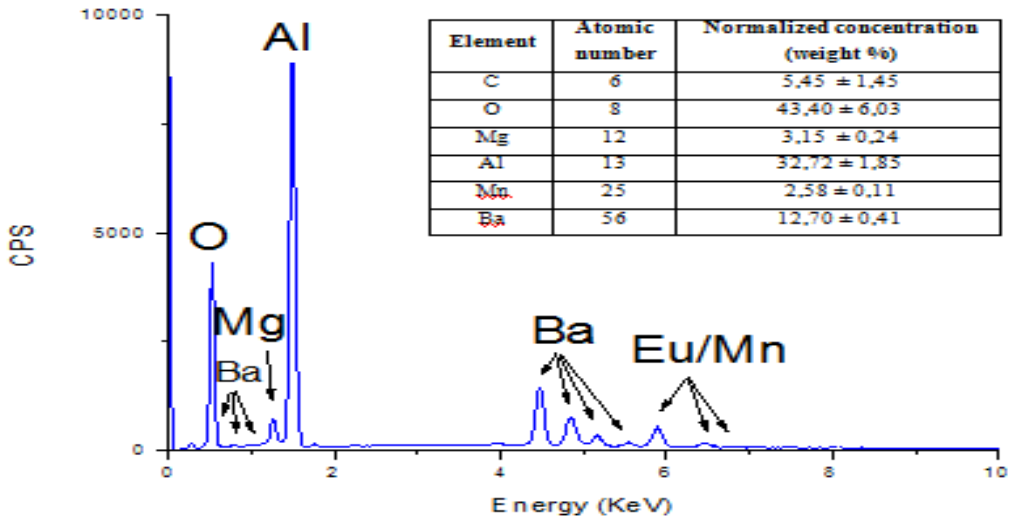

Element	Atomic number	Normalized concentration (weight %)
C	6	5,45 ± 1,45
O	8	43,40 ± 6,03
Mg	12	3,15 ± 0,24
Al	13	32,72 ± 1,85
Mn	25	2,58 ± 0,11
Ba	56	12,70 ± 0,41

Figure 3.19 – EDS spectra and quantitative results

Lifetime measurement

The lifetime measured for this sample is of 5,50ms. A one exponential fitting has been done for the decay curve monitored at 514nm, that is the maximum emission peak given the PL spectrum. As for the rare earth, the de-excitation probability is much lower than that of organic compound, since the transitions are mostly photon-radiationless, thus lifetimes of the excited states are much longer (up to tens of milliseconds). The method used for the lifetime analysis was the MCS (Multi channel scaling) and the measurement performed with a SpectraLED 377nm excitation.

3.2.3b – PFLI-G: DISCUSSION

For what concerns all three inorganic pigments, a fundamental starting point is given by the XRD software matching. The presence of dopants in the crystals, though, could not be spotlighted; here EDS elemental analysis became useful. The presence of one or other fluorescence activators was further confirmed by particular peaks or intensity ratios in the PL/PLE spectra. Photoluminescence spectra for the inorganic phosphors samples are well known since these compounds are widely applied and frequently combined, mostly in fluorescent lamp.

Many phosphors tend to lose efficiency gradually by several mechanisms: the activators can undergo change of valence (usually oxidation), the crystal lattice degrades, atoms

(often the activators) diffuse through the material, the surface undergoes chemical reactions with the environment with consequent loss of efficiency or build-up of a layer absorbing either the exciting or the radiated energy, etc.

In the case of PFLI-G sample, the XRD pattern present a good match with $BaMgAl_{10}O_{17}$ (BAM), while EDS showed the presence of Manganese and/or Europium atoms. The Mn^{2+} doping is evidenced by the sharp peak in the PLE spectra at 427nm, corresponding to its ^4E-$^4A_1$ ions electronic transitions [29] and the shape of the emission curve with the peak at 515nm (Mn^{2+}-doped BAM is employed as green phosphor). The Europium co-doping is than confirmed by PL spectra, having regard the broad band centred at 450nm (Eu^{2+}-doped BAM is currently used as blue phosphor), and the broad and intense PLE curve which corresponds to the 4f-5d transition of Eu^{2+} ions [30]. Therefore the powder has been unambiguously identified as $BaMgAl_{10}O_{17}:Mn^{2+},Eu^{2+}$. The spectral overlap between the emission of Eu^{2+} and excitation of Mn^{2+} suggests that an energy transfer from the two ion types occurs.
The long lifetime of 5,50ms is in accord with literature data. The long decay time of Mn^{2+} emission is caused by the parity forbidden $^4T_1 \rightarrow {}^6A_1$ transition, while Eu^{2+} doped BAM has a transition time on the order of microseconds due to the allowed $4f^65d^1$- $4f^7$ transition of Eu ions. Therefore as the Eu^{2+} concentration is increased, the decay time is gradually decreased, owing the fact that the transfer exist between unlike luminescent centres[30].

Fluorescence influencing factors

The stability of BAM:Eu is not good: this phosphor undergoes degradation of colour quality and luminescent efficiency both during the baking process while manufacturing (thermal damage, caused by the oxidation and migration of the Eu^{2+} ions) and the aging process (i.e. UV irradiation damage). BAM crystallizes in spinel blocks spaced by the so-called conduction layers (created by the mobility of the Ba^{2+} ions): when Europium ions are doped in BAM, they replace Barium, causing instability in those sites and easily undergoing oxidation (mostly photo-oxidation and without migration). In contrast to Eu^{2+}, Mn^{2+} substitutes for Mg^{2+} and is incorporated into the spinel blocks instead of the conduction layers, occupying only one site. Therefore Mn ions are much more stable and much more difficult to be damaged than Eu ions, remaining unchanged during UV irradiation. The emission of Mn as an acceptor in BAM:Eu^{2+},Mn^{2+} is strongly

dependent on Eu as donor. Therefore, despite the stability of Mn^{2+}, the emission intensity will be inevitably reduced if the Eu^{2+} ions are damaged during UV irradiation [31]. The Eu oxidation mechanisms have therefore to be considered not only when testing the properties of BAM:Eu^{2+},Mn^{2+} before and after ageing, but also during the grinding process.

3.2.4 – PF-R7

3.2.4a - PF-R7: RESULTS

The sample appears as a whitish powder, red glowing when excited in the long-UV (365nm). The powder is not soluble in water (in which it gives precipitate plus suspension), ethanol or ethyl acetate (in which it gives precipitate).
Mainly thanks to the XRD and EDS analyses, the sample has been identified as $Y_2O_2S:Eu^{3+}$.

Photoluminescence

The PL spectra at 365nm (red line) shows three main sharp peaks at 706, 626 and 616nm, attributable to emissions from a rare earth (Europium). The excitation curve, for the 626nm peak, covers the spectra from 260 to 420nm with few sharp peaks in the 395-480nm region.

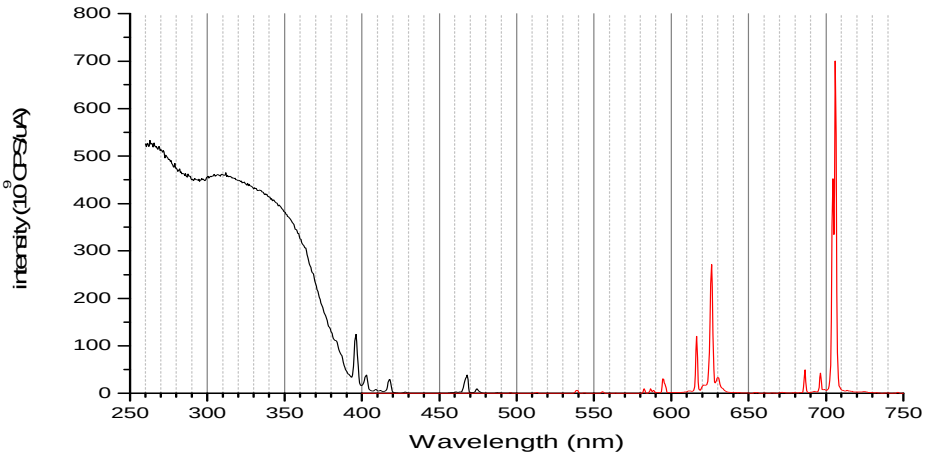

Figure 3.20 – PL/PLE spectra for PF-R7

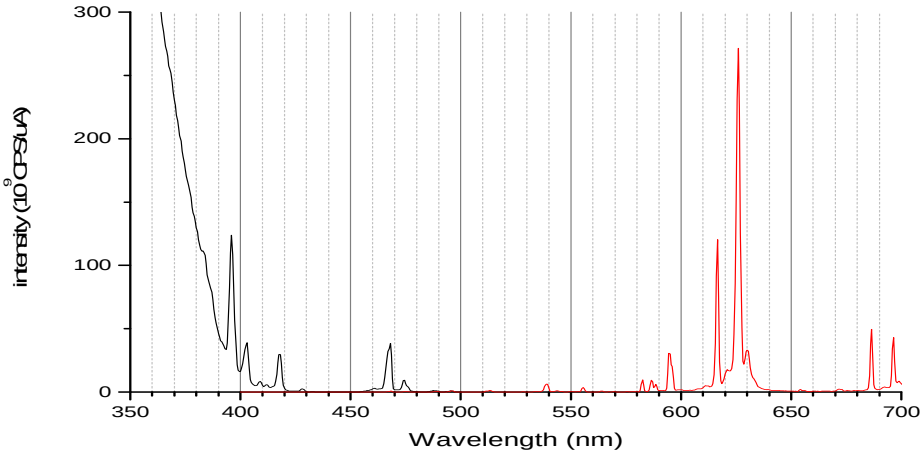

Figure 3.20b – PL/PLE zoom of PF-R7

X-ray diffraction

The diffraction pattern gives a 54% match for Yttrium Oxide Sulfide (with chemical formula:Y_2O_2S). The relatively low match could be attributable to lattice alterations caused by the production process.

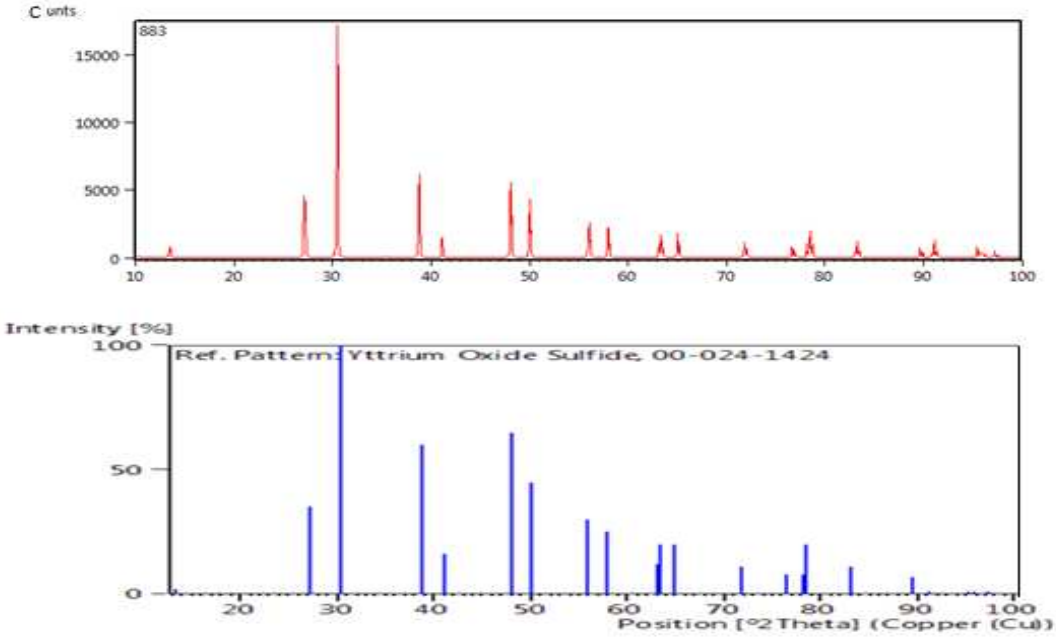

Figure 3.21– XRD pattern of the sample and reference pattern for PF-R7

EDS elemental analysis

The elemental analysis confirms the XRD match, showing the presence of a rare earth (Europium) as dopant.

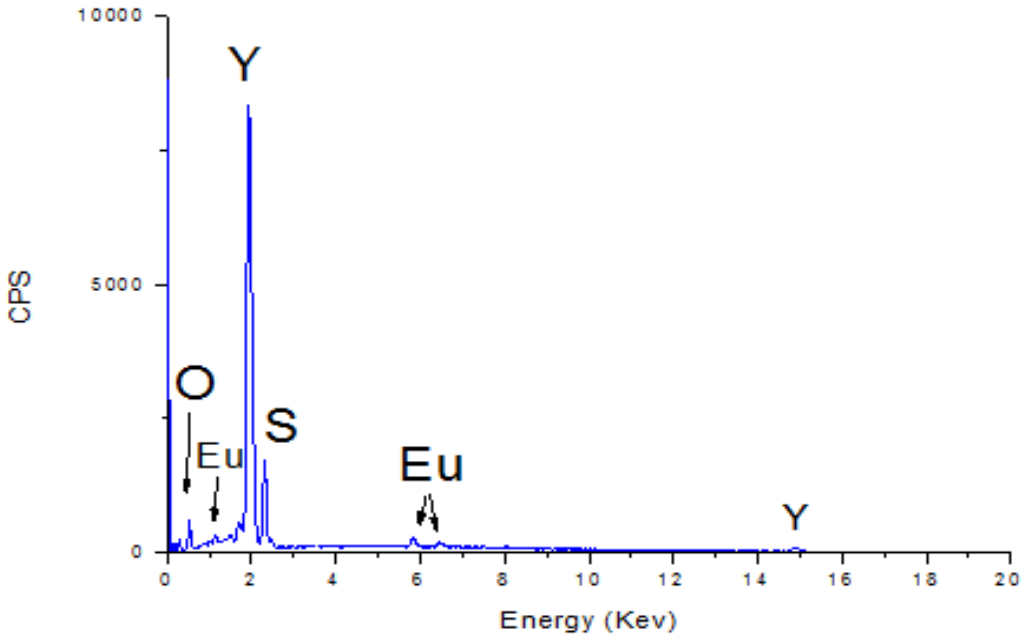

Figure 3.22 – EDS spectra

Lifetime measurement

For this sample, a double exponential fitting had to be employed for the decay curve monitored at 626nm. In this case the decay is described by

$$I = \alpha_1 e^{-\frac{t}{\tau 1}} + \alpha_2 e^{-\frac{t}{\tau 2}}$$

Where τ_1 and τ_2 are the fast and slow components of decay time and α_1 and α_2 are fitting parameters, respectively. The double exponential decay behaviour is often observed when the excitation energy is efficiently transferred from the donor to the activator. The average decay time can be calculated as

$$\tau = \left(\alpha_1\tau_1^2 + \alpha_2\tau_2^2\right)/\left(\alpha_1\tau_1 + \alpha_2\tau_2\right)$$

The revealed lifetime is τ = 0,64ms, much lower than that of PFLI-G. The method used for the lifetime analysis was the MCS (Multi channel scaling) and the measurement performed with a SpectraLED 377nm excitation.

3.2.4b – PF-R7: DISCUSSION

In this case the XRD pattern present a 56% match with yttrium oxysulfide (Y_2O_2S). The low degree of match is explained by the presence, visible in the EDS spectra, of Europium. Eu3+ are clearly doping ions as can be seen by the sharp peaks in the red range noticeable in the PL spectrum. The phosphor has therefore been identified as trivalent-europium-doped yttrium oxysulfide. The PLE spectrum of bulk samples is governed by the charge transfer bands of O-Eu (266nm) and S-Eu (325nm). The systematic behaviour in the energy needs to transfer an electron from the valence band to a trivalent lanthanide, and then the final state in the transition is the ground state of the divalent lanthanide ion. In Y_2O_2S crystal, there are two anions, one is O^{2-} and the other is S^{2-}, therefore there are two charge-transfer transitions: from the 2p orbital of O^{2-} to the 4f orbital of Eu^{3+} and from the 3p orbital of S^{2-} to the 4f orbital of Eu^{3+}, respectively[32]. The lifetime measured for the ^5D_o->$^7F_2$ transition (626nm) is of 0,64ms, in accord with what reported in literature for bulk systems. For nanometric crystals (<15nm) the lifetimes reported are significantly shorter[33] owing to the centroid shift and the crystal-field splitting [34].

$Y_2O_2S:Eu^{3+}$ has been used as a red ‘‘no mill” phosphor for decades [35].Many studies on the synthesis, control of particle morphology, and tuning luminescence properties have been carried out during 1970s, and 1980s. It is usually prepared by high-temperature solid state reaction, however, the fabrication of good $Y_2O_2S:Eu^{3+}$ red phosphors is not an easy task, the synthesis of nanocrystals (NCs) is even more difficult [37].

Fluorescence influencing factors

The europium ion is expected to occupy the yttrium site in $Y_2O_2S:Eu^{3+}$. The electron transition of $Y_2O_2S:Eu^{3+}$ occurs from the ^5D_J (J=0, 1, 2, 3) levels to ^7F_J (J= 0 to 6) levels. Some emission lines are eliminated by the selection rule and some are too weak to be observed. The strongest red-emission lines at 626 and 616 nm are due to transition from $^5D_0$ to $^7F_2$ level, working by electric dipole transition mechanism [34]. This transition is known to be hypersensitive to crystal-structure and chemical surroundings. In the orange-emission lines, the wavelengths of 530 nm, 583nm 587 and 590 nm emission light are produced by the electron transition $^5D_1$-$^7F_2$, $^5D_0$-$^7F_0$, $^5D_1$-$^7F_3$ and $^5D_0$-$^7F_1$ and work by magnetic dipole transition mechanism, insensitive to the crystals structure and chemical surroundings. At wavelengths larger than 626 nm, only two

small peaks should be observed for the electron transition from $^5D_0$ to $^7F_4$ [36]. Unlike what is expexted, a strong emission is reported at 706nm.

As for the case of PFLO-G, the presence of Europium ions in substitution of other ions causes the phosphor to easily undergo degradation of colour quality (e.g. mechanical stresses). Moreover it is well-known that the charge-transfer band is sensitive to the ligand environment (the bonding energy between the central ion and ligand ions), sensitivity that becomes more and more important in the nanometric size (<20nm). The particle size reduction causes a shift in the PLE curve (reduction of the excitation correspondent to the S-Eu CT band), therefore the fluorescent output for the same long-UV excitation (365nm) will be reduced accordingly.

3.2.5 – PFLI-Y

3.2.5a - PFLI-Y: RESULTS

The sample appears as a whitish yellow powder emitting in the yellow-green region of the spectrum when excited in the long-UV (365nm). The powder is not soluble either in water (in which it gives precipitate plus suspension), ethanol or ethyl acetate (in which it gives precipitate).

The powder has been unambiguously identified as a mixture of two inorganic sulfides: $(Zn^{2+}Cd^{2+})S$ and $Y_2O_2S:Eu^{3+}$

Photoluminescence

The emission curve for a 365nm excitation shows three sharp peaks at 616, 626 and 706nm and a broad band centred at 545nm. The excitation curve, for the main emission peak at 706nm, covers the spectra from 260 to 400nm, with a few sharp peaks from 395 to 475nm specular to the sharp emission peaks.

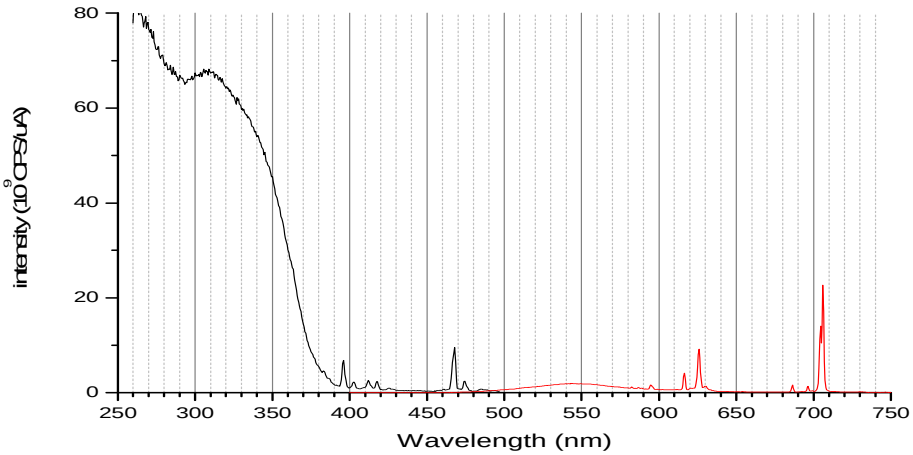

Fig. 3.23 – PL/PLE spectra for PFLI-Y

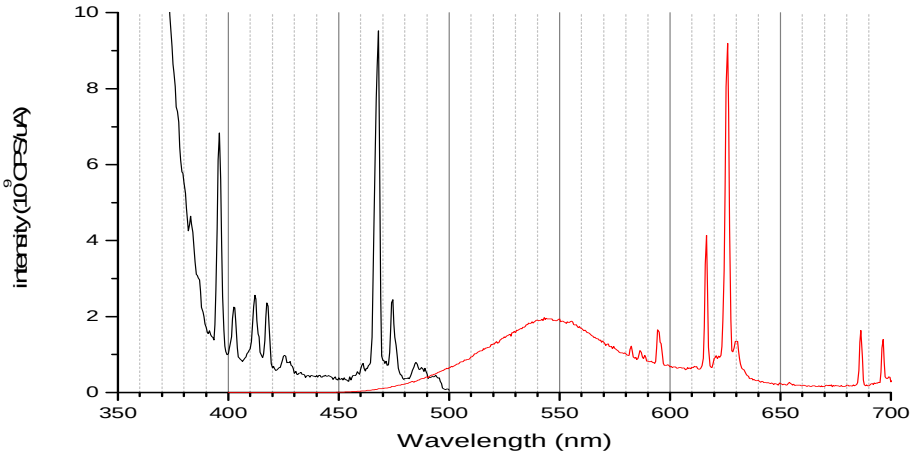

Figure 3.23b – PL/PLE specra - zoom

X-ray diffraction

The diffraction pattern gives match for a mixture of Zinc Cadmium Sulfide, with chemical formula ($Zn_{0.78}Cd_{0.22}$)S (a yellow powder showing green-yellow fluorescence), and Yttrium oxide sulfide with chemical formula Y_2O_2S (a greysh powder showing red fluorescence).

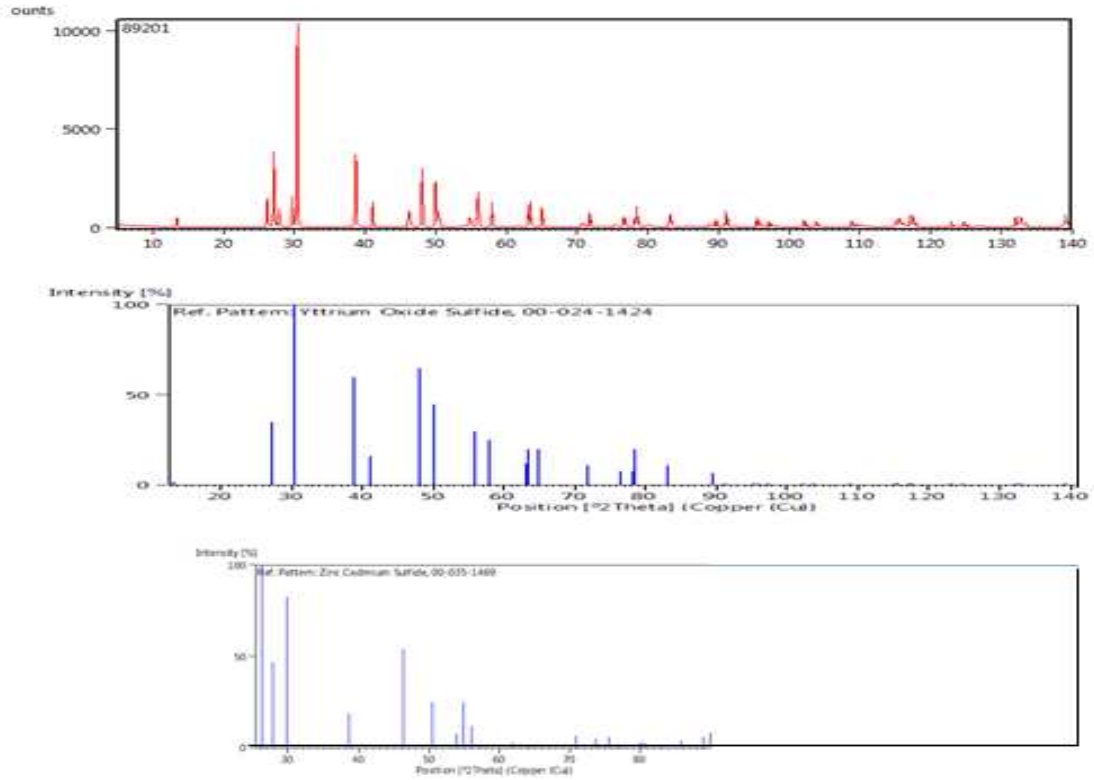

Fig.3.24 – XRD pattern of the sample (red line) and reference pattern for Y_2O_2S (blue lines) and (ZnCd)S (grey lines)

EDS elemental analysis

The elemental analysis confirms the XRD results, showing the presence, as in PF-R7, of Europium dopant other to Cd, Zn, S, Y and O atoms.

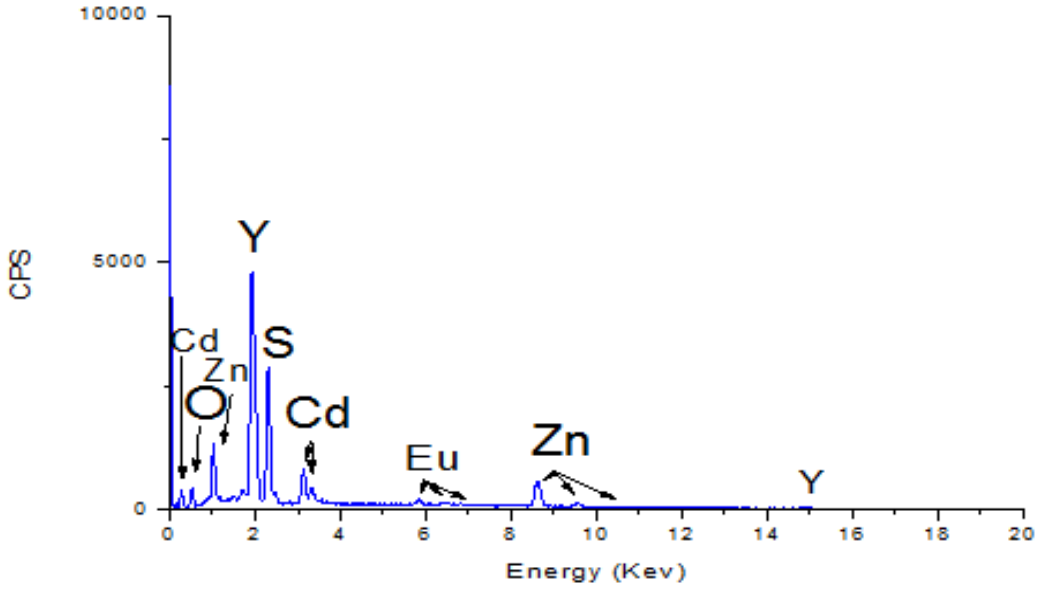

Figure 3.25 – EDS spectra for PFLI-Y

3.2.5b – PFLI-Y: DISCUSSION

Similarly to the peaks of PF-R7, the emission curve for a 365nm excitation shows three sharp peaks, and a broad band centred at 545nm. This combination of sharp and broad bands already led to the interpretation of the powder as a mixture of two different inorganic phosphors. As seen in Chapter 2 (Fig. 2.5), the broad band presented in the PL spectra, centred in the green visible range, happens to disappear owing to UV exposure, leading to a change in the glowing colour from yellow to red, thus the powder is a mixture of two different compounds with different emissions and fluorescence decay. Milling tests, in which the two compounds rapidly separate (see Chapter 4, Fig. 4.10), also suggest the presence of Sulphur, since as the fluorescent crystals are broken Sulphur smelling fumes are released. The diffraction pattern confirms the presence of two inorganic compounds containing Sulphur: $(Zn^{2+}Cd^{2+})S$ and Y_2O_2S. As for the previous sample, the presence of Eu3+ as dopant was confirmed by EDS , thus the second phosphor was identified as $Y_2O_2S:Eu^{3+}$

ZnS-type phosphors have been used since the 50s in television tubes [38, 39].CdS, a mid-band gap semiconductor (2.4 eV), is an important member of the II-VI group of elements, widely used as a phosphor material in LED devices. As ZnS is a phosphor material with a wide band gap energy of 3.7 eV, passivation of the CdS with ZnS can greatly enhance the luminescence properties. $Cd_{1-x}Zn_xS$ is a prominent ternary alloy among II–VI compound semiconductors for the fabrication of multilayer p–n junction's devices without mismatch of lattice parameter and electron affinities [40]. The polycrystalline structure of ZnS phosphors powder is a mixed phase of both cubic and hexagonal and the spectra showed shift of peak position from blue (green) to red as the CdS contents of the phosphors is increased.

Fluorescence influencing factors

While yttrium oxisulfides are relatively resistant to UV degradation, regarding the (ZnCd)S part of the mixture, it degrade by reduction of the metal ions by captured electrons: the M^{2+} ions are reduced to M^{+}; two M^{+} then exchange an electron and become one M^{2+} and one neutral M atom. The reduced metal can be observed as a visible darkening of the phosphor layer [41]. The ease of degradation that characterize $(Zn^{2+},Cd^{2+})S$ phosphors in respect of $Y_2O_2S:Eu^{3+}$ is the cause of the fast colour-change in fluorescence of PFLI-Y observed in Chapter 2.

3.3 CONCLUSIONS

Once selected the commercial additives presenting light-fatness properties (PFLO-G and PFLO-R, PFLI-Y, PFLI-G and PF-R7), pigments analytical characterization has been performed employing various techniques, accordingly to the needs of each one of them for an unambiguous identification. This study is vital in order to avoid interactions with other additives, to identify dedicated coating formulations and to define the pigments chemical and physical behaviour through ages.

Organic samples

Both the organic pigments are identified by the manufacturer as pigmented melamine-formaldehyde copolymers, flushed as a sub-micron dispersion into a high quality printing ink varnish.

The fluorophore in sample PFLO-G (green) has been identified as 2-(2'-hydroxyphenyl)-4(3H)-quinazolinone (HPQ). The pigment processing (e.g. particle size) and the matrix polarity, pH and viscosity have to be considered when working with this kind of phosphor in order to evaluate the fluorescence output.

Sample PFLO-R (red) is instead luminescent thanks to an organo-metallic complex: $Eu^{3+}(TTA)_3(TPPO)_2$. In this case the presence of O-H groups, which extensively reduces the luminescence emission intensity, has to be considered when selecting the support for the luminescent material (e.g. silica) and making sure not to underestimate parameters as humidity when monitoring its performances. Since the luminescence intensity is very sensitive to the coordination environment of the metal ions, the matrix (i.e. the strength of the complex-polymer interaction) could confer chemical and thermal stability as well as mechanical resistance to the complex and improve the photoluminescence properties of the complexes.

Inorganic samples:

Sample PFLI-G has been identified as $BaMgAl_{10}O_{17}:Eu^{2+},Mn^{2+}$. In this kind of Europium doped aluminates, the Eu^{2+} oxidation mechanism has to be considered not only when testing the properties before and after ageing, but also during the grinding process, in order to avoid unwanted degradations.

Sample PF-R7 has been identified as $Y_2O_2S:Eu^{3+}$. As for the case of PFLO-G, the presence of Europium ions in substitution of other ions causes the phosphor to easily undergoing degradation of colour quality (e.g. mechanical stresses). Moreover, especially when reaching the nanometric size, the charge-transfer band is sensitive to the ligand environment. Reducing the particle size will therefore cause a reduction of the fluorescent output for a certain long-UV excitation (365nm).

For what concerns sample PFLI-Y, the powder has been unambiguously identified as a mixture of two inorganic sulphides: $(Zn^{2+}Cd^{2+})S$ and $Y_2O_2S:Eu^{3+}$. Regarding (ZnCd)S, ZnS and CdS phosphors degrade by reduction of the metal ions observed as a visible darkening of the phosphor layer. The ease of degradation that characterize (Zn,Cd)S phosphors in respect of $Y_2O_2S:Eu^{3+}$ causes the modification in fluorescence output previously observed for PFLI-Y. Although this pigment was not embedded and tested in Chapter 5 and 6 as the other four, the grinding process has been applied in order to evaluate the effects of a bland milling on this kind of mixtures.

REFERENCES

[1] *Principles of Instrumental Analysis* VI edition, D. A. Skoog, F J. Holler, S. R. Crouch, Thomson Brooks Cole, 2007

Section 3.2.1

[2] *Melamine formaldehyde:curing studies and rreaction mechanism,* D. J. Merline, S. Vukusik, A. A. Abdala, Polym.Journal., 2012

[3] *The handbook of infrared and raman characteristic frequencies of organic molecules,* D.LinVien, N.B. Colthup, W.G. Fateley, J.G. Grasselli, Academic press, 1991

[4] *A fluorescent chemical sensor for Fe3+ based on blocking of intramolecular proton transfer of a quinazolinone derivative,* X. Zhang, G. Chenga, W. Zhang, G. Shen, R. Yu a, Talanta vol 71, Elsevier , 2007

[5] *Synthesis of quinazolinone analoges using sodium perborate as catalys*t, MKidwai M.Priya, Indian J. Chem. Vol 47B, 2007] a

[6] *Excited-State Proton Transfer: from Constrained Systems to 'Super' Photoacids to Superfast Proton Transfer* . L. M. Tolbert, K. M. Solntsev, Acc. Chem. Res. Vol 35, 2002

[7] *Pholymorph-dependent solid state fluorescence and selective metal-ion-sensor properties of HPQ*, P.A. Savarimuthu, Chem. Asian J. vol7, 2012

[8] *2-2'phosphoryloxyphenyl 4-3H-quinazolinone derivatives as fluorogenic precipitating substances of phosphatases*, Z.Huang E. terpetschnig, W.You, R.P. Haugland, Anal. biochem. Vol 207, 1992

[9] *Ground- and excited-state intramolecular proton transfer in 3,5-dibromosalicylic acid*, G.A. Ibanez, G. Labadie, G.M. Escandar, A.C. Olivieri, J. Mol. Struct. Vol 645, 2003

[10] *.Application of Excited state intramolecular proton transfer (ESIPT) principle to functional polymeric materials*, S. Park, S.Y. Park, S. Kim, J. Seo, Mol. Research vol 16, 2008

[11] *Fluorescent molecular probes-I. The synthesis and biological properties of an ELF[R]glucuronidase substrate that yields fluorescent precipitates at the enzymatic activity site*, Z. Diwu , Y. Lu , R. H. Upson , M. Zhou , D. H. Klaubert , R. P. Haugland, Tetrahedron vol53, 1997

[12] *An automotive spacer allows first-time incorporation of a unique sold-state fluorophore into a detection probe for acyl hydrolases*, X. Zhang, M. Waibel, J. Hasserodt, Chem. Eur. J. vol 16, 2010

Section 3.2.2

[13] *Modulating the photoluminescence of europium-based emitting polymers: Influence of the matrix on the photophysical properties*, J. Garcia-Torres, P. Bosch-Jimenez, E. Torralba-Calleja, M. Kennedy, H. Ahmed, J. Doran, D. Gutierrez-Tauste, L. Bautista, M. Della Pirriera, Journal of Photochem. Photobiol. A: Chemistry Vol 275 , 2014

[14] *Bright electroluminescence from a chelate phosphine oxide EuIII complex with high thermal performance*, H. Xu, K. Yin, L. Wangc, W. Huang, Thin solid films vol 516, 2008

[15] *Application of Chelate Phosphine Oxide Ligand in EuIII Complex with Mezzo Triplet Energy Level, Highly Efficient Photoluminescent, and Electroluminescent Performances*, H. X.u, L.Wang, X. Zhu, K. Yin, G. Zhong, X. Hou, W. Huang, J. Phys. Chem.Vol 110, 2006

[16] *Synthesis of a functionalized europium complex and deposition of luminescent Langmuir–Blodgett (LB) films*, R. D. Adati, F. J. Pavinatto, J. H. S. K. Monteiro, M. R. Davolos, M. Jafelicci, O. N. Oliveira, New J. Chem. Vol 36, 2012

[17] *www.nist.gov* – National institute for standard and technology database

[18] *Comprehensive study of the luminescent properties and lifetimes of Eu3+ and Tb3+ chelated with various ligands in aqueous solutions: influence of the synergic agent, the surfactant and the energy level of the ligand triplet*, N. Arnaud, J. Georges, Spectrochimica Acta Vol 59, 2003

[19] *New europium(III) complexes containing hybrid ligands with hard and soft complexation centres*, L. Prodi, M. Montalti, N. Zaccheroni, G.Pickaert, L. Charbonniere, R. Ziessel, New J. Chem. Vol 27, 2003

[20] *Simultaneous time-resolved fluorescence and thermal lens measurements: Application to energy transfer studies in europium chelates*, J. Georges, J.M. Mermet, Spectrochim Acta vol 49, 1993

[21] *A Comprehensive Strategy to Boost the Quantum Yield of Luminescence of Europium Complexes*, N. B. D. Lima, S. M. C. Gonçalves, A. A. M. Simas, Nature Scientific reports, 2013

[22] *Preparation, photo- and electro-luminescent properties of a novel complex of Tb (III) with a tripod ligand*, T. YU,Y. Zhao, D. Fan, Z. Hong, W. Su, Spectrochimica Acta Part A: Molecular and Biomolecular spectroscopy Vol 69, 2008

[23] *Preparation and fluorescent properties of europium (III) complexes with β-diketone ligand and 2,2-dipyridine or 1,10-phenanthroline*, D. Wang, C. Zheng, L. Fan, J. Zheng, X. Wei, Synthetic Metals Vol 162, 2012

[24] *Handbook on the Physics and Chemistry of Rare Earths* Vol. 35 Chapter 225, K.Biennemans, Elsevier, 2005

[25] *Sintesi di complessi fotoluminescenti dei lantanidi con il legante tris(benzotriazolil)borato*, F. Sartor, Tesi di laurea Università Cà Foscari Venezia, 2012

[26] *Synthesis, Crystal Structure, and Luminescent Properties of 2-(2,2,2-Trifluoroethyl)-1-indone Lanthanide Complexes* , H. Li , P,Yan, P. Chen , G. Hou , G. Li, Inorg. Chem. Vol 51, 2012

[27] *Time-resolved spectroscopic study of Eu(TTA)3(TPPO)2 chelate in situ synthesized in vinyl-triethoxysilane-derived sol–gel-processed glass*, G. Qian, Z. Yang, M.Wang, Journal of Luminescence Vol 96, 2002

[28] *Lanthanide-based emitting materials in light-emitting diodes*, A. De Bettencourt-Dias, Dalton Trans. Vol 22, 2007

Section 3.2.3

[29] *Energy transfer and significant improvement moist stability of BaMgAl10O17:Eu2+,Mn2+ as a phosphor for white light emitting diodes*, W. Ke C.C. Lin R. Liu M. Kuo, J.of Electrochem.Soc. Vol.157, 2010

[30] *Effects of Eu2+ co-doping on VUV photoluminescence properties of BaMgAl10O17:Mn2+ phosphors for plasma display panels*, T. Moon G.H. Hong H. Lee E. Moon B.V. Jeoung S. Hwang J.S. Kim B.G. Ruy, Electrochem and S.S. Letters, 2009

[31] The ultraviolet irradiation degradation of fluorescent lamp used BaMgAl10O17:Eu2+,Mn2+ phosphor, J. Zhang , M. Zhou, B. Liu, Y. Wen, Y. Wang, J.of Luminescence Vol.132, 2012

Section 3.2.4

[32] *The Eu3+ charge transfer energy and the relation with the band gap of compounds*, P. Dorenbos, J.of Luminescence Vol 111, 2005

[33] *Eu3+ doped yttrium oxysulfide nanocrystals – crystallite size and luminescence transition(s),* J. Dhanaraj , M. Geethalakshmi , R. Jagannathan , T.R.N. Kutty, Chem Phys. Letters Vol.387, 2004

[34] *The influence of charge-transfer and rydberg states on the luminescence properties of lanthanides and actinides*, G. Blasse, Struct. Bond. Vol 26, 1976

[35] *Rare earth activated yttrium and gadolinium oxy-chalcogenide phosphors,* M.R. Royce, US Patent 3418246, 1968.

[36] *Spectral properties of Eu3+-activated yttrium oxysulfde red phosphor,* Y. Tsenga, B.Chioub, C. Pengc, L. Ozawac, Thin solid films Vol.330, 1998

[37] *Combustion synthesis and luminescent properties of the Eu3+-doped yttrium oxysulfide nanocrystalline*, Z. Fu, Y. Geng, H. Chen, S. Zhou, H. K. Yang, J. H. Jeong, Optical Materials Vol. 31, 2008

Section 3.2.5

[38] *An Introduction to Luminescence of Solids*, H. W. Leverenz, Wiley, 1950

[39] *Tunability of physical properties of (Cd:Zn)S thin film by Close Space Sublimation Process (CSSP)* M. Zakriaa , A. Mahmooda, A. Shaha, Q. Razaa, Taj,M. khana, E. Ahmedb, Progress in Natural Science: Materials International vol 2, 2012

[40] *Synthesis and Optical and Electrical Properties of CdS/ZnS Core/Shell Nanorods*, A.Datta, S.K. Panda, S. Chaudhuri, J. Phys. Chem. Vol 111, 2007

[41] *Applications of Coordination Complexes: Metal Compounds as Phosphors*, J. S*ilver,* Platinum Metals *Rev.*, 2004

Chapter – 4 –

GRINDING

4.1 - INTRODUCTION

Once selected the additives it is necessary to disperse them into a matrix, avoiding any "clustering" phenomena (flocculation) and preparing the particles for being included into a stable coating formulation in order to test their properties. Decreasing the commercial particle size of the pigments to the nanometric range could allow obtaining a colloidal system, reducing the settling tendency of the pigments. A mechanical grinding process is usually needed in this sense. Alternatively, the needed pigment particles may also be obtained using emulsion or suspension polymerization techniques [1]. The minimum amount of fluorescent pigments in aqueous dispersion is usually 0,5% (0,08-8% dye materials, see section 1.3.3) with about 0.3% to about 6% by weight of dispersant [1]. Depending on the applying technique, pigments having particles with mean size of about 10nm to about 250nm are particularly useful in pen inks while for applications such as screen printing ink, textile printing ink and paper coating, pigment particles having a mean size of 250nm to 1µm are desired.

Another aim of the research was to study the particle size influence on fluorescence output intensity, fluorescence lifetime decay and lightfastness properties of the selected pigments. Numerous luminescence studies underline the importance of the molecules clusters size in relation to their excitation wavelength, i.e. the emission intensities at a certain excitation wavelength [2-9] moreover molecular arrangement in particles or crystals, shape, particle size and distribution, surface character, and interaction of pigments and medium may determine the physical properties (and the chemical structure) of organic pigments. Hence, the dispersion method is important for advanced applications [10]. As the diameter of the particle decreases, its optical behaviour changes. Most of the time, it is not possible to demonstrate a close optical properties' dependence on the particle size. Definite changes in the character of pigments can be made to improve mixing and dispersion in medium and even the optical properties and weathering characteristics of paints may be modified. The wetting characteristics of the materials change in accordance with the chemistry of the surface layer. Low degree of wetting gives a flocculated, high sedimentation volume with rapid settling, while high degree of wetting gives a stable suspension which settles slowly to a small but densely packed sediment. A wetting agent for pigments in aqueous suspensions reduces the

surface tension of water and the interfacial tension at the solid-water interface. A dispersing agent may have little effect on the surface tension of water but acts to overcome the adhesive forces between particles.

Before the optimum particle size can be calculated the refractive index must be known at various wavelengths throughout the visible spectrum, since the optical dispersion of most pigments is so great that the transparent or white pigments, as well as the coloured, must be treated as materials of complex refractive index.[11]

Pigments are found in a distribution of particle sizes which is caused by the production processes [12]:

- Primary particles: particles not destroyable during normal grinding processes;
- Aggregates: primary particles connected together by their surfaces, difficult to destroy;
- Agglomerates: clusters up to several 100μm formed in a pigment powder or in pigment preparations which are not enough stabilized. The dispersion of agglomerates is the main process during the grinding;
- Flocculates: interactions between the particles caused by binders or additives which are adsorbed on the pigments surfaces causing changes in the photoluminescence properties. Permanent de-flocculation is normally achieved with a minimum inter-particle distance of 20nm.

Mechanical dispersion was performed on the two primarily selected pigments (PFLO-G and PFLI-G) and, because of its particular mixture nature, also on PFLI-Y. The particle size distributions were then obtained by laser diffraction (low angle laser light scattering, LALLS), measuring the angular variation in intensity of light scattered as a laser beam passes through a dispersed particulate sample, using the Fraunhofer theory of light scattering.

In both cases the employment of dispersing agents is necessary: the evaluation of grinding effectiveness by means of particle size measurements and the fluorescence emission intensity output led to the choice of the most suitable dispersant for each pigment's category (organic and inorganic). In order to select the optimal size to be used for a coating, a possible correlation between fluorescence intensity output and particle size was investigated. Different types of dispersants can be used in function of

the kind of pigment: ionic (acting electrostatically), non-ionic (acting sterically), or a combination of these two. The principal purposes of a dispersant are:

- Grinding support: short dispersing time, optimum degree of grinding;
- Grind viscosity reduction: high pigment content, fluidity;
- Dispersion stabilization: colour strength, gloss, colour shade stability;
- Flocculation or coagulation prevention;

For this evaluation three different dispersants were tested: two inorganic dedicated and one organic dedicated. The inorganic mixture (PFLI-Y) was tested in combination with both the dispersants in order to evaluate their performances.
Whenever the particle size should be bigger than needed to keep the particles in dispersion, the addition of a thickening agent will be required to oppose the settling. Once chosen the thickener basing on its chemical stability and compatibility with the other compounds of the formulation, the possibility to add it directly in the grinding phase was therefore examined (see Chapter 5).
Once found the most suitable grinding method and particle size for each pigment, as well as the other component needed to obtain a stable dispersion, the influence of the pigment concentration on the fluorescence output and its correlation with formulation dilution and coating thickness has been studied.

Bead milling

The bead-mill technique of grinding [13] afford to destroy agglomerates by means of mechanical forces (shear forces are transferred by the liquid phase of the grinding onto pigments) and physical and chemical interactions (wetting and entering of the liquid components into pores of agglomerates, the adhesion forces between pigment particles are substituted by interaction forces of liquid molecules a tenth power lower than the adhesion forces).
A bead-mill setup (Figure 4.1) is composed by a rotating cylindrical container inside of which there is a milling base (binder, dispersant, additives, solvents) and a grinding medium creating a cascade during the rotation. The grinding medium shape is sometimes spherical, so then the technique is called ball-mill. Physical factors controlling the dispersion effectiveness of a ball-mill are:

- Bead-mill size and speed (rpm)
- Beads load (relative volume), composition (density), size and shape
- Mill-base charge relative volume, viscosity, density and composition (ratio pigment/ binder/solvent).

In particular the bead size and shape influence respectively the shearing contacts and the area needed for dispersing the pigment and the final particle size distribution. The more the pigment remains on the grinding mills, the more its particle size will be reduced, eventually reaching the fluorescent particle break down (e.g. lattice disruption).

Figure 4.1 – Bead-mill scheme

Ultrasonic grinding and mechanical dispersion

Other grinding methods use ultrasounds for breaking apart the agglomerates. This could be done either by ultrasonic bath or sonicator. Though the particle size reached with these methods is usually larger than the one obtained with a bead-mill technique, it still can be sufficient in order for the pigment not to impair the aesthetic properties of a coating.

4.2 - DISPERSING TECHNOLOGY

Dispersing process

The role of the dispersants is to make the dispersion process easier and more stable. In paint production, the dispersion phase is the most time- and energy-consuming stage, due to the different surface tensions of the liquids (e.g., resin, solvents) and the solids (e.g., fillers, additives). Pigments and extenders are supplied to paint factories as agglomerates: the grinding process incorporates these solid materials into a liquid

vehicle or grinding resin obtaining a dispersion of particles, which can be as small as the primary particle size. The process consists of three stages:

- *Wetting*: replacement of air and water covering the pigment by the resin;
- *Grinding:* mechanical break-up and separation into primary particles;
- *Dispersing:* distribution of the particles in the liquid vehicle;

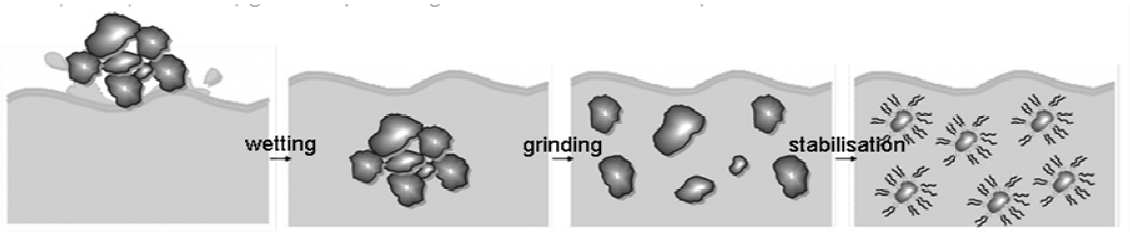

Figure 4.2 – dispersing process stages

Solubilized binder resins as well as polymeric dispersants stabilize the dispersed state of pigments by adsorbing onto the pigment surfaces and causing steric repulsion between pigment particles. It is therefore important to consider the interaction between resin and pigment. Two kinds of particle properties affect wetting, influencing the surface tension properties of pigment and vehicle. One is hydrophobicity or hydrophilicity of the surface, the other is the geometrical structure of the pigment agglomerates, as shown by the Washburn equation (explaining the rate of penetration of a liquid into a powder):

$$V = dh/dt = \frac{r\sigma Cos\theta}{C^2 \cdot 2\eta h} = \frac{r}{C^2} \cdot \frac{W}{2\eta h}$$

Where "h" is the depth (or height) of penetration during the time "t", "σ" the surface tension of the wetting liquid, "η" its viscosity, "θ" the wetting angle, "r" the mean radius of capillaries, "C" the structural coefficient associated with parameters of the porous structure, "W" the energy (heat) of wetting.

Hydrophobic pigments show larger contact angles which lead to longer penetration times and lower wetting rates: under this condition, the geometrical contribution (that is, the mechanism of pigment particle agglomeration, gap width and length between pigment particles) is remarkable [14].

The amount of dispersing agent required depends on the actual surface area of the additive to be dispersed. The smaller the particle size, the higher the actual surface area, hence the larger the area the dispersant has to cover. For a paint mill-base, the addition of 40% more dispersant on pigment content is recommended, once the optimum dose

(corresponding to the minimal viscosity) has been determined, for ensuring a safety margin [15].

The dispersing agents could be classified as “Low-molecular-weight” (1,000 and 2,000 g/mol) and “High-molecular-weight” (5,000 and 30,000 g/mol).

Electrostatic or “Ionic” stabilization – Inorganic pigments

Low molecular weight types can be polymeric dispersants or surfactants, categorized as anionic, cationic, electro-neutral and non-ionic. Their effectiveness is determined by the adsorption of the polar group onto the pigment surface and the behaviour of the non-polar chain in the medium surrounding the particle. Molecules with only one polar group attach themselves to the pigment surface while their non-polar chains extend into the resin. If the molecules have more than one polar group, they arrange themselves in such a way that the free polar groups form hydrogen bonds and build a physical structure with the pigments. The polar groups containing charged ions such as metallic oxides, have affinity for inorganic pigment surfaces, while not being effective for pigments consisting of uncharged, covalently bonded carbon, hydrogen, oxygen and nitrogen atoms (organic).

Drawbacks of surfactant are: a) Water sensitivity provided to the final coating; b) Foam formation leading to surface defects (e.g.. fish eyes, craters) on the final coating and, if it occurs at the milling stage, loss of production capacity; c) Interference with inter-coat adhesion. Despite this, specific surfactants have been developed to minimize these defects, and some provide other advantages to the final paints such as de-foaming or wetting of difficult substrate.

Dispersants that build up a charged double layer around the pigment are generally used to stabilize pigments in water. Ionic dispersing agents act by coating the surfaces of inorganic mineral particles as the result of an attraction to the charges that develop on particles, process known as ‘adsorption’. Ordinarily, resins are neutralized by more than the equivalent amount of amines (anionic systems, pH 8-9) or acids (cationic systems, pH 5-6) in order to obtain sufficient solubility. The charge of the pigment particles therefore depends on the pH value of the suspending medium (positively charged at low pH values and vice versa) [14]. The electrostatic repulsion prevents the pigments from re-agglomerating. However, the stabilizing charge can easily collapse when subjected to external influences such as impurities and other ions, or if other pigments with different zeta potentials are added.

Steric or " Non-ionic" stabilization – Organic (and inorganic) pigments

High-molecular-weight dispersing agents are linear or branched molecules with a polyurethane or polyacrylate structure and pendant anchoring groups, which easily adsorb onto the surface of organic pigment particles. Adsorption is achieved through hydrogen bonding, dipole-dipole interactions and London-Van der Waals forces. This kind of dispersing agents are effective also for the inorganic pigments thanks to the simultaneous bonding to numerous sites on the surface. The remaining backbone creates then a steric stabilization. [15]

One fundamental requirement for steric stabilization is to fully solvating the chains, leaving them free to extend within the medium, providing as such a good barrier to inter-particulate attractions (i.e. flocculation). The nature of the polymeric chain (i.e. its compatibility with the whole medium) and its amount are therefore critical to the dispersant performances, and it extends throughout the final drying stages of any applied coating [16].

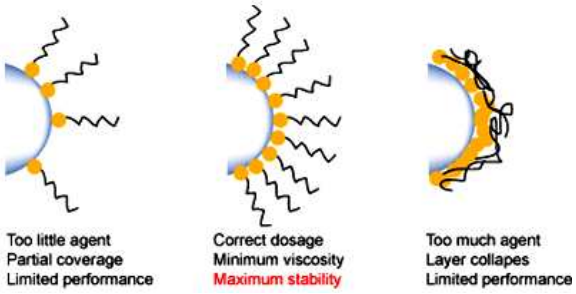

Figure 4.3 – Polymeric dispersant amount and steric stabilization

The great steric repulsion generated by the addition of polymeric dispersants changes the minimum in the potential energy curve (Figure 4.4), and thus reduces the overall viscosity.

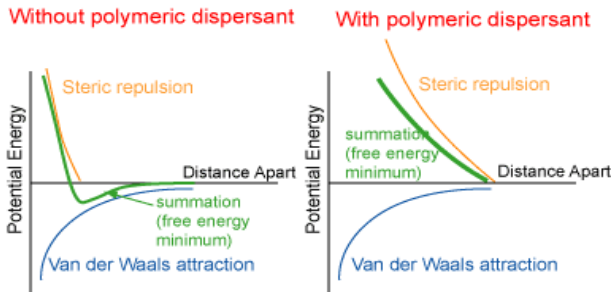

Figure 4.4 – Potential energy curve changes due to the dispersant presence

This stabilization mechanism occurs in solvent-based systems and in water-reducible systems which contain solvated resins. Comprising pigment affine groups (polar) and resin-compatible chains (nonpolar), these dispersing agents do not only stabilize the pigment dispersion, but they also function as wetting additives.

Anchoring groups in polymeric dispersants

The anchoring of the dispersant to the particles could be conducted through [16]:

- *Solvent-Insoluble Polymer Blocks*: it is possible, for example, to disperse a pigment in an aliphatic hydrocarbon using a polymeric dispersant based on poly(tert-butylstyrene) chains, which are solvent-soluble, and polystyrene chains, which are not solvent-soluble.
- *Ionic or Acidic/Basic Groups*: examples of functional groups that can be used to anchor polymeric chains to charged or acidic/basic surfaces include amines; ammonium and quaternary ammonium groups; carboxylic, sulfonic, and phosphoric, acid groups and their salts ; and acid sulphate and phosphate ester groups.
- *Hydrogen-Bonding Groups (Figure 4.5a)*: pigments may have hydrogen-bond donor or acceptor groups, such as esters, ketones, and ethers. Polyamines and polyols are used to anchor via hydrogen bonding, either donor or acceptor. Polyethers can be used to anchor via hydrogen-bond acceptance.
- *Polarizing Groups (Figure 4.5b):* polyurethanes are commonly used as polarizable anchor groups.

a) 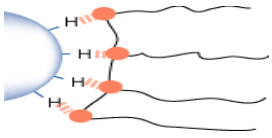 b) 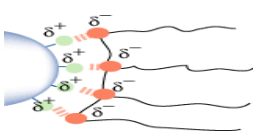

Figure 4.5 - Anchoring of a polymeric dispersant by hydrogen bonding (a) and through polarizing groups (b).

Most polymeric anchor chains probably anchor via a mixture of electrostatic forces (hydrogen bonding and/or polarization) and van der Waals forces. One of the mechanisms may be dominant, but the most effective polymeric dispersants probably maximize the effect from all three mechanisms.

4.3 - PARTICLE SIZE MEASUREMENT

Several analytical techniques give particle size information: laser diffraction, dynamic light scattering, photo-sedimentation, molecular sieving, electrical conductance, microscopy, capillary hydrodynamic chromatography, light obscuration counting, field low fractionation, Doppler anemometry, and ultrasonic spectrometry. Some give only a mean size, whereas others give a complete particle size distribution. The specific particle sizing method chosen depends on the type of size information needed and the chemical and physical properties of the sample.

In general, the particle size is described by a single quantity, such as a diameter, volume or surface area. The particle size distribution is a plot of the number of particles having a particular value of the chosen quantity versus that quantity or a cumulative distribution representing the fraction of particles bigger or smaller than a particular size. Since the particles being described are three dimensional, the usual approaches are to assume the particles spherical, allowing the particle size to be described by only its diameter (d). Examination of the samples under microscope is usually wise because the range of sizes and shapes present can then be estimated. Most particle size methods are sensitive to particle shape and all are limited with respect to the particle size range. For many techniques, particle sizes are best obtained by suspending the particles in a fluid in which the particles are insoluble that disrupt any cohesive forces that could lead to coagulation or agglomeration of the particles.

Low-angle laser light scattering (LALLS)

The LALLS technique [17], also called laser diffraction, is one of the most commonly used methods for measuring particle sizes and size distributions from 100nm to 2mm. The technique is popular because of its wide dynamic range, precision, ease of use, and adaptability to samples in various forms. The measurements are made by exposing the sample to a beam of light and sensing the angular patterns of light scattered by particles of different sizes, producing an accurate and reproducible measurement of the size distribution.

The beam from a continuous-wave laser, usually a He-Ne laser, is collimated and passed through the sample, where scattering from particles occurs. The beam is then

focused on a detector array where the scattering pattern is measured. The scattering pattern is then analysed according to theoretical models (using Mie or Fraunhofer theories) to give the particle size distribution. The instrument used for the particle size analysis in this thesis exploit the Fraunhofer theory, that approximate the particles to matter transparent, spherical, and much larger than the wavelength of the incident beam. It monitors the concentration of particles in the beam by means of an obscuration detector located at the focal point of the lens. If no particles are present in the beam, all the light falls on the obscuration detector, otherwise they block some of the light and scatter the rest onto the elements of the detector array creating the so-called “airy pattern” (different for different particle radii).

When particles of different sizes are present, the intensity pattern can be considered to be the summation of the airy patterns for individual particles. The relationship between the intensity distribution of the scattered light and the particle size distribution for the case of Fraunhofer diffraction is

$$I(x) = I_0 \int_0^{\infty} \left(\frac{2J_1(x)}{x} \right)^2 f(d)dd$$

where I(x) is the intensity distribution of the scattered light, f(d) the particle size distribution coefficient, and d the particle diameter. In terms of scattering angle 0° and with a size parameter $\alpha=2\pi r/\lambda=\pi d/\lambda$:

$$I(\theta) = I_0 \int_0^{\infty} \left(\frac{2J_1(\alpha\theta)}{\alpha\theta} \right)^2 f(d)dd$$

This equation can then be solved by iterative methods.

The particle size distribution *f(d,)* is usually calculated on the basis of volume. The value at each particle diameter represents the percentage of particles having diameters less than or equal to the expressed value. Thus, the particle size is reported as a volume equivalent sphere diameter: “d0,5= x” means that 50% of the particles have diameter equal or less than that “x” value.

4.4 – EXPERIMENTAL

All the experiment were carried out at the same pigment concentration (5% w/w on the mill base). For what concerns the bead-mill grinding the basic setup [13] was followed: half-filled jar and mill base covering the top layer of grinding media. The media used were ceramic spherical beads in different sizes, in order to perform process parameters (called 1° and 2° milling condition) having different impacts on milling time and performances. The 1° milling condition will be referred to as “Small beads” and the second as “Mixed beads”. A 4-5% pigment suspension in water was grinded in 4cm diameters jars. The first dispersant used was Joncryl HPD 96-E (from BASF) for all pigments, then Solsperse 46000 (from Lubrizol) and Pat-Add DA103 (from PATCHAM) for the inorganic pigments.

Joncryl HPD 96-E is a 31% ammonia based high molecular weight and high acid value dispersion resin solution at pH 8,5 for high concentrated pigment dispersions to be used in water-based inks. The styrene acrylic resin backbone enhances both the rate and degree of absorption on a wide range of pigment surfaces, this resin is also a foaming agent thus usually needs a defoamer co-additive. Solsperse 46000 is a 50% polymeric dispersant recommended for dispersing various pigments in resin free dispersions for water-based paints, with a wide range of compatibility in various resin systems. Pat-Add DA103 is a 45% solids polymeric dispersing agent at pH 8 containing sodium salts and working as polyelectrolyte for inorganic pigments in water. It is designed for use in dispersion paints, enabling high pigment loading in the mill base and lowering pigment flocculation and settling tendencies.

Sample	Type	Dispersants	Experiments
PFLO-G	Org.	Joncryl HPD 96-E	1° Mill. Cond. – 4 batches (Jars A, B,C and D for different sampling time) 2° Mill. Cond. – 2 batches
PFLI-Y	Inorg.	Joncryl HPD 96-E Pat-Add-DA103 Solsperse 46000	1° Mill. Cond. – 2 batches each dispersant 2° Mill. Cond. – 2 batches only for Joncryl HPD 96-E (Jars A and B)
PFLI-G	Inorg.	Pat-Add-DA103 Solsperse 46000	1° Mill. Cond. – 2 batches each dispersant

Table 4.1 – Pigments milling conditions

The active-dispersant percentage was meant to be in rate 1:1 w/w (solid) with the pigment. Joncryl and Solsperse dispersions were made 5%, while Pat-Add dispersions had to be 4% due to the hygroscopic tendency of the dispersant increasing the viscosity of the milling base.

The size of the particles in dispersion was monitored several times during the milling by means of laser diffraction (Malvern Master Sizer 2000, analyses model TiO_2, n= 2,741+i0,1). In order to do that, the grinding had to be stopped momentarily: different "stops" were taken for the same milling condition, permitting a general evaluation of the ease of re-aggregation. When using the first dispersant (Joncryl HPD 96-E) the process lasted 20 days, while for the others the milling was stopped as soon as the fluorescence intensity started lowering. Fluorescence measurements were carried out with Jaz portable spectrometer (see Chapter 1.2) on glass vials containing 0,4ml of dispersion. As previously stated, this choice was determined by the need to perform a fast-measurement of the fluorescence output in order to avoid sedimentation phenomena during the analysis. The parameter used were: 1, 2 and 5 seconds of integration, 1 scan to average and 1cm from the probe. For an initial screening of the milling ability of the different classes of compound (organic and inorganic), only PFLO-G and PFLI-G samples were milled. The milling of PFLI-Y, following the fluorescent output at the two characteristic wavelengths of the mixture (546,5 and 627,5nm for the portable spectrometer), aimed to evaluate the effectiveness of the different dispersants. The sampling time was based on the fluorescence trend. For PFLI-Y and PFLO-G with Joncryl HPD 96-E the sampling was performed at: 24, 46, 69, 92, 104, 126, 148, 168, 264, 336, 480 hours (alternating A and B jar). For PFLO-G the sampling was performed also at 4.5, 7.5, 14, 24.5, 24.8, 30, 46 hours (from both C and D jars). For what concerns the dispersions with Solsperse 46000 and Pat-Add DA103 the sampling times were: 4, 7, 24, 30, 46, 69, 92, 116, 126, 148, 168 hours.

Ultrasonic grinding and mechanical dispersion

After the choice of the appropriate dispersant for each pigment type in the bead mill phase, the dispersion by means of ultrasonic bath and mechanical disperser was performed maintaining the selected dispersant (Joncryl HPD 96-E for the organic pigments and Pat-Add DA103 for the inorganic ones).

It was not possible to perform this grinding experiment along with the particle size measurements, therefore the evaluation for this section were merely qualitative.

In this context, the influence of the presence of an anti-settling thickener on the particle size reducibility during grinding was tested, in order to: (a) optimize the production process using the thickener directly in the initial phase of the process (adding it to the liquid slurry before gelling in the case of Xanthan gum) and (b) check if the thickener causes stability/compatibility issues. Few thickeners were chosen basing on the availability of watersoluble products, their neutrality (pH ~7), stability and influence on coating's transparency. The rheology modifiers with the above mentioned characteristics were: Acrysol RM5000 (Dow), Bentone DE (Elementis specialties) and Xanthan gum (Sigma Aldrich). Acrysol RM-5000 is a 19% non-ionic urethane (HEUR) based on a new solvent-free technology, a Newtonian rheology profile for excellent flow and levelling and high film build, combined with excellent water and alkali resistance. Bentone DE additive is a 94% hyperdispersible powdered hectorite clay used as a high concentration pregels to simplify paint manufacture, for formulations with diminished post thickening, excellent pigment suspension, excellent sprayability, superior syneresis control and good spatter resistance. Xanthan gum is a natural gum high molecular weight anionic polysaccharide widely used in pharmaceutical formulations as thickening agent and stabilizer. The experiment was conducted with and without the presence of the previously selected dispersants. The thickeners were used in three different concentrations in the range suggested by the manufacturer (0,1-1% w/w) and the dispersants were used in the same ratio as in the bead-milling section (1:1 w/w with the pigment). These formulations were coated and the thickener that gave the best performance (transparent, plasma-removable and homogeneous coating), Xanthan gum, was integrated in the grinding process. The filming resin (see Chapter 5.5 I°) was also added to check the presence of any difference in stability caused by the interaction pigment-matrix in a possible final formulation.

A first grinding trial was carried out both with ultrasonic bath and a IKA Ultra-Turrax T8 basic disperser on formulations in water, with and without dispersant. The thickener concentrations were 0%, 0,1%, 0,4%, 0,7% with 25% of filming resin (Primal AC-339, acrylic emulsion polymer), for a final concentration of pigment in matrix of 2,5%. The pigments used for these trials were an inorganic and an organic pigment: PFLI-G and PFLO-R available among the ones chosen during the first screening (Chapter 2), evaluating any interaction dispersant/thickener also in terms of viscosity. The inorganic pigment was also tested with the dispersant Joncryl HPD 96-E (for organic pigments) to check the behaviour of the different dispersants in this type of grinding.

First the Xanthan gum in water gel was prepared stirring at a temperature of 60°C, then the other component were added under vigorous stirring until homogeneously mixed. Ultrasonic bath was performed for 25 minutes while the Ultra-Turrax sonication for 5 minutes; the mixing/grinding process was followed using a UV-light source at 365nm. The stability of the dispersions (presence of any separation or precipitation phenomena) was checked under UV-light after 48h. Basic formulations, further refined in Chapter 5, were obtained in this way and used for preliminary aging tests.

4.5.a - BEAD-MILL RESULTS AND DISCUSSION

4.5.1 - PFLO-G

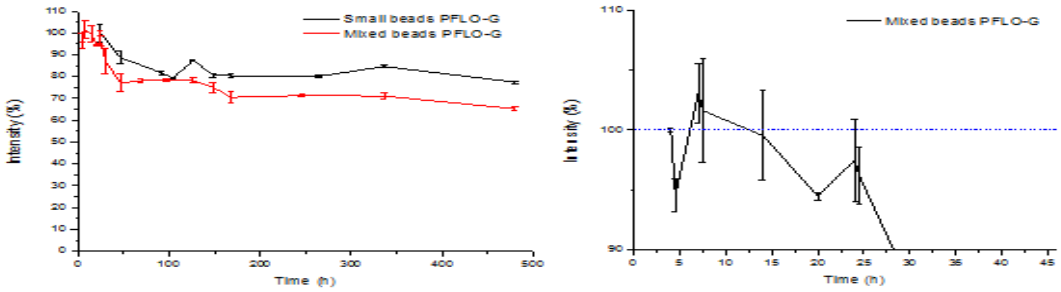

Figure 4. 6 – Fluorescence maximum intensity in function of milling time

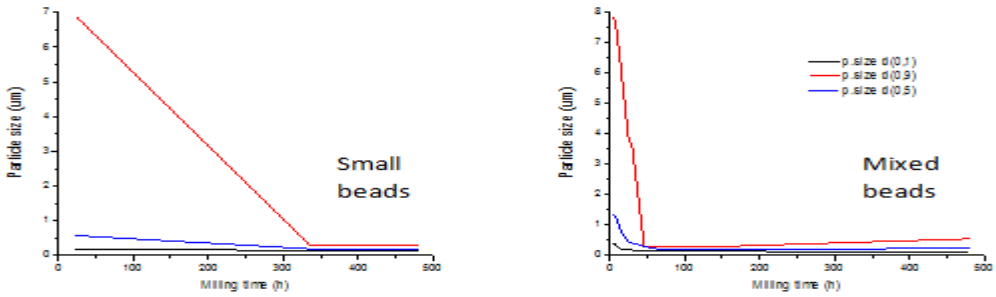

Figure 4.7 - Particle size as function of milling time (hours), pre-tests with different milling conditions (i.e. beads sizes) and Joncryl HPD 96-E

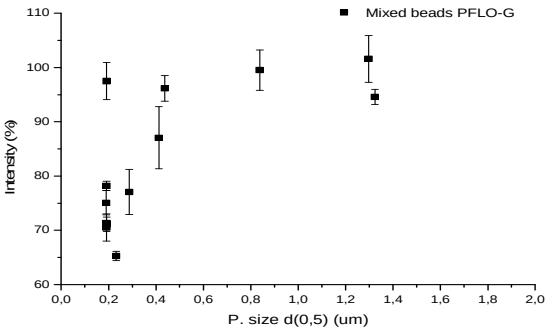

Figure 4.8 – Particle size as function of the main peak's fluorescence intensity, for the 2° milling condition ("Mixed beads") with Joncryl HPD 96-E

1° test -"short" PFLO-G milling				2° test -"long" PFLO-G milling			
Time (hours)	d(0,1) µm	d(0,5) µm	d(0,9) µm	Time (hours)	d(0,1) µm	d(0,5) µm	d(0,9) µm
4,5	0,367	1,324	7,816	24	0,14	0,192	0,284
7,5	0,357	1,297	7,711	46	0,138	0,193	0,287
14	0,218	0,838	6,361	69	0,137	0,191	0,279
24,5	0,175	0,437	3,927	92	0,137	0,19	0,279
30	0,174	0,412	3,559	104	0,137	0,191	0,282
46	0,161	0,287	3,449	126	0,137	0,191	0,284
				148	0,137	0,192	0,286
				480	0,105	0,232	0,549

Table 4.2 – Particle size distributions for different milling time and sampling experiments, for the 2° milling condition ("Mixed beads").

In Figure 4.6 the signal intensity is plotted as a function of milling time. The intensity value is in percentage and refers to the signal revealed during the first sampling, i.e. 4h after the milling starting point. For both milling conditions the fluorescence varies rapidly during the initial milling hours, firstly increasing until around 7h and then reaching a plateau after approximately 46h to the 75% of the initial intensity. This values refers to the shaked suspension taken from the jars while milling, however, when the particles were embedded in a coating the fluorescence output increase a lot for the milled particles in comparison with the non-milled ones (see Chapter 5.6).

As can be seen in Figure 4.7, the first milling condition reaches the average size of 280nm in 11 days. The second condition reduces the particle to this size already after 24h; however, between 126h and 20 days the average size grows, until 0,55micron in 20 days.

These tests led to the decision to mill the organic pigment PFLO-G (and, for extension, PFLO-R) with the second milling condition in order to reduce the grinding process time. Aiming to obtain different particle size distributions for the photo-oxidation ageing tests, the selected milling times are 20h and 120h corresponding to approximately 500nm and 190nm ("50% of the particles having diameter less than or equal to") according to the first milling tests. However, the data were obtained for two different sampling processes (Table 4.2) therefore, considering the possible ease of re-agglomeration, different agglomeration/deagglomeration rates need to be taken into account. The particle size distributions measured at the two chosen milling time for the actual grinding processes are indeed very similar (Table 4.3) even though the actual distribution shows some differences (Fig.4.9). This observation clearly demonstrate the instability of the PFLO-G dispersion, which tends to re-agglomerate as soon as the grinding process is stopped for the laser diffraction measurements, lowering down the process fastness. The d(0,9) obtained (i.e. the maximum particle size) ranges from 8 to 0,5µm during the whole milling process. The bigger the particles are, the more they fluoresce. However, it can be seen from Figure 4.8 that for the same measured particle diameter (d(0,5)) different intensity values are reported. This phenomenon is caused by the continuous de-agglomeration/re-agglomeration process, accompanied by a deterioration of the particles, hence in their fluorescence.

Sample	**ID**	**Milling time**	**d(0,1)**	**d(0,5)**	**d(0,9)**
PFLO-G	GO1d	20h	0,140µm	0,194µm	0,302µm
	GO5d	120h	0,135µm	0,186µm	0,273µm
PFLO-R	RO1d	20h	0,139µm	0,194µm	0,290µm
	RO5d	120h	0,142µm	0,199µm	0,298µm

Table 4.3 – Organic samples, particle size reached after different bead-milling time

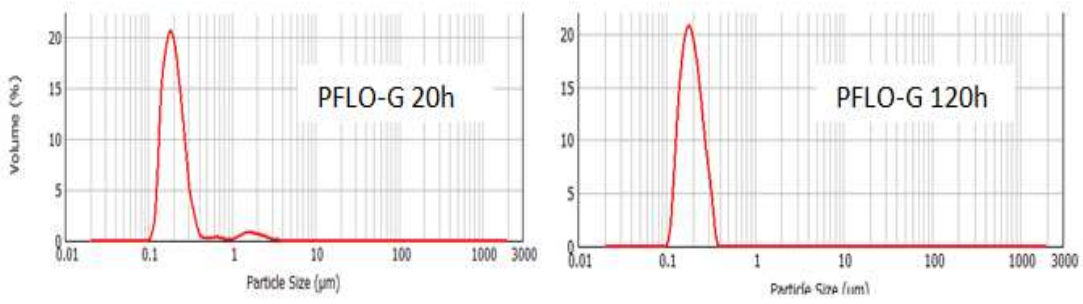

Figure 4.9 – PFLO-G particle size distributions at different milling time.

For what concerns the emission peak position, while milling it showed a 5nm blue-shift (20th day), using the 1° ("soft") milling condition. Using the 2° (and "harder") milling condition, there was a 8nm blue shift instead. This difference is not caused by the particle size, the same for both the sample after 20 days of milling, but rather by a change in the energetic levels distances caused by the stronger action of the beads.
Four new samples were obtained in this process: GO1d, GO5d, RO1d, RO5d. The optical properties of these samples, compared to the non-milled samples GO and RO (respectively PFLO-G and PFLO-R in 1:1 w/w combination with Joncryl HPD 96-E dispersant) were then object of the evaluations in Chapter 5 and 6.

4.5.2 – PFLI-Y

The 1° milling condition with Joncryl HPD 96-E presents a decrease in the fluorescence intensity of the highest peak (green) after 126h, the ratio green/red peaks varies during the milling: after 104h it began to form a red precipitate. The pigments are being separated (Fig.4.10b) and the re-agglomeration became an influent process. The 90% average particle size, and so the maximum particle size present, was reduced from 298µm to 23µm in 20 days of grinding. While the fluorescence is still visible for the previous sample, the 2° milling condition with Joncryl HPD 96-E led to the disappearance of fluorescence already after 24h, probably due to the strong action of the milling beads on the sample (Fig. 4.10a).

a) 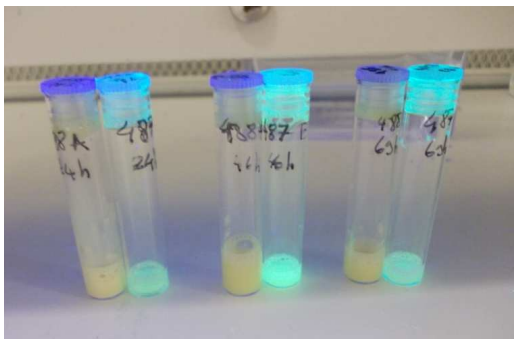 b) 

Figure 4.10 – a) fluorescence from the samples of PFLI-Y milled with the 1° (blue-green fluorescence) and the 2°(not-fluorescent) milling conditions for the samples levied at 24, 46 and 69h; b) Evidence of the presence of two different inorganic pigments in the sample

Fig.4.11 shows the fluorescence intensity in function of milling time for the peaks relative to mixture's composing pigments, at 546,5nm and 627,5nm (emission measured by portable spectrometer). Data were collected for all three the dispersants tested, however the fluorescence output of the sample milled with Joncryl (specific for organic molecules) was not comparable to the other two samples, hence not shown in the plot.

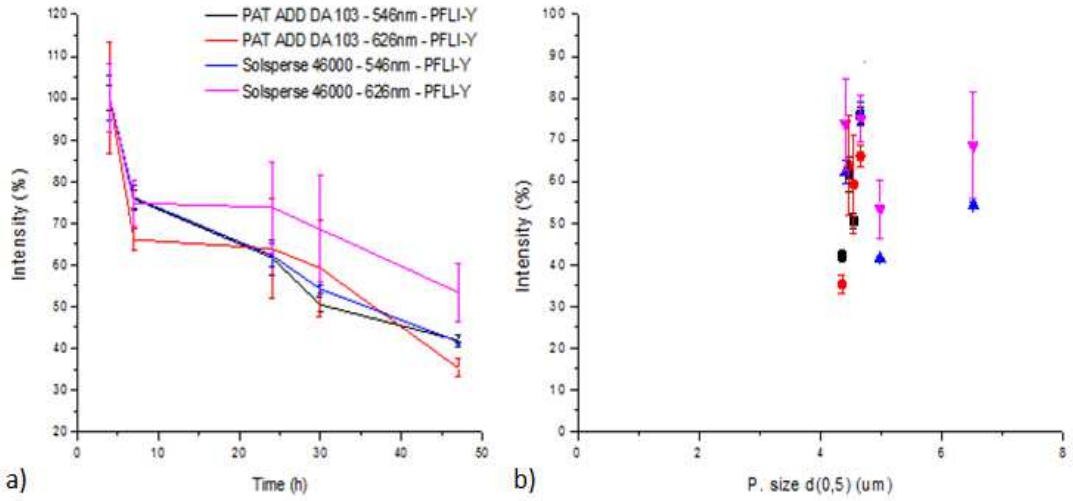

Figure 4.11 – Fluorescence intensity as a function of milling time (a) and as a function of particle size (b), using the two inorganic-dedicated dispersing agents and monitoring the main peaks for the two pigments present in the mixture.

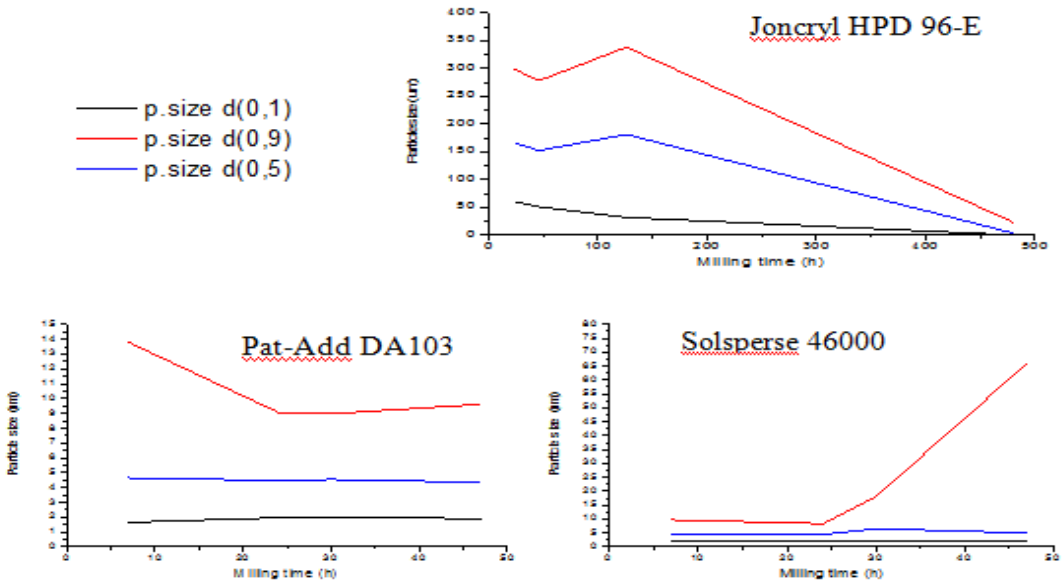

Figure 4.12 – Particle size (d(0,5)) as a function of milling time for the 1° milling condition, obtained with the organic-dedicated dispersant (Joncryl HPD 96-E) and inorganic-dedicated (Pat-Add DA103 and Solsperse 46000) dispersants.

The plots relative to the particle size measurement on the samples milled with the three different dispersants show how the effect of the dispersing agent type could be influent (Fig.4.12). In the presence of organic-dedicated dispersant, indeed, the particle easily agglomerate instead of being grounded. Even with the other dispersants, the pigment didn't give a stable dispersion, with the particles precipitating, because of their size, and re-agglomerating. It has to be noted that the settling rate is not necessarily the same for both the pigment in the mixture, thus the intensity ratio between the two peaks, measured on a single spot of the dispersion's vial, varies accordingly. The pigment was also milled with two inorganic-dedicated dispersants: in this case the maximum fluorescence intensity of both the monitored emission peaks is reached already after 4h of milling. Figure 4.12 shows that the milling process was not happening: the average particle size reached with Pat-Add DA103 is 4,5 to 5µm and the maximum particle size goes from 10 to 15µm; with Solsperse 46000 the values are 4,5µm to 6,3µm for the average size and 8µm to 70µm for the maximum. As stated in section 4.2, in the presence of different pigments to be milled the stabilizing charge of the inorganic-dedicated dispersants can easily collapse. The red glowing pigment fraction (Y_2O_2S:Eu) seemed to present a lower settling rate and a higher fluorescence intensity compared to that of the yellow-green peak (ZnCdS). When the pigment is milled in Solsperse 46000, the fluorescence output, especially that of the red glowing pigment, is higher compared to Pat-Add DA103. This intense fluorescence could be explained by the particle size measurements correlation, 50% of the particles varies in a narrow range for the dispersion in Pat-Add DA103, while for the dispersion in Solsperse 46000 the particle easily re-agglomerate during each milling pause (Fig. 4.11b). However bigger particle sizes milled with Solsperse gave the same fluorescence output than smaller particles milled with Pat-Add.

4.5.3 – PFLI-G

After the considerations about inorganic- and organic-dedicated dispersants, this inorganic pigment was milled directly with Solsperse 46000 and Pat-Add DA103 (inorganic-dedicated). Giving the results of the previous experiment for PFLI-Y, the two dispersant were tested also in order to select the best performing dispersing agent for the RiskReactor inorganic samples.

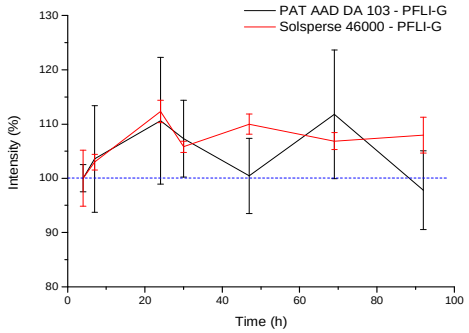

Figure 4.13 - Fluorescence intensity as function of bead-milling time for PFLI-G milled with different inorganic-dedicated dispersants.

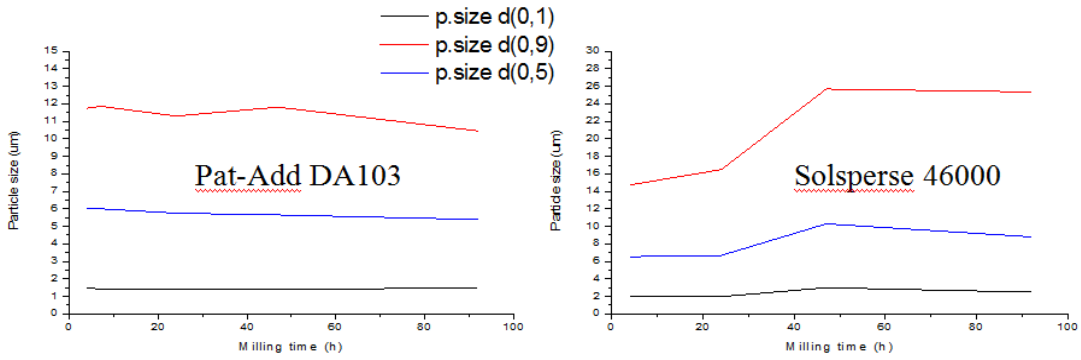

Figure 4.14 - Fluorescence intensity as function of particle size for the two different dispersants

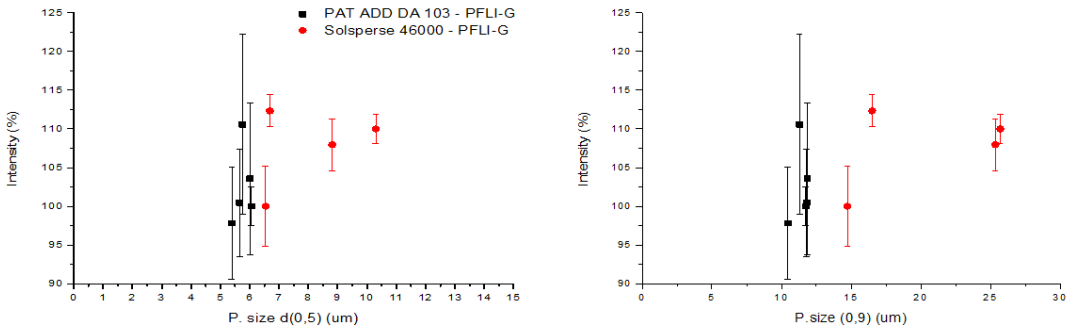

Figure 4.15 - Particle size distribution d(0,5) and d(0,9) as a function of the fluorescence output

In Solsperse 46000 the fluorescence signal increases till 24h (Fig. 4.13), yet as shown in Fig. 4.14 the increasing is due to agglomeration. As can be seen from the particle size measurements in function of milling time, the Pat-Add DA103 dispersions seems to be more stable, arriving at the maximum fluorescence and the lowest reachable particle

size already at 24h. As in the case of the mixture, the milling process of the 2-6µm particles (commercial d(0,5) particle size) was not happening. The reached particle size values are similar to that of PFLI-Y although the agglomeration process is less significant: the maximum particle size was of 10-12µm with Pat-Add and went up to 25µm with Solsperse, while the average size was 5,5-6µm with the former and 6-10,5µm with the latter.

Owing to the agglomeration caused by Solsperse 46000, Pat-Add DA103 was selected as preferred inorganic-dedicated dispersant.

4.5.b - ALTERNATIVE DISPERSING METHOD RESULTS AND DISCUSSION

To disperse with Ultra-Turrax appears as a valid and simpler way both to reduce the pigments particle size and to stabilize them, at least for the inorganic pigments since the particle size reached was around 5 microns. Ultrasonic bath method was discarded, not being powerful enough to mix the formulations or to grind the dispersion even without any thickening agent, and dispersion by means of Ultra-Turrax instrument was performed.

A thickener giving transparent , removable and homogeneous coating, Xanthan gum (an anionic polysaccharide commonly used as food thickening agent and stabilizer), was tested as additive during the grinding process, owing to the need to prevent the particles from settling. Without the presence of thickener, the average particle size of the bigger particles were indeed visibly reduced for the organic pigment PFLO-R from 300µm (d (0,9) measured for the commercial powder) to 300nm already in 5 minutes using Joncryl HPD96-E as dispersant. This type of grinding could therefore grant a simpler way to achieve de-agglomeration and smaller particle sizes compared to the bead-milling process. Visually following the first grinding trial with UV illumination, it can be seen that an effective vortex during the sonication is obtained only with thickener concentrations of 0,1% or less. However, it is still necessary to counteract the pigment precipitation, therefore more than 0,7% of gum in the total dispersion’s water content should be used. As expected, the formulation results more homogeneous in the presence of the dedicated dispersant as shown in Fig. 4.16.

a)  b) 

Figure 4.16 – a) PFLO-R 1% formulation with and without the presence of dispersant (Joncryl HPD 96-E) ; b) Phase separation for the PFLI-G 5% formulation with Pat-Add DA103

After 48h from the mixing/grinding with mechanical disperser the formulations made with dispersant for inorganic pigments (Pat-Add DA103) showed phase separation (Fig. 4.16b), while the formulations with dispersant for organic pigments (Joncryl HPD 96-E) seemed to be stable but also filled by air bubbles.

Regarding the inorganic pigment, its particle size distribution did not seem to change, but by means of Ultra-Turrax mechanical disperser the colour of the pigment itself under visible light becomes progressively darker (from white to black) influencing, albeit not very much, the fluorescence output (Fig.4.17). The same happens with other inorganic pigments from the same manufacturer, because of the crystal damaging caused by mechanical and thermal stresses.

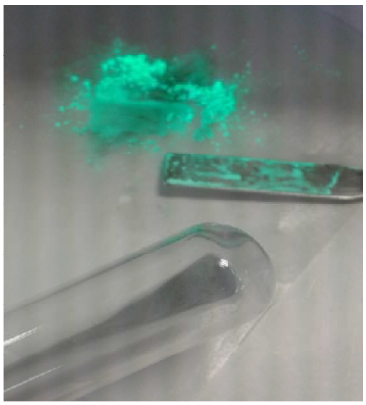

Figure 4.17 – Inorganic pigment (PFLI-G) colour changes due to pressure (spatula) and thermal (mechanical disperser – in test tube) stresses. The powder in the back (off-white in visible light) is here illuminated with a 365nm UV-source.

4.6 - CONCLUSIONS

The selected commercial fluorescent additives have been grounded in order to study the correlations between their fluorescence emission output (when excited at 365nm) and their particle size. The first grinding technique employed was bead-milling, focusing on those pigments that gave the best results in terms of light-fastness in the screening part (Chapter 2): PFLO-G and PFLI-G. Another peculiar inorganic sample, PFLI-Y, was grounded in order to evaluate the effectiveness of the dispersing process on a mixture of two fluorescent compounds. The ultrasonic-grinding and mechanical dispersing technique were also exploited for the particle size reduction of two available samples, PFLO-R as organic and once again PFLI-G as inorganic pigment, in order to evaluate the milling ability of these techniques in comparison to the bead-milling.

Basing on the bead milling results, the optimal grinding conditions to be used were individuated, in order to obtain samples having different particle sizes to be embedded in a coating and further tested (Chapter 5 and 6). This milling for the organic pigments was performed for 20h and 120h, with the second milling condition (called “mixed beads”) and dispersant Joncryl HPD 96-E; the milling of inorganic pigments was shown to be ineffective, therefore their fluorescent properties were not further studied in relation to particle size. All the not-milled pigments were of course mixed with the dispersant in order to obtain 5% dispersions (mixtures), as for the milled ones. Despite its negative effects on the inorganic pigments particle size, the organic-dedicated dispersant Joncryl HPD 96-E was used in all the mixtures owing to the need of comparison between the different coatings formulations prepared in the next chapter.

ID	Sample (milling time)	P.Size d(0,5) (µm)
GO	PFLO-G (none)	~ 4
GO1d	PFLO-G (20h)	0,194
GO5d	PFLO-G (120h)	0,186
RO	PFLO-R (none)	~ 4
RO1d	PFLO-R (20h)	0,194
RO5d	PFLO-R (120h)	0,199
GI	PFLI-G (none)	~ 6
RI	PF-R7 (none)	~ 6

Table4.4 – Final samples identification

Organic pigments bead milling

For PFLO-G, the dispersant Joncryl HPD 96-E gives good milling results: a mean particle size reduction from 6µm to 0,2µm (with maximum particle size of 0,3µm) already in 24h, with a dedicated bead size's mix ("second milling condition"). The highest fluorescence output is obtained after 7h 30'correspondent to a mean particle size (d(0,5)) reduction from 6µm to 1,3µm and a maximumparticle size of 7,7µm. However, the fluorescence intensity reduction do not overcome the 25% of the initial fluorescent output even for the 20 days milled samples.

The experimental results have been extended to the other selected organic pigment PFLO-R. Four new samples were obtained in the final milling process: GO1d, GO5d, RO1d, RO5d. The optical properties of these samples, compared to the non-milled samples GO and RO (respectively PFLO-G and PFLO-R in 1:1 w/w combination with Joncryl HPD 96-E dispersant) were then object of the evaluations in Chapter 5 and 6.

Inorganic pigments bead milling

In order to obtain stable dispersions and homogeneous coating from PFLI-Y and PFLI-G, two dedicated dispersants were tested, both using the first milling condition (i.e. the so-called "Small beads") in order not to destroy the fluorescent particle. According to visual assessment and particle size measurements, more stable dispersions and narrower size distributions were obtained with Pat-Add DA103. For both pigments, after 4 days milling no appreciable difference in the particle size distribution is shown, despite a decrease in fluorescence output. The best fluorescence performance of PFLI-G is obtained after 24h correspondent to a d(0,5) reduction from 6µm to 5,8µm and a maximum particle size of 11,3µm. For the sample with two mixed pigments (PFLI-Y), the best fluorescence performance is obtained after 4h correspondent to a mean particle size reduction from 6µm to ~5µm and a maximum particle size of ~15µm.

The inorganic pigments can therefore not be milled with a bead-mill method.

Ultrasonic grinding and mechanical dispersion

The results obtained in the bead-mill section show that no grinding happens with the inorganic pigment and only a mild milling is needed for the organic ones to reach their maximum fluorescence output.

This suggests the use of a simpler way to de-agglomerate the pigments particles: two methods were compared: ultrasonic bath and mechanical dispersion (IKA Ultra-Turrax

T8 basic). Ultrasonic bath method was discarded since it wasn't powerful enough to disperse the pigment, even without any thickening agent. The dispersion by means of Ultra-Turrax, instead, is shown to be as effective as the bead-milling in reducing the pigments particle size; on the other hand, it seems to be a less controllable method (in terms of particle size) compared to the bead-milling. Although sonication was not the method used for reducing the particle size in this study (further studies has to be done regarding the setup characteristics), it is shown to be a valid alternative to the bead milling, especially if the purpose is to grind the pigments to the minimum particle size reachable sparing time.

On the other hand, even the grounded pigments tended not to give stable dispersions. In order to counteract the precipitation, the addition of thickening agents and the possibility to add it directly while mechanically dispersing, was tested. Homogeneous and shelf-stable dispersions were obtained only with a Xanthan gum concentration higher than 0,7% , which leads to a viscous dispersion that needs to be diluted. However the thickener cannot be added directly during the grinding step, thus the next step was to adequately incorporate the mixture of pigment and dispersant in water with pre-prepared Xanthan gum gel. The need to perform the particle size measurements right away before stabilizing the dispersions, implies the thickener addition to be the limiting step of all the subsequent embedding processes.

REFERENCES

Section 4.1

[1] *Aqueous dispersions of fluorescent pigments*, United States Patent US5294664A, R. Morrison, 1994

[2] *Synthesis, characterization and fluorescence performance of a waterborne polyurethane-based polymeric dye*, H. Xianhai, X. Zhang,J. Liu, J.Dai, J. of Luminescence Vol.142, October 2013

[3] *Synthesis and fluorescent investigations of VBL-based waterborne polyurethane dye*, Hu X., Zhang X., Dai J., Liu J., Journal of Luminescence 131, 2011

[4] *Synthesis and characterization of a novel waterborne stilbene-based polyurethane fluorescent brightener*, X.Hu, X.Zhang, J. Dai, Chinese Chemical Letters 22, 2011

[5] *Effect of Fluorescent Particle Size on the Modulation Efficiency of Ultrasound-Modulated Fluorescence*, Y. Liu, B. Yuan, J. Vignola, Intern. J.of Optics Vol.2012, 2012

[6] *Effects of crystal size, structure and quenching on the photoluminescence emission intensity, lifetime and quantum yield of ZrO2:Eu3+ nanocrystals*, S. D.Meetei , S. D. Singh, J.of Luminescence Vol. 147, 2014

[7] *Functionalised, photostable, fluorescent polystyrene nanoparticles of narrow size-distribution*, M. Pellach, J. Goldshtein, O. Ziv-Polat, S. Margel , J.of Photochem. and Photobiol. A: Chemistry Vol. 228, 2012

[8] *Effect of solvent, host precursor, dopant concentration and crystallite size on the fluorescence properties of Eu(III) doped yttria*, P. K Sharma, R. Nass, H. Schmidt, Optical Mat. Vol.10, 1998

[9] *Size dependent efficiency in Tb doped Y2O3 nanocrystalline phosphor*, E.T. Goldburt, B. Kulkarni, R.N. Bhargava, J. Taylor, M. Libera, J.of Luminescence Vol.72, 1997

[10] *Dispersion of organic pigments using supercritical carbon dioxide*, W.T. Cheng, C.W. Hsu, and Y.W. Chih , J. of Coll. and Interf. Science vol 270, 2004

[11] *Physics and chemistry of pigments*, C. E. Barnett, Industrial and engineering chemistry vol. 41, 1949

[12] *Polymeric dispersing agents, Munzing chemie GMBH, EDAPLAN, 2000*

[13] *Paint Flow and Pigment Dispersion. A Rheological Approach to Coating and Ink Technology 2° ed*, T.C. Patton, 1979

Section 4.2

[14] *Clay-assisted dispersion of organic pigments in water*, Y. Lan , J. Lin, Dyes and Pigments vol. 90, 2011

[15] *www.dispersions-pigments.basf.com* – BASF, The chemical company

[16] *www.uniqchem.com* – UNIQchem, Additives for coating inks and plastic applications

Section 4.3

[17] *Pigment dispersion in water-reducible paints*, T. Kobayashi, Progress in Org.Coat. vol 28, 1996

[18] *Principles of Instrumental Analysis VI edition*, D. A. Skoog, F J. Holler, S. R. Crouch, Thomson Brooks Cole, 2007

Chapter – 5 –

COATING

PREPARATION

5.1 – INTRODUCTION

One of the aims of this thesis was to formulate a fluorescent protective coating. In the light of considerations on the fluorescence variability due to the embedment of the luminescent particles in a matrix, however, the focus moved to the study of the pigments behaviour, leaving aside the formulation context. In order to test the performances of the selected additives, a coatable waterbased formulation was anyhow needed to permit the study of the pigments when exposed to UV light. Typically, the coating systems are solvent-based resin composition. The use of such compositions requires extra safety precautions, while waterbased coating formulations is less toxic and less polluting. A coating formulation must contain, in addition to water and pigment, a polymer as film-forming element. As a project goal, the coating had to be easily removable by a cold plasma torch and transparent. Owing to experimental needs, the coating must contain the minimum number of ingredients in order to restrain the variables number when studying the influence of the additives on the matrix ageing (and vice versa). Sections 5.2 , 5.3 and 5.5 explain the process that led to the coating composition formulation to be aged.

Once added to a formulation, the pigments' fluorescence properties could change, owing to the new environment characteristics to which the molecules are subjected, as stated in Chapter 1. The prepared formulations were coated on glass slides (widely available and inexpensive) for the fluorescence decay tests and on silicon wafers for the coating yellowing and removability tests. The deposition method used in the first place was bar-coating (a simple and fast method to obtain coating with a certain fixed thickness), then spin- and dip-coating were introduced in order to obtain homogeneous coating with a repeatable thickness. The selected matrix influence on the fluorescent output of the samples and the correlation with the pigments' concentration and coating's thickness were examined in Section 5.6.

5.2 - STABILIZATION OF THE DISPERSIONS:

THICKENING AGENT ADDITION

The pigment needed to be provided in the form of dispersion, hence the necessity to stabilize the compositions obtained in the grinding process (5% suspension of pigment in water and polymeric dispersing agent). The main issue for this research was to prevent the re-agglomeration of the settling pigments and to avoid change in the particle size to which the fluorescence output is correlated. The precipitation of particles in a mixture could be avoided in two ways: reducing the particle size and adding various additives in order to obtain the so-called “colloidal stabilization” or counteracting the particles settling increasing the mixture viscosity (adding a rehology modifier). As stated in the previous chapter, three systems of coating stabilization can be used in aqueous medium to maintain the "potential barrier" (i.e. the energy that particles shouldn't be able to overcome on expense of their heat energy in order to maintain the dispersion steady): a) the use of ionic surfactants or chemicals which produce ions, b) the adsorption of non-ionic surfactants or corresponding chemical modification of the polymer phase (or surface only) with non-ionic lipophilic fragments c) the combination of ionic and non-ionic stabilization, widely used in technologies of latexes, emulsions and paints, allowing to achieve prominently high dispersion stability toward the action of various destabilizing factors. Although in this sense experiments with various combination of filming resins and surfactants were performed, the concrete research of dedicated additives for each pigment would have been a time consuming process, therefore the addition of a rheology modifier was the preferred choice giving the basic experimental needs.

The main thickener’s features sought for this study were:

- Transparency (no influence on the coating appearance);
- Removability by means of cold plasma torch;
- Physic-chemical stability under a wide range of conditions;

As reported in Chapter 4.5, the selection made during the ultrasonic-grinding experiment led to the choice as thickening agent of a polysaccharide (Xanthan gum). The concentration selected for the 5% pigment dispersions stabilization was 1% , thus

obtaining a viscous system (gel) which needed a severe dilution when incorporated in the final coating formulation.

Hence, an experiment regarding the coatability (e.g. the coating homogeneity) of formulations with different ratios of pigmented gel, filming resin and dilution water was performed. The stabilization of the pigment dispersion, became as such the limiting stage of all the coating process. It determined the ratios of the selected components (including the pigment content) and, as will be seen later on, the final coating thickness.

The speed at which viscosity recovers following application (and removal of the shearing force) will directly influence the properties of the film. Slow viscosity recovery causes good levelling, good gloss, but possible sagging, while fast viscosity recovery reduce the flow and cause no sag, but brush marking, orange peel and reduced gloss. For typical coating, the viscosity at high shear rates must be sufficiently low to allow application, but not so low that the film applied is too thin and has insufficient covering power.

Not only the coating properties, but also the fluorescence of a compound is affected by the viscosity of the medium, increasing with increasing viscosity since the energy transfer is reduced by a reduction in the number of molecular collisions [1]. The thickener presence influence on fluorescence was clearly detected, and examined in Section 5.6.

Rheology modifiers

Aqueous coatings are dependent on the use of rheology modifiers to achieve the required balance of application properties for a given market. Generally, a combination of modifiers is used to provide the best balance between container viscosity, application viscosity, anti-settling properties, spatter resistance, flow and levelling properties[2].

Typically to correct pigment settling problems in aqueous systems, thickeners such as fumed silica or clays such as montmorillonite hectorite or attapulgite have been used. However, these are difficult to use as post add correction, to disperse during the manufacturing and require high shear mixing equipment to achieve adequate dispersion. Other thickeners acting as stabilizing agents to deter sedimentation include: natural gums as Xanthan gum (but also: alginate, Arabic gum, guar gum, tragacanth gum and locust bean gum), cellulose derivatives such as carboxymethyl cellulose and hydroxyethyl cellulose, and modified starches[3]. Furthermore, polyacrylic-acrylate

thickeners could provide resistance to pigment settling, for example ASEs, HASEs, HEURs and LDPs. Alkali-swellable emulsions (ASE) increase viscosity overlapping and tangling after swallowing when the high percentage of acid groups distributed throughout their polymer chains is neutralized. Hydrophobically modified alkali-swellable emulsions (HASE) also contain long-chain hydrophobic groups referred to as 'associative'. The combination associations (intra-molecular, inter-molecular and with the other hydrophobic elements in a formulation) has a significant effect on rheological properties. Hydrophobically modified ethoxilated urethane resins (HEUR) also belong to the associative category of thickeners, but unlike HASE, they are non-ionic substances not depending on alkali for the activation of the thickening mechanism [4]. Liquid dispersion polymers (LDPs) are water-soluble acrylic polymers in mineral spirit (thus, do not require neutralizing to become water 'soluble') suitable for formulations covering a wide pH range [2].

Xanthan gum, the selected thickener, is a high molecular weight polysaccharide gum, containing D-glucose, D-mannose and D-glucuronic acid and prepared as the sodium potassium or calcium salt. It is a gelling agent which gels show pseudoplastic behaviour, the shear thinning being directly proportional to the shear rate. For coating formulations pseudoplastic and thixotropic behaviour are preferred, granting the fluid to flow freely when applied and reverting to a gel-like state on standing. When this gum is mixed with certain inorganic agents such as magnesium aluminium silicate, or inorganic gums, synergistic rheological effects occur (as happened in the presence of the pigment samples). The pH is neutral and its aqueous solutions are stable over a wide pH range (pH 3-12) and temperature range. Xanthan gum is an anionic material, therefore, precipitation from the solution occurs when in the presence of cationic surfactants, polymers or preservatives. Also polyvalent metal ions as calcium can cause precipitation under highly alkaline conditions.

5.3 – MATRICES FOR PROTECTIVE COATINGS

In the C.H. conservation field the treatments for the protection superficial layers are intended to confer hydrophobicity, without harming the substrate vapour permeability, and prevent the pollutants to reach the surface and their penetration. Ideal coating properties should be: flexibility, transparency, adhesion, cohesion, lack of colour, long-term durability (UV resistance and chemical stability to pollutants), reversibility, easy and rapid application with no risks for the operators. [5] The development of formulations of more than one component requires research efforts aimed to the definition of the correlations between composition, phases' structure, compatibility, miscibility, viscosity, penetration depth and protection and consolidation functionality modulated in correspondence with the characteristics of the substrate to be treated.

The binder (or resin) is the film-forming element of a coating or adhesive. It provides adhesion to a substrate, binds pigments and extenders together, and determines important properties such as durability, flexibility and gloss. When using polymeric emulsions, curing is performed by coalescence, the binder particles being fused together as water evaporates [2]. For a precise evaluation of the matrix to be used, all the formulation components should be regarded as important; for example the organic samples contain MF resins, that are known to have un-stabilizing effects on latexes compositions [6].

Among the available filming matrices for waterbased coating fulfilling the removability and transparency precondition, an acrylic binder commonly used for restoration purposes was used for the final coating (i.e. the support for the additives aging test in Chapter 6). However, two other project-related matrices were used during the pre-tests.

Acrylic resins

Acrylic resins include a wide range of polymers and polyaddition copolymers obtained by radical polymerization of acrylic or methacrylic monomers. The acrylic systems can be divided into three different types: preformed polymers in solution, reactive monomers capable of reacting in situ and dispersions and emulsions of preformed polymers. Speaking of protective formulations for C.H. conservation, aqueous

emulsions present macromolecular aggregates dispersed as micelle, having low penetration ability, bad film-forming ability, and usually more hydrophilic surfaces compared to the solution. On the other hand they avoid toxicity and have less environmental impact than solvent-based protectives. The polymers applied in concentrations between 1% and 50%, with brush, roller, spray, airbrush or capillarity absorption, depending on the type and concentration of the polymer and on the substrate porosity. Acrylic polymers used in surface treatment of the stone are: poly-methyl acrylate (PMA), polymethyl methacrylate (PMMA), polyethyl metacrylate (PEMA) and copolymers P [EMA / MA]. As a host polymer matrix for rare earth ions and organic dye doping, PMMA is widely used thanks to its low optical absorption, refractive index tailorability with molecular weight, simple synthesis, and its low cost. However its employ comprise solvents use. The acrylic copolymers have been, on the other hand, widely used in surface protection of stone materials of different nature and origin. Through the copolymerization of two or more monomer units is possible to synthesize products with intermediate characteristics between those of the homopolymers. For example, the values of glass transition temperature (Tg) of copolymers [EMA / MA] depends on the composition (molar or weight ratio of the two components). In particular the Tg increases with the increase of the content of EMA from 8 ° C, Tg of PMA (100%), to 65 ° C which corresponds to PEMA (100%). The versatility of the processes of polymerization and the high number of acrylic monomers available, allow to optimize the production in order to obtain final products with the desired chemical structure and molecular weight, thus with the functional characteristics needed for the particular use[7].

The matrix used for the pigments embedding was Acryl33, a 46% mixture of MMA, EA and EMA polymers in water with excellent alkali resistance that should dry to form a water resistant film. It is typically applied in: fixing and unifying of interior plasters and frescoes, mortar sealing to improve adhesion and elasticity, mechanical strength improving, pigments binding and documents protection. The pH of the liquid product is around 9.5, but it drastically decrease in coating (pH 7) and when the coating are aged (pH3). Glass transition temperature close to the environmental temperature, high transparency, good yellowing resistance, excellent resistance to UV rays, permanent flexibility and elasticity are the main coating features proposed by the manufacturer, while the emulsion shows excellent thermal, chemical (resistance to soluble salts,

including those bivalent, and pH variations) and mechanical stability and more importantly a good compatibility with fillers and pigments. [8]

Acrylic polymers deterioration

The phenomenon of degradation in organic materials consists in the continuation of the drying and hardening process, which led to the formation of the polymer film. Solar radiation and heat cause the absorption of a photon by the chromophore group, triggering the processes of radical species formation. The radicals give hydrogen extraction and crosslinking reactions, already involved in the film formation, and a progressive yellowing of the surfaces, fragility increase and solubility variation. The molecules can also undergo beta-scission, which involves loss of material of low molecular weight that can volatilize or be trapped in the film as mobile component. The crosslinking reactions involve structure stiffening and increase the fragility, while the beta-splitting leads to a mechanical properties loss. In addition acrylates, may undergo reactions of hydrolysis of the ester bonds, with consequent release of the pending groups. These are small volatile molecules that are then released. The main consequences of such reactions are the loss of mechanical properties (and protective efficiency, concerning C.H. conservation). The formation of OH groups as a result of hydrolysis, in fact, makes the structure more polar and therefore less hydrophobic [9], that is why water resistance decreases strongly in aged samples and in correspondence of alkaline and acid conditions. The deep structural changes due to electromagnetic radiation exposure are detectable by FTIR analyses through the enlargement of the peak at 1731cm-1 (C = O, ester) and the appearance of new absorption bands at 1780 and 1665cm-1.[7]

Polymers stabilization

Stabilisation is essentially based on three different processes: antioxidants and UV stabilizers addition, molecular structure modification, blending technology improvement. In particular, UV stabilizers could be absorbers (carbon black, iron oxides, benzophenone derivatives), quenchers(nickel based complexes) or radical scavengers (HALS =hindered amine light stabilizers). The ability to develop polymeric systems that better resist chemical environmental aging is linked to the development of new additives, antioxidants and UV stabilizers, characterized by greater efficiency and

further characterized by low vapour pressure at processing temperatures and exercise, low propensity to migrate to the surface of the article with the formation of deposits (chalking or blooming) and high resistance to extraction by the solvent with which the polymer is in contact during use. On the other hand, the modification of polymers by fluorinated monomers inclusion along the chains of acrylic copolymers creating high energy covalent bonds, increases resistance to: UV rays, oxidation and temperature changes, microorganisms, aggressive chemicals in a wide temperature range, heat and fire, wear, dynamic stresses. Furthermore, the fluorinated polymers are characterized by a high light transmission ability and a surface energy reduction (wetting and excellent performance against foreign substances adhesion). Therefore, in relation to the nature and structure of the substrates to be treated, the in situ polymerization of fluorinated acrylic copolymers may represent an interesting opportunity for the development of new fluorinated surface endowed with high chemical and photochemical stability.[7]

In this sense the addition of a fluoro-alkyl-functional water-borne organo-siloxane, Dynasylan F 8815, acting as modification agent on oxidic carboxy and hydroxyl-functional substrate was experimented in order to confer hydrophobicity to the coating.

5.4 - EXPERIMENTAL

Pre-tests: coating matrices and surface tension control

The coatability of some basic formulations without any additive or dispersion stabilizer was evaluated as a pre-test. These formulations contain: 0.1%, 0.3% and 0.5% of pigment respectively, 1:1 w/w with the dispersing agent, 20% or 10% of filming matrix and water. The samples tested were PFLO-G and PFLI-Y (un-milled commercial powder) and the dispersing agents Joncryl HPD 96-E and Pat-Add DA103 respectively. The formulations were coated by means of bar-coating method on glass slides, in order to obtain a final thickness of 10µm. Since the coating appeared to suffer from bad wettability and inhomogeneity, the addition of some extra-additives, as surfactants and thickeners, was experimented. Coatings were made with various concentration of four different types of surfactants, one anionic (Dodecylbenzenesulfonic acid, from Acros), one cationic (CTAB, from Sigma Aldrich) and two non-ionic (Polyoxyethylene(10)tridecylether, from Sigma Aldrich and Surfynol 104E, from Air products) and two types of thickening agents, one polysaccharide (Xanthan gum, from Sigma Aldrich) and one non-ionic urethane (Acrysol RM-5000, from Dow). The surfactants were added in different percentage from 0% to 2% and the thickeners from 0% to 5%, also in combination, to the pigment in water formulations. The same formulations were made also without the inclusion of pigments (so-called “blanks”) both with and without adding the dispersing agent, in order to evaluate the interaction between dispersants and matrices. The matrices used in the pre-tests were Primal AC-339 (48% acrylic polymer emulsion in water, from Dow) and Acrilem IC-390 (45% silane modificated acrylic pre-crosslinked copolymer emulsion in water, from ICAP-SIRA).

Hydrophobization

After the pre-tests the matrices used were Acrilem IC-390 and Acryl33 (46% poly-acrylates emulsion in water, from Bresciani).

A parallel experiment was conducted adding to the formulations containing both these filming-agents the hydrophobizing agent Dynasylan F 8815 (a fluoro-alkyl-functional water-borne organo-siloxane, from Evonik), in ratio 1:1 with the matrix, both with and without the presence of Xanthan gum as thickener.

Thickener addition and dilution

The thickener selected in the ultrasonic grinding stage, Xanthan gum, was added in the concentration of 1% to the milled pigment suspensions (prepared in the previous chapter), heating the samples up to 60°C and stirring vigorously using a magnetic stirrer. The ratio gum/suspension being fixed, obtaining 5% pigment dispersions in the form of gels, the parameters of matrix concentration and dilution water varied. In order to define the optimum ratio gel/matrix/water, coating tests were performed without the presence of pigment particles (even though their presence influences the gel viscosity). In the pre-tests the ratios pigment/dry resin used were varied from 1% to 5%, the latter giving a good fluorescent output with thick (10µm) films. Therefore, for this test on thin coatings, hypothetical pigment concentrations of 2,5%, 5% and 20% were used. The matrix dilution was varied from 3% to 206% in order to explore a wide range of concentrations. The resin emulsion was added stirring vigorously after the diluted dispersions recovered the environmental temperature.

De-foaming additives

In order to eliminate the formed foam the addition of anti-foamer Defoamer TEGO Foamex 805N (from Evonik)was evaluated. The bad result obtained in terms of coating homogeneity led to the choice of ultrasonic bath sonication as foam-remover method.

Formulations for the intensity/thickness/concentration correlation experiment

In order to correlate fluorescence intensity and pigment concentration, a fixed coating thickness is preferred (i.e. the coating formulations must have the same viscosity), thus the ratio Xanthan gum/dilution water (i.e. the ratio dispersion/water) have been fixed to be 1:1550 (i.e. 6,5% of dispersion gel in water). However, the rates gum/matrix end up being changed, and this influenced the thickness of the coating coated by means of a dip-coater (as much as by means of coating bar). The changes in coating thickness were measured using a profilometer (Alpha-Step IQ-KLA Tencor). This permitted to obtain fluorescence intensity vs thickness curves for each concentration (1, 10, 20%) of each pigment sample. The samples considered in this study were only those with smaller particles (i.e. GO5d and RO5d for the organic samples and GI and RI for the inorganic ones). The data regarding the non-milled samples are obtained from the pre-test

formulations. The error bars are calculated from the error on the thickness combined with that on the intensity for three different zones on the same sample. The fluorescence data were collected with a Fluorolog3 from Horiba Jobin Yvon (See Chapter 3), equipped with Xenon lamp for PL/PLE analysis and NanoLed-370 and Spectraled-370 for the lifetime decay measurement.

Substrates and deposition method

The substrates used were microscope-glass slides (2x3cm) and silica wafers (1x2cm). In order to activate the substrates and homogeneously coat the formulations, all the substrates were washed with soap, then with acetone and then cleansed with a NH_3/H_2O_2 bath for 24h; after that they were rinsed with distilled water and dried with compressed air.

In the pre-tests the bar coating method was used for the deposition, then dip- and spin-coating were considered, in order to obtain reproducible coating thicknesses (DIP COATER D KSV and SCS G3P-12 from Cookson Elecronics Equipment). The spin coating deposition is mainly controlled by the rotation speed (RPM) since the centripetal acceleration causes the deposition by spreading of a central drop. The thickness depends on the polymer nature (viscosity, surface tension, etc…) and spin coating parameters such as rotation speed, acceleration and the presence of vapour suction. Several trials were performer with RPM from 300 to 3000 and 30seconds cycles. This technique is not optimal for the coverage of wide surfaces with water-based formulations owing to the slow solvent evaporation; therefore dip-coating was evaluated. The stages through which a thin film is deposited by dip coating technique are: immersion, extraction, deposition, drainage and evaporation. The instrument consists of a worm screw, driven by an electronic device that regulates the speed of rotation and consequently extraction. This mechanism allows to contain a continuous vertical displacement The ascent speed of the sample is the variable that can be controlled in order to obtain films with a certain thickness (that also depends on factors such as the viscosity of the solution, gravity, surface tension between liquid and vapour and effects due to the evaporation). The extraction rates tested were 20, 40, 100, 200 mm/min all for 1,2 and 3 times, with a 15 min oven drying process in between. Concerning the fluorescence intensity/thickness/concentration study, 1%,10% and 20%

coatings (this time containing the pigments) were brush-coated in order to obtain different realistic thicknesses (applying 1,2,and 3 coat) and fastening the process.

5.5 - RESULTS AND DISCUSSION I° : COATING PREPARATION

5.5.1 - COATING STABILIZATION PRE-TESTS: FILMING MATRICES AND SURFACTANTS

Simultaneously to the first grinding tests, coating pre-tests were performed on the unmilled dispersion of the fluorescent pigments, using concentrations from 0,5% to 5% on the matrix and a 3% to 30% matrix dilution. From the pre-tests for 10µm coatings from pigmented formulations without addition of dispersion stabilizer, a 1% ratio of organic pigment on matrix already gave a good fluorescent output, while, the inorganic pigment reached the same fluorescent intensity with a 5% ratio, as expected. When adding the dispersant, interactions with the filming resin impaired the coating's wettability and homogeneity properties, at least in the case of the formulations with Joncryl HPD 96-E and Primal AC-399 (Fig 5.1). However, the presence of dispersing agent seemed inevitable in the grinding step and its presence affected positively the fluorescence output (although giving a matt coating). These considerations led to the experimentation of other two available matrices: Acrilem IC390 and Acryl33 (former "Primal AC-33").

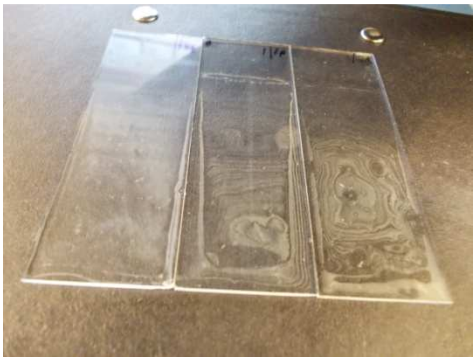

Figure 5.1 – Blank coatings showing the interactions between Joncryl HPD 96-E and Primal AC-399

Several defects, like fish eyes and air draft sensitivity, were observed. These defects are mainly caused by differences and changes in the surface tensions of liquid, substrate and contaminants (Fig.5.2). Effective wetting of a solid takes place when the liquid has a lower surface tension than the solid. When the surface tension of the liquid paint is high, the system is more sensitive to wetting defects. In general, modern synthetic resins have higher surface tension than those based on natural fatty acids and aqueous systems have high surface tension due to their polarity. Surface control additives and levelling agents like polysiloxanes and polyacrylates are used in the coating industry to prevent surface defects during paint application and improve the resistance and appearance of dry film adjusting the surface tension of the liquid.

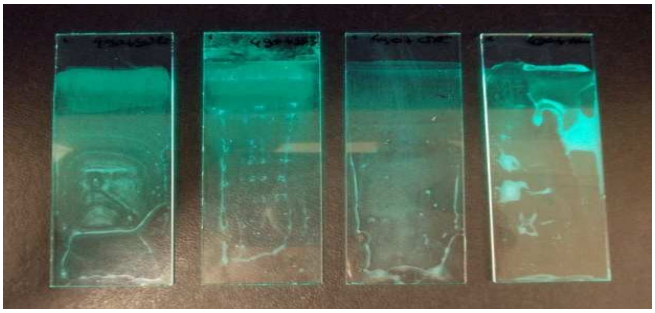

Figure 5.2 – PFLO-G formulation coated in the presence of different surfactants (from the left to the right: non-ionic, non-ionic, cationic, anionic)

Also the presence of pigment particles and their size had to be considered during the preparation of a well-coated film (Fig. 5.3). For example, sample PFLO-G in the form of nanometric sized particles (<0,5µm) created a lot of issues to the coating, independently on whichever dispersant, surfactant or thickener (or combination of the three) was employed.

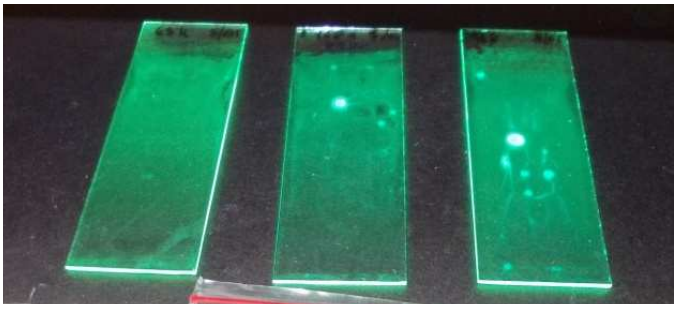

Figure 5.3 – Coating from formulations containing PFLO-G milled 3, 7 and 11days (1° milling condition)

For what concerns the inorganic pigment PFLI-Y, a well coated formulation was obtained combining non-ionic thickeners and surfactants, i.e. not influencing the electronic stabilization occurred with Pat-Add DA103 dispersant.

Well-coated, completely transparent and removable preparations were formulated with 10% Acrilem IC-390 and 0,5% of pigment powder. For the inorganic pigment the formulation included 1,1% of Pat-Add DA103 and 0,5% of HEUR, while for the organic pigment 1,6% of Joncryl HPD 96-E was added. Despite obtaining good results using Acrilem IC-390 as matrix, Acryl33 was preferred as matrix for the actual coatings to be aged because of its wide use in the restoration field. Both matrices do not present water-repellency properties.

Once added Xanthan gum as thickening agent (see Chapter 4), some evaluation on its stability in the presence of different matrices and dispersant have been possible. The gum is stable in the presence of matrix but presents a little phase separation (gum-latex) when in the presence of dispersing agents. This separation is more visible in the presence of JoncrylHPD 96-E than in the presence of Pat-Add DA103 and is enhanced by the presence of the pigments (especially by PFLO-G).

As seen in the grinding step, Joncryl HPD 96-E acts as foaming agent. Foam is an undesired side effect, promoting surface defects such as craters and weak points in the dried film, only stable in systems that contain surfactant-like substances with the ability to migrate to the air/liquid interface of the paint and thereby reduce surface tension. These bubbles accumulate and deform, thereby deforming the surface of the coating: the air cannot escape because lamellae are formed. Without surfactants, drainage of the liquid would cause the lamella to thin and ultimately break. Their presence prevents the lamella from thinning by counterflow of liquid due to a surface tension difference, which results from interface stretching and repulsion by the surfactants at the interfaces caused by steric and electrostatic mechanisms. To prevent stabilizing effects and eliminate foam, a defoamer is required that destroys existing foam and/or prevents foam formation and /or releases air, assisting air bubbles to rise to the surface. It must be insoluble in the paint system and mobile so it can enter the lamella at the point where it has to spread at the interface and displace the surfactants, and have lower surface tension than the surfactant, causing fast thinning and collapse of the lamella. A wide range of chemical structures can be used with water-based systems on account of their generally higher surface tension, so mineral oil defoamers and silicones are highly

effective. The performance of a defoamer is difficult to predict due to the multiplicity of materials used in a formulation and the method of application, so evaluation of the respective system is crucial for a selection and optimal dosage determination. In the case of our samples, after some compatibility trials with the available defoamer TEGO Foamex 805N presenting bad coating optical features ("oil stain" visible on the coating), it was preferred not to add a defoamer in order to maintain the coating formulation as simple as possible, therefore the foam generated in the various mixing process was removed by placing the sample batches in an ultrasonic bath for few minutes according to the amount of foam generated.

5.5.2 - DISPERSIONS STABILIZATION

As soon as the particle size have been measured after grinding, the "dispersions" were separated from the milling beads and under vigorous stirring, heated up to 60°C. Transparent grade Xanthan gum, to the measure of 1% w/w on dispersion, was then carefully added, keeping stirring until the formation of a homogeneous and transparent gel (about 40min). The same process was followed for the non-milled samples in 5% water/dispersant suspension (GI, RI, GO, RO).
The gels obtained contain therefore 1% of Xanthan gum and 5% of pigment.

5.5.3 - COATING HYDROPHOBIZATION

The principal deterioration phenomena in the C.H. field are related to the presence of water in the materials porosity. A protective coating should therefore be hydrophobic without creating a barrier to vapour permeability. The protective products in this sense could be divided in: monomers dissolved in organic solvent (in situ polymerization) and polymers, applied in solution or water emulsion. For what concerns the acrylic resins, the water-repellence feature is lost in few month after the application. Therefore they cannot be listed as protectives. However, hydrophobization could be obtained in two ways: mixing the acrylic resin to one siliconic resin or preparing an inorganic-organic hybrid, as an acryl-siloxane or acryl-fluorinated copolimer. In this sense the addition of

a fluoroalkyl organosiloxane (Dynasylan F8815) was experimented. Although this additive was reported to give good water repellence results in combination with Primal AC399, the exclusion of the latter from the matrices list, because of its interaction with the dispersing agent, led to the need of performing other tests in combination with Acrilem IC390 and Acryl33, which gave similar results. Drawbacks of the use of this additive are the insertion of inorganic bonds Si-O, not removable by plasma treatment [8 in Ch.6] and the subtraction of coating transparency. Moreover the polymerization process turned out to be very sensitive to temperature gradients and foam presence. In the presence of dispersing agent, but more extensively in the presence of Xanthan gum, flocculation occurs. Clearly this hydrophobing agent is not assessable to a coating based on a xanthan gum-gelled fluorescent pigment dispersion.

5.5.4 - CONCENTRATION AND DILUTION TESTS

The coatability (and the coating homogeneity) of formulations with different ratios dispersion/matrix/water was then evaluated. Table 5.1 shows the different matrix dilution experimented, and it was designed in order to test a 26% dilution (medium dilution selected from those typically used for Acryl33) with different pigment concentrations. The table shows the parts of water and Acryl33 to be added to 1 part of dispersion, the pigment percentage corresponding to 0.23, 0,92 and 1,84 dry resin parts are therefore 20%, 5% and 2,5% respectively. The percentages were selected on the basis of the pre-tests, showing good fluorescent output for 5% coatings, but this time the pigments were not included in the formulation.

Acryl33 dilution [% on water]		**Dry resin*** **[parts] - (46% emulsion on 5% gel [parts])**		
		0,23 – (1:2)	**0,92 – (1:0,5)**	**1,84 – (1:0,25)**
Dilution Water [parts]	**1,94**	25,8%	103,2%	206,2%
	7,75	6,5%	25,8%	51,6%
	15,50	3,2%	12,9%	25,8%

* Supplied as Acryl33 (46% dispersion)

Table 5.1 – Concentration/dilution experiment

The highest dilution did not show phase separation in formulation and the coatings (very thin) are also more homogeneous than for the other dilution (no floating). On horizontal surfaces, floating is seen as hexagonal patterns, called Bénard cells. The observed Bénard cells morphology is due to the film-formation during the solvent evaporation because of the "no-flow point" reaching; in pigmented systems, the pigments settle in different areas, depending on their mobility. Floating and bad wettability defects are usually avoided by minimizing surface tension differences during the drying process, in this case are avoided thinning the coating and lowering the resin concentration. The selected Acryl33 concentration was therefore 3,2% on water (i.e. only 1,5% of solid content); this super-dilution is unusual, but necessary to obtain well-spread and defects-free coating. This level of dilution could also cause problems trying to obtain realistic film thickness (from superposition) but, more importantly, could cause anomalous pigment spreading while coating (mostly in spin-coating). Having the pigment concentration in the dispersion fixed, and selecting this ratio gel/Acryl33/water, the concentration of pigments in the final coatings was automatically determined as 20%.

As shown in Table 5.2, the matrix content was then varied in order to obtain coatings with different concentration of pigment once dried (1% , 10%, 20%) and perform the concentration/thickness/fluorescence intensity tests.

Pigment (5% mixture) **: Xanthan gum** (pure powder) [parts]	**Pigment on resin** [dry %]	**Resin** (46% emulsion)**: pigment** (5% gel) **: Water** [parts]
1 : 0,01	20	1 : 2,00 : 31,00
	10	1 : 1,00 : 15,50
	1	1 : 0,10 : 1,55

Table 5.2 – Pigment on matrix concentrations for the concentration/thickness/intensity experiments

5.5.5 - COATING DEPOSITION

Before the deposition, the substrates were cleaned profoundly since the initial contact angle (60° for the glass slides) made it impossible to adequately coat water-based

formulations. After soap, acetone and NH_3/H_2O_2 cleansing in a row, the contact angle was lowered from 60° to 16° degrees.

After several deposition trials by means of coating bar and spin-coater , during the pre-tests and the hydrophobization experiment, dip-coating was preferred as deposition method thanks to the better coatability of the low-evaporation-rate waterbased formulation and the method reproducibility. In particular when speaking of dip-coated surfaces, the presence of foam could cause bad deposition, therefore the samples were left in ultrasonic bath until foam-disappearance.

The solvent evaporation could cause the formation of different concentration-zones, starting from the support's borders. The extracting rate is the principal variable of the dip-coating deposition: the faster the extraction rate (mm/min), the more uniform and thicker the coating will appear. The best results, during the dilution/concentration experiment, are obtained with an extraction rate of 20mm/min repeated on the same sample for three times, reaching a 300nm thickness (i.e. the same average thickness obtained by brush coating of these formulations) homogeneous coating. The rate selected for the pigmented coating to be aged was then 40mm/min, with only two subsequent depositions, followed by a 30min oven drying at 65°C. The thickness measured for these samples are of 190±15nm for all the additives (independently from the dispersion initial viscosity due to each pigment). Obviously the "blank" samples (without pigments), do not contain Xanthan gum, therefore more coating steps are needed in order to reach the same thickness. Normally, this thickness cannot be considered valid for the needs of the subsequent plasma removability test, in spite of this, the PANNA cold plasma torch parameters could be adjusted in order to monitor the removability of these thin films, comparing the removal rates of different samples.

This kind of deposition gave good results for what concerns the organic pigment, that are maintained in dispersion thanks to the presence of the organic-dedicated dispersing agent (and the continuous stirring). However, the inorganic pigments are not dispersed adequately and therefore settle down before being deposited. For this reason the inorganic pigmented formulation (GI and RI) were coated by means of brush-coating, in order to evaluate adequately the fluorescence/yellowing and removability properties of the coating (see Chapter 6) (Fig. 5.4).

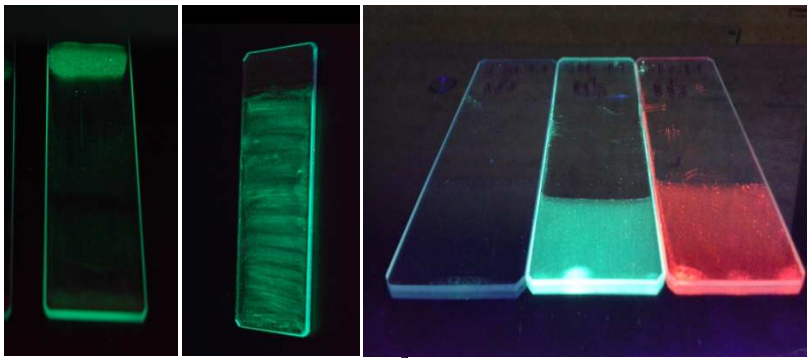

Figure 5.4 – inorganic pigment coated with coating-bar, brush and dip coater, compared to two dip-coated organic pigments(on the right)

5.6 – RESULTS AND DISCUSSION II°: PIGMENTS IN THE COATING

The coated samples are formulations containing the pigments PFLI-G (“GI”), PF-R7 (“RI”), PFLO-G (“GO”, “GO1d”, “GO5d”) and PFLO-R (“RO”, “RO1d”, “RO5d”). As seen in the previous chapter the organic samples identified as “1d” and “5d” correspond to the milled pigments (i.e. ~190nm particles, with different processing times). Another sample was then coated: “GO5d+RO5d” (or “GRO5d”), that is the mixture of the two organic pigments in their smallest particle size. All the samples have a 20% concentration of pigment on the dry filming-resin, the latter included (therefore 10% of GO5d and 10% of RO5d). The high pigment content, due to the dispersion stabilization limiting step, grant the monitorability of the fluorescence in a long period of time and a good fluorescence output also from coating as thin as 200nm.

When the pigments are dispersed in a matrix, the resulting spectrum is a combination of a number of factors: (a) the reflectance of the non-fluorescing materials; (b) the absorbance of the fluorescent material due to the excitation of electrons to a higher energy state; (c) the emission spectrum of the fluorescing material.

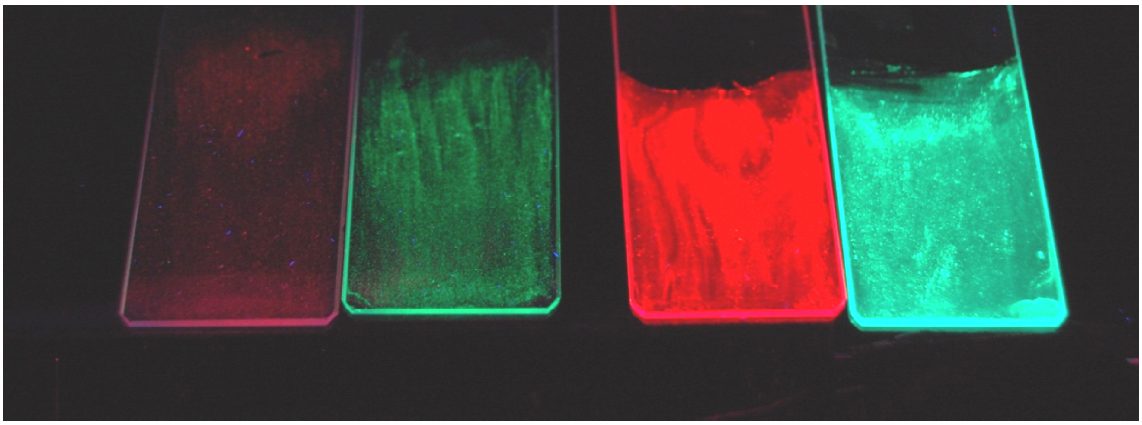

Figure 5.5 – inorganic (brush-coated, on the left) and organic (dip-coated, on the right) pigment fluorescent coating under 365nm UV light

From the PL spectra it is possible to observe an evident decrease of the 706nm peak in the samples containing Eu^{3+} (reds, the inorganic one in particular), while nothing changes for the green samples. The PL spectrum of "GRO5d" is simply the superposition of green and red samples emissions (Fig. 5.7a). The fluorescence intensity varies a lot for different particle sized sample (for the milled sample, PFLO-G and PFLO-R) as shown in Fig.5.6: although in the grinding stage (Chapter 4.5), i.e. when not in the presence of thickening agents, a decrease in the fluorescence output was observed, for these samples the smaller were the particles the higher was the fluorescence intensity. For what concerns PFLO-R (organo-metallic chelate) also the processing time is quite important: although the samples milled for 20h and that milled 120h have almost the same particle size, the longer processing degrade the molecules, decreasing their fluorescence output.

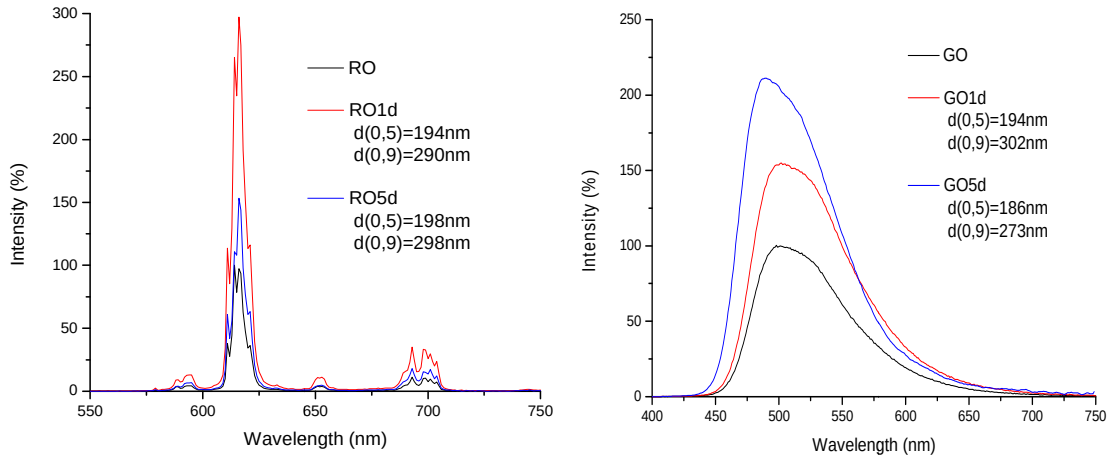

Figure 5.6 – Organic pigments intensity in function of particles size

a) 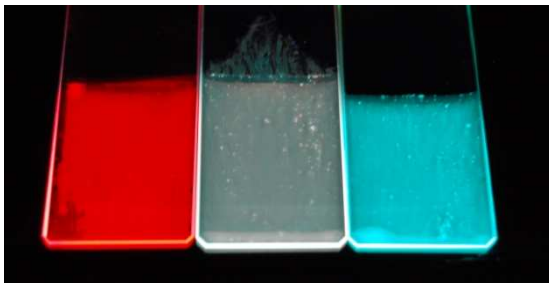 b) 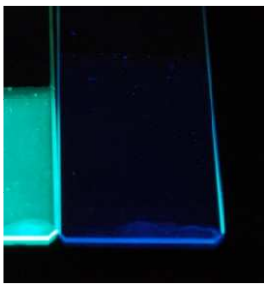

Figure 5.7 – a) Organic 120h milled pigments and their 1:1 mixture; b) Emission of a coating from a 20% watersoluble fluorophore (dye) formulation

When embedded in the matrix, all the 9 PLE spectra show the same drastic intensity decrease for wavelength longer than 350nm. The PLE spectra obtained from the "mixture" sample remain unchanged compared to the single pigments samples (with halved intensities for halved concentrations), showing that there is no interaction in the fluorescence mechanism of the two luminescent materials.
In order to evaluate the properties of the pigments, also a formulation containing a watersoluble fluorophore (dye) was coated, maintaining the concentration at 20% as for the pigments. As can be seen from Fig. 5.7b, the fluorescence output from the pigments is not even comparable to that of the dye, and the same applyes to its lightfastness as explained in Chapter 6.

5.6.1 – FLUORESCENCE LIFETIME DECAY

Table 5.3 reports the lifetime ("τ obs", in milliseconds) observed for the fluorescent pigments powders in Chapter 3, and the relative samples identification names when embedded in Acryl33 matrix. The lifetime value for a fluorescent watersoluble organic additive (TINOPAL dye) is also presented as comparative data for the organic emitter HPQ (PFLO-G). The FLT analysis showed the different fluorescent behaviour of the samples in a matrix, also in relation to the matrix UV ageing (Tab. 5.4).

Sample	Compound	τ obs [ms]	Sample in matrix ("M") ID
PF-R7	$Y_2O_2S:Eu^{2+}$	0,64 ± 0,008	RI
PFLI-G	$BaMgAl_{10}O_{17}:Mn^{2+},Eu^{2+}$	5,50 ± 0,008	GI
PFLO-R	$Eu^{3+}(TTa)_3(TPPO)_2$	0,72 ± 0,003	RO
PFLO-G	HPQ	$6,29*10^{-6}$ ± 0,008	GO
TINOPAL	unknown	$1,02*10^{-6}$ ± 0,080	DYE

Table 5.3 – Powder samples identification and observed lifetimes

ID	τ obs M [ms]	τ obs M aged [ms]	τ obs M 1d [ms]	τ obs M 1d aged [ms]	τ obs M 5d [ms]	τ obs M 5d aged [ms]	τ obs M 5d mixture [ms]	τ obs M 5d mixture aged [ms]
RI	0,49 ± 0,003	0,43 ±0,004						
GI	5,39 ± 0,008	5,39 ±0,008						
RO	0,57 ± 0,001	no signal	0,69 ± 0,001	no signal	0,70 ± 0,001	no signal	0,67 ± 0,001	no signal
GO [$*10^{-6}$]	6,11 ± 0,001	5,27 ±0,009	6,72 ± 0,010	3,84 ± 0,015	4,58 ± 0,030	3,13 ± 0,015	6,35 ± 0,009	3,63 ± 0,025

Table 5.4 – Embedded samples observed lifetimes (τ obs M) for different sized particles (20h and 120h milled organic samples) before and after artificial UV ageing (14,3 years).

All the samples lifetimes are reduced when the pigments are embedded in Acryl33, for example the red and green organic sample lifetimes vary from 0,72 ms to 0,57 ms and from 6,29 ns to 6,11 ns respectively. The Dye lifetime is much faster than the pigments' (1ns) but remains in the organic compounds decay range of nanoseconds. The decay curves for all the samples are shown in Fig.5.8.

Concerning the inorganic samples, PF-R7 (RI) present a faster decay compared to PFLI-G (GI), and that is a reason for the preferred use of this phosphor ($Y_2O_2S:Eu^{3+}$) in

optoelecronics. In this case, the decay is accelerated when the coating is aged while remaining fixed for the green sample (GI).

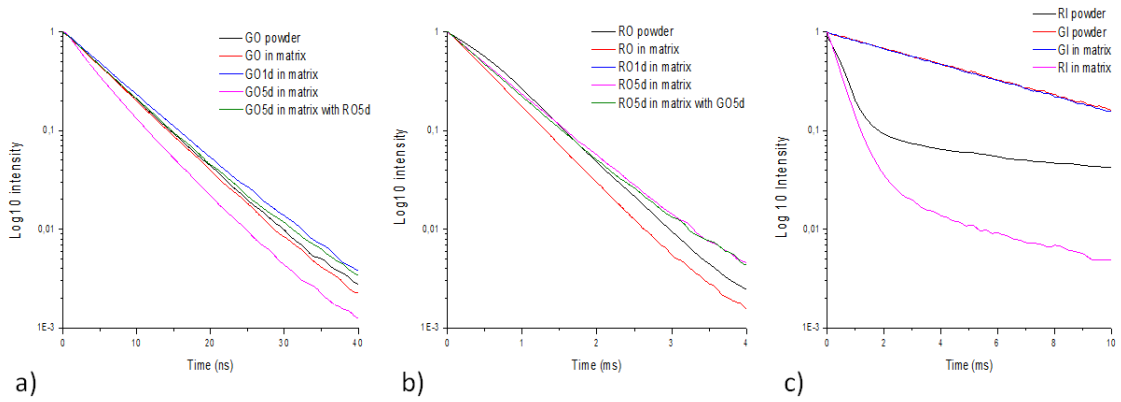

Figure 5.8 – Decay curves for: a) Green organic samples (HPQ); b)Red organic samples (Eu^{3+} complex); c) Green and red inorganic samples (Eu^{2+},Mn^{2+} doping and Eu^{3+} doping, respectively)

The organic samples decay is quite different; therefore no interaction (energy transfer) between the two pigments in terms of lifetime decay is due to happen. The differences between the lifetimes of GO5d and GO5d+RO5d (Tab 5.4) observed in Fig. 5.8a, 5.9c and 5.9d are likely to be ascribed to a HPQ internal concentration quenching, not happening for what concerns the organic complex (RO5d). The double exponential decay behaviour shown by the milled PFLO-G samples after UV ageing (Fig. 5.9) is attributable to a more efficient transfer from the donor to the activator compared to the un-aged samples. The lifetimes of the aged samples were not measurable for the red organic samples, because of the complex deterioration (i.e. low fluorescence signal).

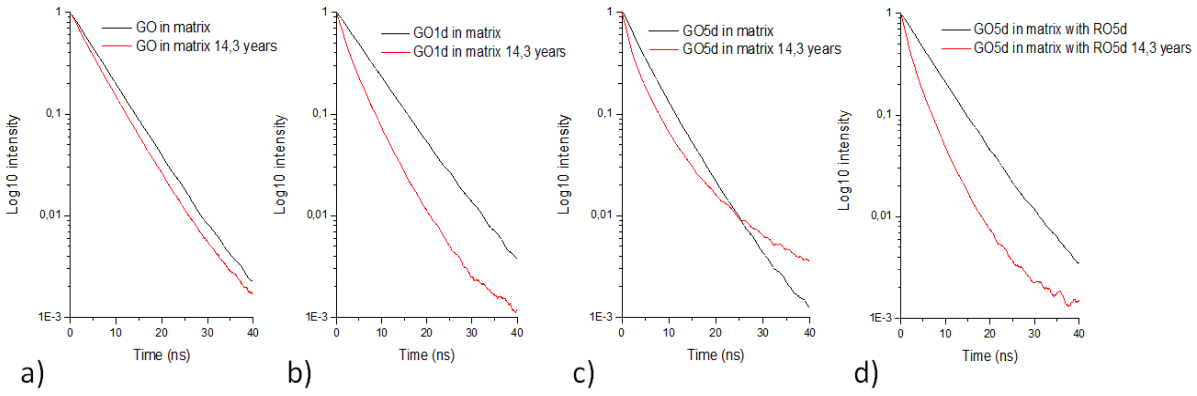

Figure 5.9 – Embedded PFLO-G samples before and after ageing: a) un-milled, b)20h milled; c)120h milled; d)120h milled, halved concentration in the presence of PFLO-R.

The samples with smallest particles (RO1d and GO5d) have a faster lifetime decay compared to the other samples embedded in the same concentration (20%). The lifetimes are, instead, even longer than the samples with bigger particle size (Tab. 5.4) when speaking of the mixture of organic pigments, i.e. for lower concentrations.

5.6.2 – THICKNESS AND CONCENTRATION: ON THE CORRELATION WITH FLUORESCENCE OUTPUT

It is known that a linear correlation between fluorophore concentration and fluorescence intensity could be observed only using low pigment concentrations (see Chapter 1.1). In order to define a useful relation and therefore obtain calibration curves for the evaluation of coatings containing the studied samples, the fluorescence output at different fluorophore concentrations (1%, 10% and 20%) was measured for the four studied samples (Fig. 5.10). The organic samples considered were only those milled for 120h, i.e. RO5d and GO5d, in order to reduce the samples number.

As shown in Fig. 5.10 and Fig. 5.13, a linear correlation is observed between coating thickness and pigment concentration only for the 20% sample for what concerns the red glowing sample (Eu^{3+} complex) and for all the concentrations for what concerns the green glowing (HPQ). The intensity vs concentration plot for 200nm thick coatings (Fig. 5.10c) shows two curves, instead. The HPQ sample present an exponential trend, approaching a plateau, while the Europium complex output as function of the concentration could be represented by a peak function, reaching a maximum around the 10% concentration. Saturation of light output with increasing doping density is primarily a kinetic problem. Excluding temperature rising, the most probable causes of saturation are: saturation due to excited state interaction and true activator saturation, i.e. excitation of a large fraction of available activator sites causing significant depletion of the ground state population.

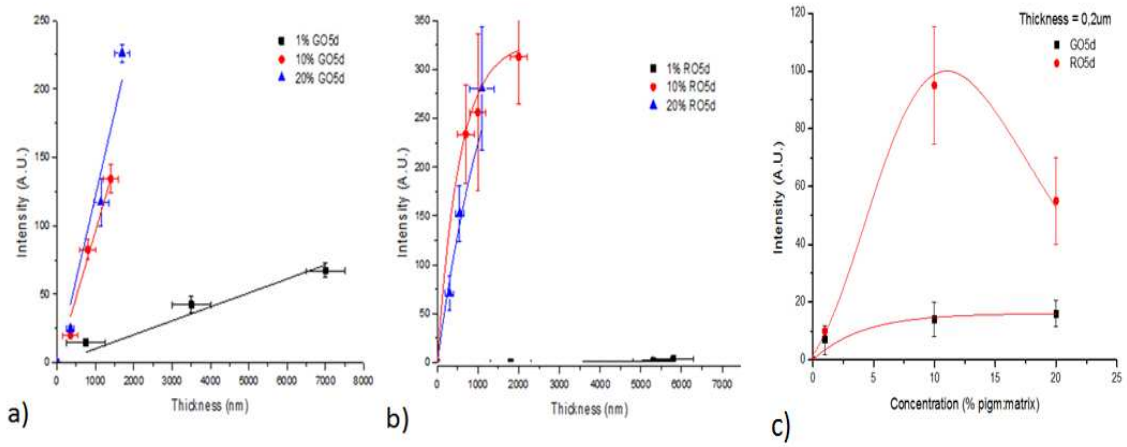

Figure 5.10 – Plots of the fluorescence output from the organic samples: a-b) as a function of the coating thickness at different concentration (a) PFLO-G 120h milled, b) PFLO-R 120h milled); c) as a function of the concentration (in 200nm thick coatings)

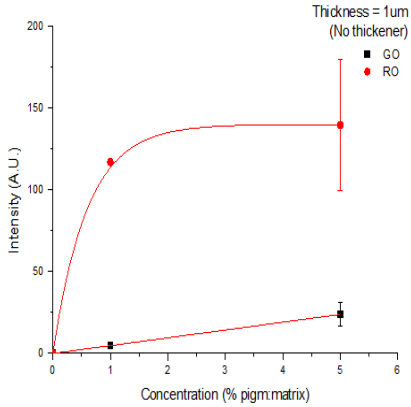

Figure 5.11 – Plots of the fluorescence output from the non-milled organic samples as a function of the concentration, in 1micron thick coatings without the thickener presence (from pre-tests)

Comparing Fig.5.10b and Fig. 5.11 it can be observed how the fluorescence output of the green glowing organic pigment (HPQ) is enhanced by the presence of thickener (increased viscosity), while the red glowing metal-organic complex is not. It has to be pointed out that the plot in Fig. 5.11 is based on the pre-tests data, therefore on the non-milled samples.

For what concerns the inorganic pigments, an exponential trend is detectable both in the thickness/intensity plots (Fig. 5.12a and 5.12b) and in the concentration/intensity plot

(Fig. 5.12c); in the latter, the Europium doped yttria (RI) present an exponential growing and not an exponential decay, though.

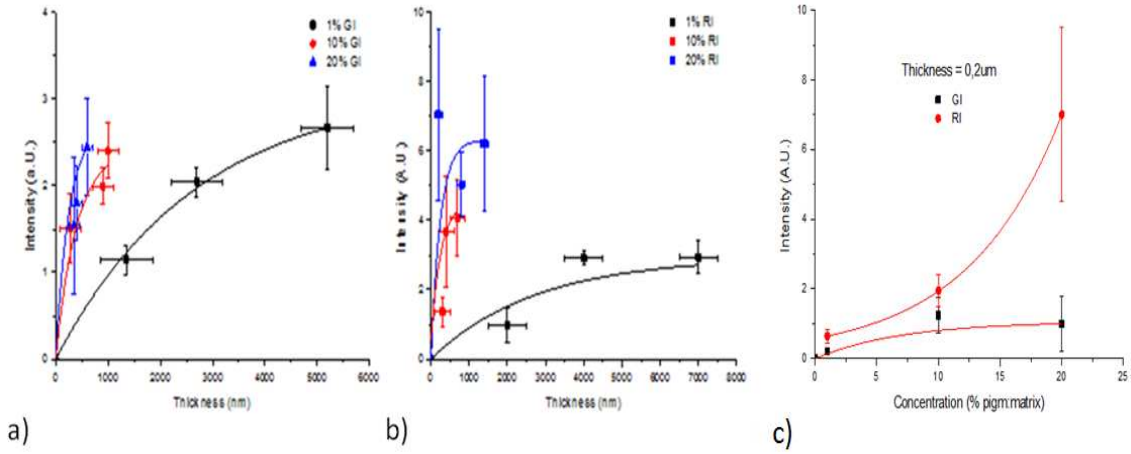

Figure 5.12 – Plots of the fluorescence output from the inorganic samples: a-b) as a function of the coating thickness at different concentration (a) PFLI-G, b) PF-R7); c) as a function of the concentration (in 200nm thick coatings)

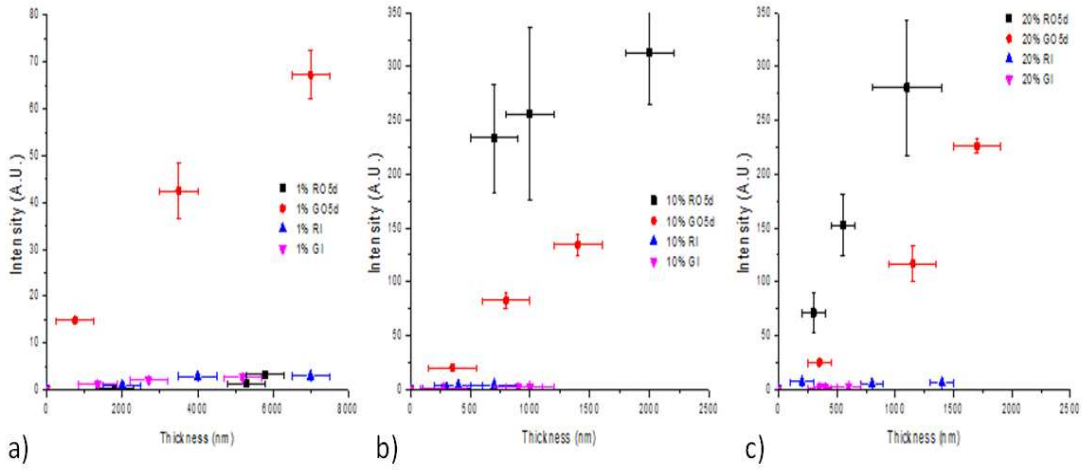

Figure 5.13 – Coatings thickness as function of fluorescent output for the four samples at different concentrations: a) 1%; b) 10%; c) 20%.

5.7 – CONCLUSIONS

The coated samples are formulations containing the pigments PFLI-G (“GI”), PF-R7 (“RI”), PFLO-G (“GO”, “GO1d”, “GO5d”) and PFLO-R (“RO”, “RO1d”, “RO5d”). Another sample was “GO5d+RO5d”, that is a mixture of the two organic pigments in their smallest particle size.

PRODUCT	**SAMPLES ID**		
	Unmilled	**Milled 20h**	**Milled 120h**
INORGANIC SAMPLES			
PFLI-G	GI	-	-
PF-R7	RI	-	-
ORGANIC SAMPLES			
PFLO-G	GO	GO1d	GO5d
PFLO-R	RO	RO1d	RO5d
PFLO-G + PFLO-R	-	-	GO5d+RO5d

Table 5.5 – Coated samples ID

All the samples have a 20% concentration of pigment on the dry filming-matrix, the latter included (therefore 10% of GO5d and 10% of RO5d). The high pigment content, due to the dispersion stabilization limiting step, grant the monitorability of the fluorescence in a long period of time and a good fluorescence output also from a coating as thin as 200nm.

The first step of the coating preparation was the stabilization of the “dispersions” obtained in the grinding section: the 5% pigment dispersions were stabilized adding 1% Xanthan gum.

Coating preparation

Three different matrices were tested but only two of them were compatible with the dispersant selected in the grinding section; one of them (Acryl33) was selected as film-

forming agent because of its wide use in the C.H. field. The addition of surface tension modifiers, one anti-foamer and one hydrophobing agent was tested, though not successfully. In particular, the fluoroalkilsiloxane used as hydrophobing agent interacts with Xanthan gum (thickener), but also with the dispersing agent when the thickener was not present, causing flocculation. After the determination of thickener needed in order to maintain the pigment dispersed, dilution/concentration coating experiments determined the exact amount of dispersion, film-forming matrix and dilution water in the formulations. The selected formulation had a 1,5% of solid resin content on water and a 20% concentration of pigment on dry resin. Several deposition methods were evaluated, and dip-coating gave the best performances in terms of homogeneous coating spreading and drying. The dip-coater extraction rate selected for the pigmented coating to be aged was 40mm/min, for two sequential deposition, followed by a 30min oven drying at 65°C, giving a 190±15nm thickness. For what concerns the inorganic pigments, giving their particle size and non-dispersability by the selected dispersing agent (as seen in Chapter 4), they had to be brush-coated in order to evaluate the performances of the matrix in their presence.

For the preparation of commercial formulations, the specific substrate, application method and storing characteristics will have to be defined.

Pigments in the coating

The fluorescence intensity varies a lot for different particle size samples: although when not in the presence of thickening agents a decrease in the fluorescence output was observed (Chapter 4), the smaller were the particles, the higher was the fluorescence intensity. For what concerns PFLO-R (organo-metallic chelate) also the processing (milling) time was found to be quite important. When embedded in the matrix, all the PLE spectra show the same drastic intensity decrease for wavelength longer than 350nm. No interaction in the fluorescence mechanism of the two luminescent materials is detected from the PLE spectra obtained from the “mixture” sample. All the samples lifetimes are reduced when the pigments are embedded in Acryl33. The samples with the smallest fluorescent particles have a faster lifetime decay compared to the other samples embedded in the same concentration (20%), while for lower concentrations the lifetimes are even longer than the samples with bigger particle sizes. In this sense the samples’ lifetimes are function of the concentration.

In order to define a useful relation and therefore obtain calibration curves for the evaluation of coatings containing the studied samples, the fluorescence output of coatings with different pigment concentrations (1%, 10% and 20%) was measured. It can be observed fluorescence output enhancement for the green glowing organic pigment (HPQ) when in the presence of thickener (increased viscosity). For what concerns the inorganic pigments, an exponential trend is detectable both in the thickness/intensity plots and in the concentration/intensity plots. A linear correlation is observed between coating thickness and pigment concentration only for the 20% sample, for what concerns the red glowing organic sample, and for all the concentrations for what concerns the green glowing one. The intensity of the HPQ sample (PFLO-G) present an exponential trend, rapidly increasing and approaching a plateau for high concentration, while the Europium complex (PFLO-R) presents concentration quenching phenomena, therefore being described by a peak function.

REFERENCES

[1] *Practical fluorescence 2° edition*, G. G. Guilbault, Guilbault ed., 1990

[2] *www.dispersions-pigments.basf.com* – BASF, The chemical company

[3] *Anti-settling agents for acqueous coating compositions,* US patent US5374687A, R.C. Cooperman, W.W. Reichert, 1991

[4] *A guide to understanding and mixing thickeners*, C.Angos, Charles Ross&son company, 2008

[5] *Water dispersed polymers for textile conservation: a molecular, thermal, structural, mechanical and optical characterization*, M. Cocca, L. D'Arienzo, L. D'Orazio, G. Gentile, C. Mancarella, E.Martuscelli , C.Polcaro , J. of Cultural Heritage Vol 7, 2006

[6] *Stable acrylic ester latex coating composition*, UK patent UK3996177, B.F. Goodrich company, 1977

[7] *Chimica, scienza e tecnologia dei materiali per la conservazione dei beni culturali*, Ezio Marusticelli, EnzoAlbano ed.,2014

[8] *www.brescianisrl.it* – BREASCIANI SRL materiali e attrezzature per il restauro

[9] *Degrado dei materiali*, Chiantore O., Scalarone D., Materiale didattico corso di Chimica dell'Ambiente e dei Beni Culturali, Univerisità degli studi di Torino, 2008

Chapter – 6 –

UV AGEING

TEST

6.1 – INTRODUCTION

Not only has the matrix a great influence on the initial fluorescent output, in relation to the coating thickness and concentration, but also on the fluorescent decay behaviour. Its deterioration (e.g. yellowing and removability) is, in turn, influenced by the presence of additives. On the other hand, the presence of different pigments, and their different particle sizes, would impact differently on the coating aspect (e.g. transparency and colour) and reversibility (e.g. removability by means of cold plasma).

Main aim of this thesis was the correlation of the intensity of the fluorescence output with the health status of a water-based coating from which it is detected. This implies, of course, the understanding of the decay processes suffered by the pigments and the coating itself. Detailed studies on the ageing/weathering of the coating, taking into account the substrate and the damaging factors implied, would make the intensity/health status study more accurate and realistic.

This chapter proposes to define the spoiling effects that a prolonged exposure to UV rays, therefore sun- or artificial- lightening, would have on a coating embedding the selected commercial fluorescent additives, also in relation to their particle size.

The coating properties evaluated were: fluorescence output (PL/PLE peaks and intensity), fluorescence lifetime decay (FLT), yellowing and removability by means of cold atmospheric plasma torch. One of the fundamental properties of a synthetic polymer for Cultural Heritage restoration is its reversibility. The commercial products cannot always maintain their characteristics; in fact, the chemical-physical modifications in time (through freeze-thaw cycles, exposure to UV radiation, and thermal cycles) could have several drawbacks such as loss of efficiency, yellowing, removal impossibility and limitations to conservative treatments. The main agents that cause or accelerate the aging of a polymer exposed to the external environment are light, temperature and humidity. The light induces chemical reactions, that can lead to a change in colour or the breaking of C-C bonds and C-O, which depends on photon energy (see Chapter 1.1 and 5.3). The oxygen acts directly or in pairs with the photolytic degradation processes through auto-oxidation, bio-oxidation, photo-oxidation and combustion. The combined effect of oxygen and temperature leads to the formation of peroxides and hydro-peroxides which are very unstable. The water may cause

breakage of the molecular chain of the polymer, with a considerable catalytic effect of the ions in solution. Air pollutants such as ozone, sulphur dioxide, nitrogen oxides, metallic residues of Cu and Fe, are actively involved in the degradation of synthetic polymers by acting as catalysts or favouring hydrolytic processes through the entrapment of water, and retaining biologically active materials. Here, the light deterioration phenomena were investigated. Among the numerous factors from which the stability of a polymer depends, including chemical nature, morphology, degree of crystallinity, formulation, film thickness and especially aging conditions, the impurities presence (i.e. additives as pigments) is one of the most important. Therefore, the samples in object were the formulations coated on glass slides and silica wafer in chapter 5: two containing the inorganic samples PFLI-G and PF-R7, and seven containing the organic samples, respectively PFLO-G (non-milled, 20h milled and 120h milled), PFLO-R (non-milled, 20h milled and 120h milled) and a 1:1 mixture of them (from the samples milled for 120h). As yardstick, a coating formulated with an available fluorescent dye, in the same concentration of the pigments (20% on dried coating), was aged and tested.

The in-depth study of the removability, yellowing and fluorescent decay phenomena, would be a valuable feature for the selection of a certain commercial fluorescent product as additive in coating formulations.

6.2 – COLOURIMETRY

Colour and yellowness

The samples colour was measured both before and after the light exposure according to the CIE-L*a*b* method (CIE = "Commission Internationale de l'Éclairage"). A Lab colour space is a colour opponent space with dimension L* for lightness and a* and b* for the colour-opponent dimensions. This space is based on nonlinearly compressed (cube root transformation) CIE 1931 XYZ coordinates, which can predict which spectral power distributions will be perceived as the same colour, not being particularly perceptually uniform, though. The colourimetric measurements are therefore based on the reflectance, that is, the rate between the flux intensity from the radiant light and that from the incident light. L*a*b* stands for a worldwide standardized method of colour

measurement, represented by a three-dimensional colour system, where L* indicates the position on the grey axis (L*=0 yields black and L*=100 indicates diffuse white), a* the position on the green/red axis, and b* the position on the yellow/blue axis. The colour difference is represented by the Δ E *, calculated from: $\Delta E^* = \sqrt{(\Delta L^*)^2 + (\Delta a^*)^2 + (\Delta b^*)^2}$ [1]. If the Δ E * is less than 4, the colours will show no visible colour change under museum conditions (exposure to the standardized amount of artificial light) for approximately 125 years. If the specimens are fluorescent, the choice of the instrument optical geometry can affect the measurement result. The spectral power distribution of the illuminating system may be altered by the reflected and emitted power from the specimen when using the integrate sphere geometry; therefore, the bidirectional geometry should be preferred.

This study focuses on the yellowing caused by the pigments and by the UV exposure. The ASTM (American Society for Testing and Materials) has developed a method for the yellowness index (Yi) calculation[2], in order to indicate the degree of departure of an object colour from colourless (or from a preferred white) toward yellow. The required coefficients in this case consist of the tristimulus values of the reflecting diffuser (X_n, Y_n and Z_n), established by the CIE. The calculation for illuminant C described in the ASTM E313 is:

$$Yi = 100 \times \left[1 - \left(\frac{0{,}847Z}{Y}\right)\right]$$

Typically, the yellowness index is measured for a reference representing the ideal white and is normalized for the thickness of the film. Here, is reported as “ΔYi”, that is, the deviation of the pigmented sample index from the blank sample index, relatively to each ageing time. When determining the non-pigmented coating yellowness, the reference is the BA sample (i.e. the sample with “filming resin only”). The normalization is not needed having films with fixed thickness.

Transparency evaluation

The appearance of a transparent product is defined by its application. The absorption and scattering behaviour of the specimen will determine how much light will pass through and how objects will appear through the transparent coating. Absorption and reflection properties influence the transmittance (direct and diffuse), determining the haze and see-through quality of the sample. The wide angle scattering diffuse light in all directions, causing a loss of contrast, while the narrow angle scattering diffuse light

in a small angle range with high concentration defining how the details can be seen through the specimen [3]. Therefore, dedicated instruments for this type of evaluation measure the transmitted light. When speaking of opacity the focus is on the hiding power. The opacifying effect is proportional to the difference between the refractive index of the pigment and that of the medium in which it is dispersed. Inorganic pigments have a high refractive index and organic pigments have much lower values. Consequently, most inorganic pigments are considered opaque, whereas organic pigments are transparent. The particle size distribution of the pigment is another factor that also plays an important role in opacity. As the particle size increases, the ability of the particle to scatter light increases, up to a maximum. It then starts to decrease. This ability to scatter light increases the hiding power of the pigment, and therefore the hiding power also reaches a maximum and then decreases as the particle size increases. Whereas the refractive index of a compound cannot be altered, the particle size of pigments can be adjusted; consequently particle size selection has become one of the principal developments in pigment technology in recent years [4]. The colourimeter used is able to perform contrast or percentage of opacity measurement. Each measurement requires three readings (over black, over white, and on white background) [5]. However, the method used for evaluate the coating hiding power relate on the L*a*b* measurement. The multiple dimensions of the visual experience of lightness, brightness, and transparency were considered: people do not perceive the lightness of surfaces by discarding information concerning the light illuminating those surfaces; rather, they perceive a pattern of illumination projected onto a pattern of surface greys [6]. The value considered was therefore L* as measure of the brightness (i.e. the attribute of a visual sensation according to which an area appears to emit more or less light, while the lightness is the brightness of an area judged relative to the brightness of a similarly illuminated area that appears to be white or highly transmitting). The L* value was measured for the different ageing times on the films, coated on the glass transparent surface, superposed to the black reference of the colourimeter: the lower the L* value, the higher the transparency. The transparency gain (or loss) due to the presence of the coating additives (dispersing agent, thickening agent and the different pigments with different particle sizes) was then evaluated in terms of ΔL^*.

6.3 – COLD PLASMA TORCH

Within the surfaces cleaning, the elimination of the dysfunctional polymer layer is expected, as a maintenance operation to be concluded with the application of another product. For example, the cleaning methods allowed on stone surfaces, classified as mechanical, chemical and physical, are: water spray, aqueous wraps (whether with aqueous or organic solvents), aqueous solutions or suspensions with complexing or solvent action, ion exchange resins, mechanical methods (scalpel, brushes, sandblasting, micro-drilling machines, ultrasound) and physical methods(laser cleaning using low energy impulses). The chemical removal does not exclude the possibility of a conveyance towards the substrate of part of the substances carried in solution, leading to the alteration of the artefact, and are often harmful both for the operators and for the environment.

Plasma removal falls both in the physical and chemical category. The plasma is defined as the fourth state of matter and is an ionized gas composed of positive ions, negative ions, radicals and electrons. When energy is added to a gas, ionization reorganizes the electronic structure of the gas and produces excited species and ions. Overall, plasma is electrically neutral but contains free charges and is electrically conductive because of this structure. The energy required to generate and sustain this ionized gas is typically provided in the form of heat, electricity or electromagnetic radiation. The plasma provides highly active species (ozone, radicals, etc) that can reduce or oxidize molecules on a surface: the main process by which atmospheric plasmas can be used for cleaning is the transformation of a film in reaction products and volatile gases released into the atmosphere (such as CO_2, CO and H_2O). Once excluded the thermal effect, the action is purely chemical and superficial, without requiring any direct contact.

In plasmas generated by the application of an electric field, energy is transferred mainly to the free electrons because of their greater mobility, and then dissipated through elastic and inelastic collisions with other species present in the plasma. The ionization collisions are needed to start and sustain the plasma, it is therefore necessary for a part of the electrons to have energy sufficient to trigger these processes. In the case of atmospheric plasmas (bootable in environmental pressure conditions), elastic and inelastic collisions between different species heat up the system, thus increasing the temperature of the neutral gas and ions. The plasma properties vary depending on the

type of generator used, the torch configuration, the pressure and the type of gas; the main descriptive parameters are electron density and temperature. Since the atmospheric plasmas are typically thermal, the research over the past 10 years has focused on reducing the heat load on the surfaces in contact with the plasma. Special configurations permit to obtain non-thermal plasmas. A very high oscillating potential difference (AC voltage) is required in non-thermal plasma since it influences the behaviour of the electrons and ions. The energy of the electric field gives energy to the electrons of the working gas, accelerating them to collide with neighbouring neutral particles exciting/ ionizing them. The excited states relax to the ground state by giving off a photon, and the result is an emission spectra of the working gas used (the plasma is visible in the plume that exit the torch). A *cold atmospheric plasma* is the ionized gas generated at atmospheric pressures and produces a plasma that is "cold" enough to be touched. The term "cold" refers to the generation of the plasma being non-thermal, but also describes the temperature of the accelerated electrons being extremely higher than the heavy particle temperature [9].

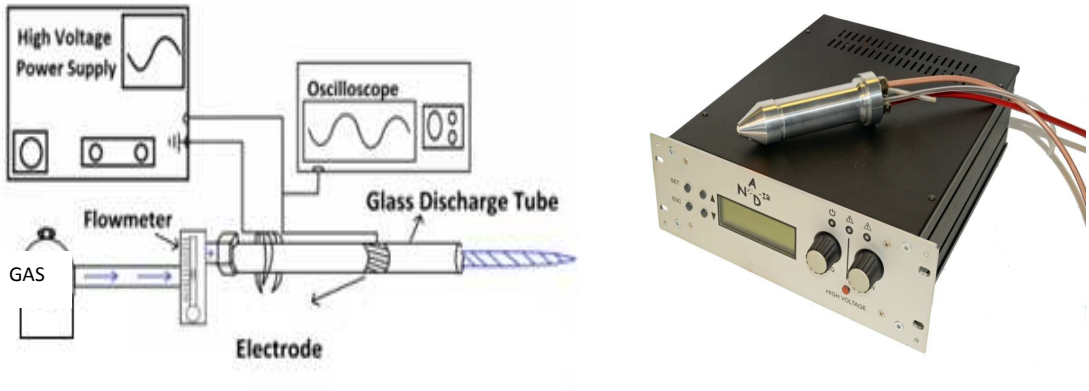

Figure 6.1 - Setup of an atmospheric plasma torch (left) and the Nadir portable cold atmospheric plasma torch (right)

The chemistry of reactive species generated depends on the initial working gas used for the plasma, as different gases will produce unique plasmas with a multiplicity of reaction initiation. The gas most commonly used is helium because of its high thermal conductivity. The gases used in this study for the removal of polymeric coating were Oxygen and Argon. The oxidizing mode is active when combining the two gases while employing only Argon the reductive effect is obtained [11].

The innovation brought by the plasma jet torches lies in their size that allows portability, low cost and versatility and selective treatment of certain areas of materials (which may be characterized by curved surfaces or complex shapes) . The instrumentation can have reduced dimensions, and the operator can direct the plasma plume on the surface of the material to be cleaned without the aid of motorized guides. Torches with a very low input power and extreme manoeuvrability have significant potential in the field of restoration.

The major advantages derivable from the use of cleaning technologies with energy source, common to plasma and laser, are:

- non-direct physical contact with the work of art;
- selectivity, due to the management of the source through appropriate parameters and - for plasma removal - for the selective interaction with organic bonds[8];
- controllability: the removal is progressive, involving a thickness of several microns or less with the instant verification of the most appropriate degree of removal;
- precision: the removal process affects only a selected area.

The major drawbacks common to the two cleaning methods are:

- risk of damaging the surface because of an inappropriate source control
- atmospheric release of removed substances
- risks for the operator caused by the emitted radiation (UV/IR)

One of the common plasmas drawbacks is also the deposition of metallic particles on the sample treated (electrode damaging); this inconvenience is avoided by the PANNA project's torch thanks to the electrode isolation from the ionizing gas[10].

The effects due to the temperature-rise depend from the different physical and thermal characteristics of the substrate. The plasma generates a process of thermal ablation due to the temperature of the plasma itself (between 50 and 300 ° C for low-power sources), thus the heat propagates to the material to be removed and to the substrate. The heating-related effects can be avoided by adjusting the parameters in order to lower the power or by changing the geometrical parameters. The PANNA project torch (Fig. 6.1) gives a high density plasma, providing a great number of reactive species and allowing working temperatures lower than 60°C in order to operate also on temperature sensitive substrates.

6.4 – EXPERIMENTAL

In order to characterize the ageing properties of the coating matrix independently on the pigments presence, “blank” samples were coated. These samples were named BA, BB, BC and BD, standing for: “filming agent only” (BA), “filming agent and dispersing agent” (BB), “filming agent and thickener” (BC) and “filming agent, dispersing agent and thickener”(BD) respectively. The four blank samples and the nine pigmented samples were coated on two different supports (2,5x3cm glass slides and 2x2,5cm silica wafers) in double copy, for a thickness of 200nm. The pigmented samples were named GI, RI (the inorganic ones), GO, RO, GO1d, RO1d, GO5d, RO5d (the organic ones), GO5d+RO5d (s mixture of the two organic pigments) and DYE. The coating formulated with the available fluorescent dye (TINOPAL SFP),in the same concentration as for the pigments (20% on dried filming matrix), was introduced as yardstick in order to evaluate the differences between the ageing properties of pigments and dyes.

UV-ageing

One sample copy was kept in the dark, while the other exposed to UV-light in a weathering chamber equipped with a Zh-type medium pressure UV lamp (MPUV), which emission is shown in Fig. 6.2, in order to artificially simulate about 15 years of solar irradiation. One minute in chamber is bound to be equal to 50min of sun exposure (“fifty times the solar irradiance (W/m^2)”); the simulated years of irradiation are calculated taking into account the seasonal variability. The ultraviolet light produced simulates only part of the UV region of natural sunlight and consequently, the test pieces are subjected to a small but destructive portion of the spectrum. Moreover, due to the lack of visible and infrared energy, the samples are not heated above the surroundings temperature in the way they would be in practical use [7].

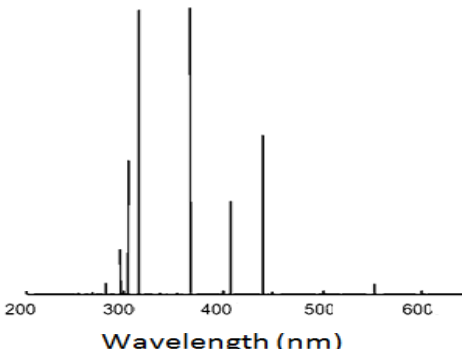

Figure 6.2 – UV lamp emission spectrum

The aged samples were extracted and the properties measured after different ageing times: 2.6, 5, 9.6 and 14,3 simulated irradiation years. These timings were determined on the basis of preliminary ageing tests (on coatings made with the non-milled powders and without the presence of thickening agent), in order to follow the luminescent materials decay curves. The non-aged samples properties were measured as soon as the coating was deposited, in order to avoid humidity-related fluorescence decay. However, the aged samples had not be maintained under constant temperature and humidity values (at least when outside the ch¬mber).

Fluorescence

The fluorescence output and the fluorescence lifetime decay were evaluated by means of a Fluorolog3 from Horiba Jobin Yvon equipped with Xenon lamp for PL/PLE analysis and NanoLed-370 and Spectraled-370 for the FLT (See Chapter 3.1). PL/PLE measurements and photographic survey were performed after every sampling time; FTL measurements were performed only at the end (14.3 simulated irradiation years) and compared to those previously obtained for the powders and the un-aged embedded pigments. The PL exciting wavelength was of 365nm, while the PLE and FTL curves were measured for the initial characteristic emission wavelength (PFLO-R=616nm, PFLO-G =525nm, PFLI-G=514nm, PF-R7=626nm).

Colourimetry: yellowing and transparency

A SP64 portable colourimeter from X-Rite, with sphere D10° geometry using a standard “C” illuminant, was employed for the yellowness and transparency evaluation on the coatings deposited on transparent glass substrates. The data were collected as XYZ and L*a*b* data, in four different zones of the same sample, and the standard deviation calculated. The yellowness calculations are based on ASTM-E313 while the colour difference calculations are based on the CIE.DE.2000 standards.

The yellowing index were calculated on the white reference surface, for each of the 14 samples (Yi) and also as a difference from the relative aged sample blank “BD” (ΔYi). Also the ΔE values, for the colour difference between un-aged and aged samples, were calculated as differences from the relative BD sample L* a* b* values above the white reference surface. The L* data were measured also above the black reference surface,

and here reported as ΔL* (differences from the relative BD sample) in order to evaluate the brightness, and therefore the transparency, of the coatings before and after ageing.

Plasma removability tests

The silicon wafer were selected as substrate for the removability tests, thanks to their transparency to the infrared radiation; in fact, in order to determine the removal efficiency, the area under the 1732cm^{-1} absorption peak was monitored (main Acryl33 absorption peak, correspondent to the esteric C=O stretching) [12] . Moreover, the silica wafers are conductive substrates granting a good plasma extraction of active species. The parameters to be controlled are essentially: sample distance from the torch, flow rate, power and treatment time. These parameters were chosen so as to grant a good monitorability of the thin coating removal. Although not completely representative of a real situation (the protective coatings present 1 to 50µm thicknesses), the 190nm thick coating removal could be monitored thanks to the adjustable features of the cold plasma torch. The radio-frequency power was chosen to be 30W, on a previous senior design work suggestion. The distance torch-sample was fixed at 2mm. Several combination of gasses (Oxygen and Argon), gas flux and voltage were tested and the removability monitored every 10 seconds acquiring infrared spectra (FTIR). The parameters combination granting a good removal monitorability was 70% voltage (11,5kV measured on the electrodes) with a 10 l/min flux of pure Argon. The fluorescent samples' removal was monitored after 20s and 50s of plasma treating in order to obtain characteristic removal curves. The removal rate of the samples was expressed in terms of removed percentage as calculated from the 1732cm^{-1} peak areas measured with infrared spectroscopy, avoiding the coating thickness influence. The equation used in the calculation implies the percent rate between the corrected area of the peak after and before plasma treatment (removed% = 100-[100$*$(A_{20s}/A_{0s})]). This ensured the method reproducibility on all the samples, not having the exact same thickness, the brush-coated samples (inorganic pigments) included. The experiment was conducted for standing single-spot etching, creating a circular spot with maximum diameter as large as the FTIR sampling spot. Therefore a removal percentage of 100% will correspond to a completely clean silica surface (although the presence of crater borders and the shape of the FTIR analysis window reduce the maximum cleaning effect value to ~90%). The samples were fixed on the IR spectrometer sample holder in order to maintain

unchanged the etching/revelation area. The etching error bars derive from the standard deviation calculated for the blank sample (BD) removal, before the ageing tests.

6.5 - RESULTS AND DISCUSSION

6.5.1 – FLUORESCENCE

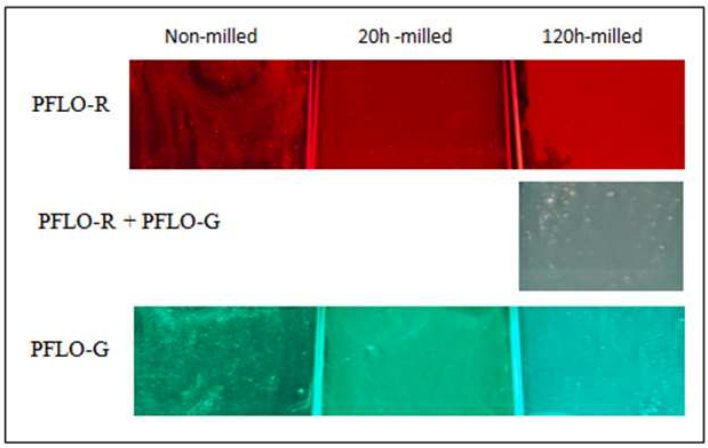

Figure 6.3 – Fluorescence output of the organic pigments' coatings under UV- light source (365nm) before the ageing test

Fluorescence lifetimes

The fluorescence decay was firstly screened ageing the 1% and 5% coating, without the presence of thickener, of the non-milled samples PFLO-R, PFLO-G and PFLI-G (see Chapter 5). The aged coatings for the actual test had a 20% concentration, granting as such the lifetimes variations (e.g. reductions) due to the particle's milling and the thickener presence, not to affect the decay curves exploration. The fluorescence decay lifetime data along the ageing are presented in Tab. 5.4. While the inorganic pigments' lifetime remained unchanged after 14.3 simulated years of irradiation, the coating containing HPQ showed a lifetime shortening dependent on the additive particle size processing time : GO (4µm particles) from 6.11ns to 5.27ns, GO1d (0,194µm particles) from 6.72ns to 3.84ns and GO5d (0,186µm particles) from 4.58ns to 3.13ns. The latter value goes from 6.35 to 3.63 when GO5d is present in the coating to the concentration

of 10% and in mixture with RO5d. The reasons for the different initial fluorescent decay of GO5d pure and in mixture have been previously discussed (see Chapter 5), on the other hand the difference in lifetime between the un-aged and aged sample is more substantial for the mixed sample for reasons that remain to be investigated. The lifetime values were not calculable, owing to the low fluorescent signal, for the samples containing the metal-organic europium complex (RO, RO1d, RO5d and RO5d in mixture).

The fluorescence emission spectrum from organic samples is not dependent on the excitation wavelength, due to the partial dissipation of excitation energy during the excited-state lifetime, therefore the wavelength selected for the PLE and FLT spectra acquisition was 525nm (and not the exact emission maximum at 500nm).

Fluorescence decay pre-tests

As can be seen in Fig. 6.6 and Fig. 6.12, the organic red glowing pigment undergo a faster decay (pre-test decay constant = 1,4) than the green glowing one (pre-test decay constant = 4,7). The green glowing inorganic pigment present an intermediate decay constant, reaching the plateau quite faster than the green organic pigment, but at the same time the percentage of intensity loss does not exceed the 35% in 10 simulated ageing years. The un-milled PFLO-G decay is not influenced by the pigment concentration in the coating (1% and 5%) but is strongly influenced by the presence of the thickener. PFLO-R decay constant, instead, remains unchanged. On the contrary, for what concerns the inorganic pigment, PFLI-G, its decay rate is proportional to the concentration.

Excitation curves

While the excitation curves for the inorganic pigments remain unchanged after UV ageing, Fig.6.4 shows the differences in the PLE spectra of the organic samples before and after 14.3 simulated years ageing. It is also evident how the particle size influences the PLE spectra and, therefore, the emission intensity at a certain wavelength as shown in Fig. 6.9 and 6.10. For the un-aged organic samples, the highest excitation intensity (under 375nm) is acquired for the 20h milled samples for both PFLO-G and PFLO-R, while after a 14.3 years ageing for PFLO-G the highest intensity is observed for the un-milled pigment. The UV-light exposure substantially impairs the excitability of the red

glowing Europium complex, at least from wavelength higher than 260nm, while the PLE intensity of the green glowing HPQ is uniformly reduced within the spectrum, but in a stronger degree for the 20h milled sample GO1d. For what concerns the organic pigments mixture (Fig.6.5), proportionally to the pigment concentration in the coating, the RO5d excitation curve remains unchanged both before and after ageing, while GO5d intensity is decreased after ageing. In mixture, the fluorescence decay constant remains fixed for the red pigment (0.25) while increasing from 3.38 (pure GO5d) to 3.84 (mixture) for the green one. As observed during the FLT evaluation, this decay slowering could be due to the lower pigment loading (while for higher concentrations self-quenching happend).

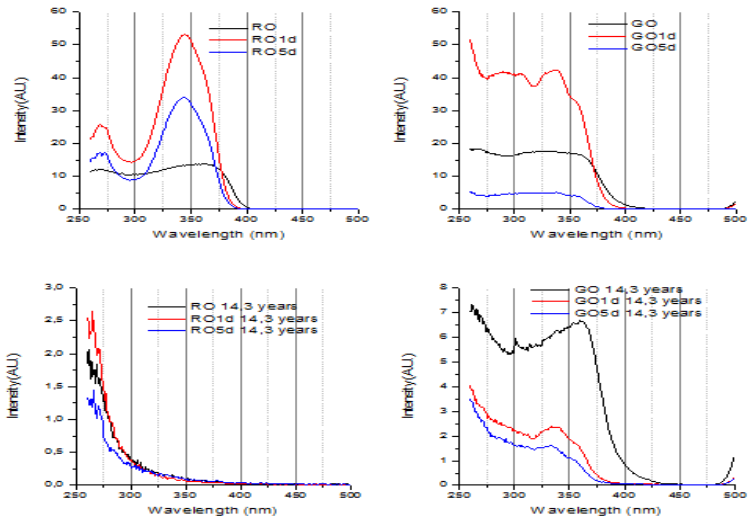

Figure 6.4 – Organic samples excitation curves: before (top) and after (bottom) 14.3 simulated ageing years, for the different sample's milling times.

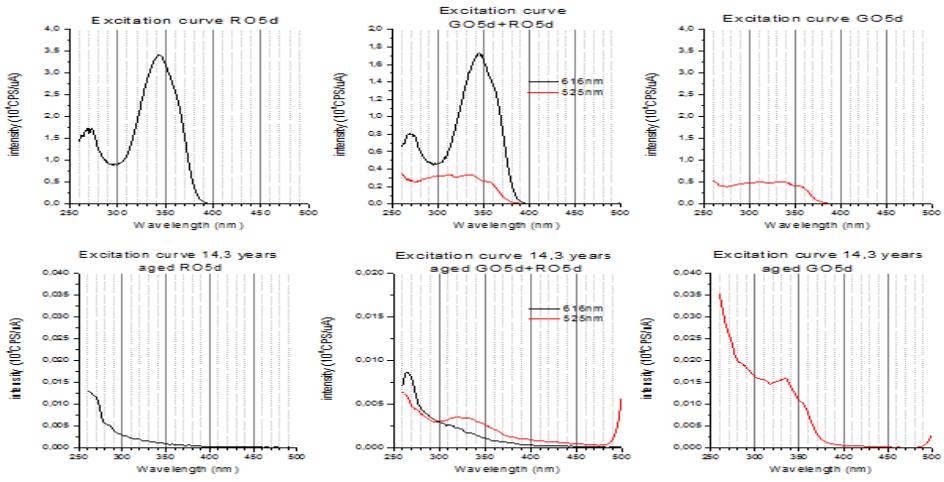

Figure 6.5 – Excitation curves for the 120h milled organic samples and their 1:1 mixture (in the middle): before (top) and after (bottom) 14.3 simulated ageing years

Fluorescence decay curves simulation

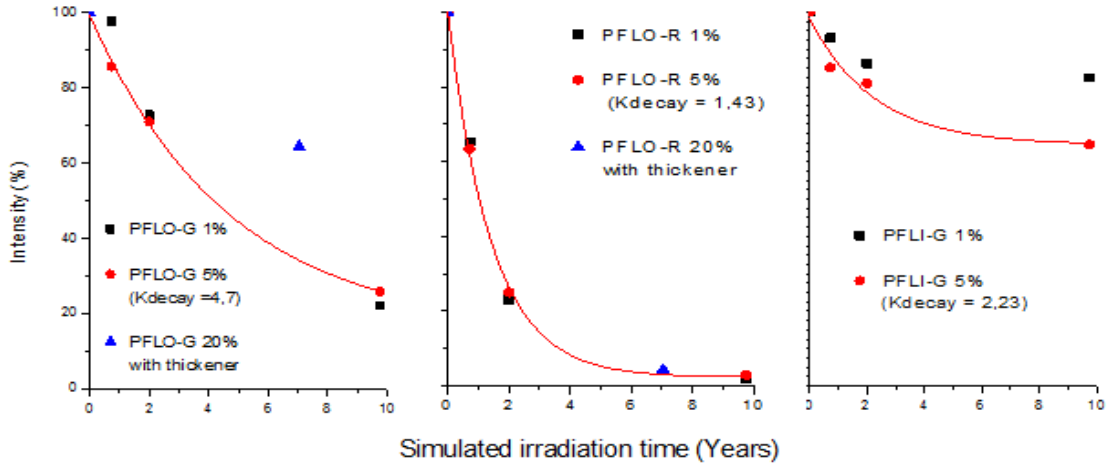

Figure 6.6 –Fluorescence percentage loss and exponential decay constants from ageing pre-tests of coating with different concentrations of PFLO-G, PFLO-R and PFLI-G

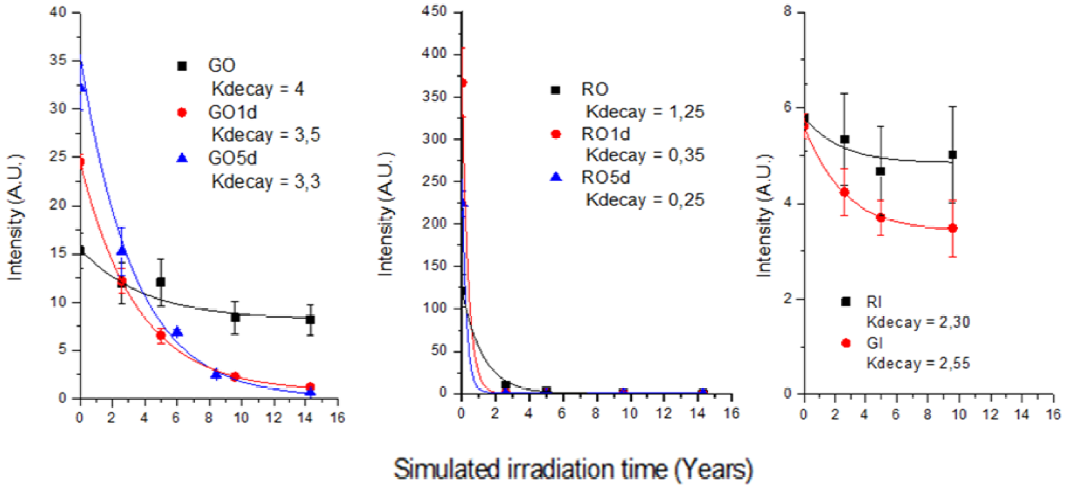

Figure 6.7 – Fluorescence decay curves and exponential decay constants from the actual ageing test of all the samples: PFLO-G (right), PFLO-R (middle), PFLI-G and PF-R7 (left)

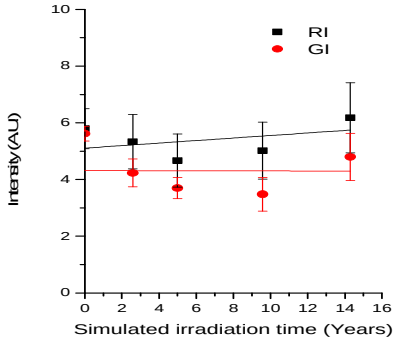

Figure 6.8 – Inorganic pigments decay trend until 14.3 simulated irradiation years

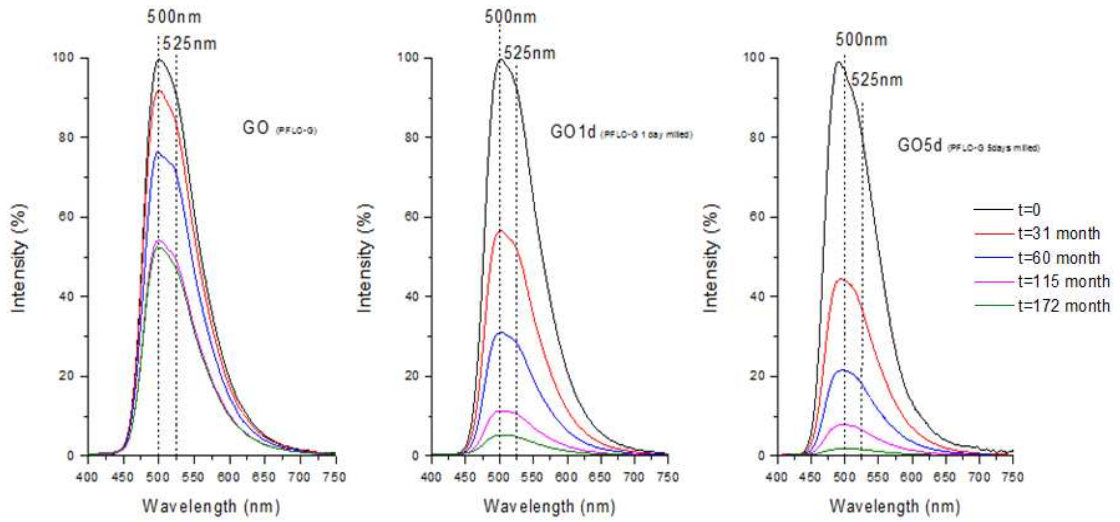

Figure 6.9 – PFLO-G, PL spectra showing the percentage intensity loss after different ageing periods (simulated irradiation times in months)

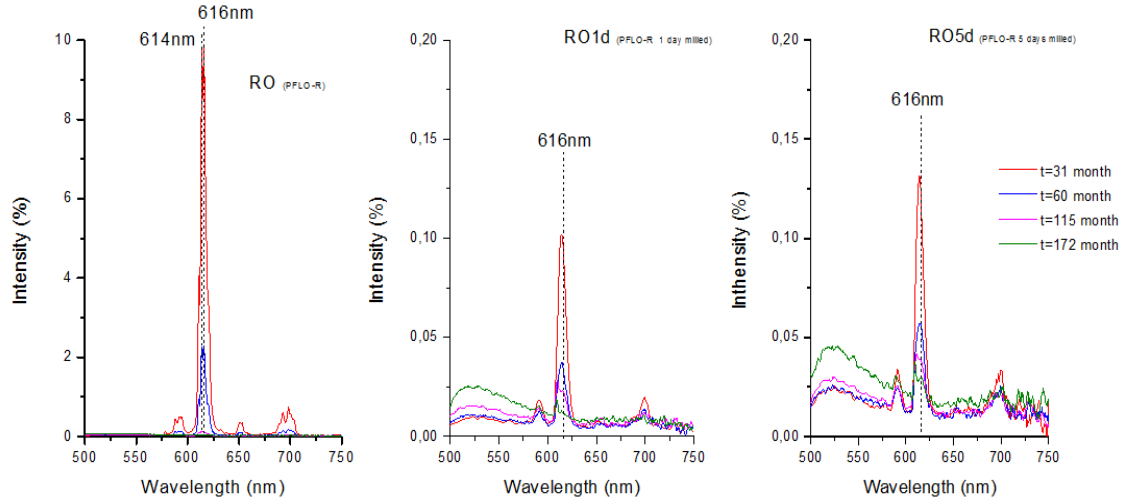

Figure 6.10 – PFLO-R, PL spectra showing the percentage loss of intensity after different ageing periods (simulated irradiation times in months). The t=0 spectra (100%) is not reported.

The decay curves obtained for the aged samples (Fig.6.7) showed some differences from those obtained in the ageing pre-test. The un-milled sample decay constant decrease for the organic samples and increase for the inorganic, going from 4.7 to 4 for PFLO-G, from 1,43 to 1,25 for PFLO-R and from 2,23 to 2,55 for PFLI-G. What is more important, in Fig.6.7 is shown also the much faster decay followed by smaller sized organic pigment particles (as can be seen in Fig. 6.9 and 6.10). The decay

constant are decreased from 4 to 3,3 in the green sample and from 1,25 to 0,25 in the red sample.

Although the inorganic samples seemed to follow an exponential decay as the organic (Fig. 6.6 and 6.7), after 14.3 simulated ageing years the measured fluorescence intensity is the same (error bars granted) of the initial intensity (Fig. 6.8). Moreover, the output signal seemed to be increased as shown in Fig. 6.11 and as reported in chapter 1 for the pigments initial screening. This phenomenon is most certainly due to the matrix deterioration accompanied by the un-covering of the inorganic particles.

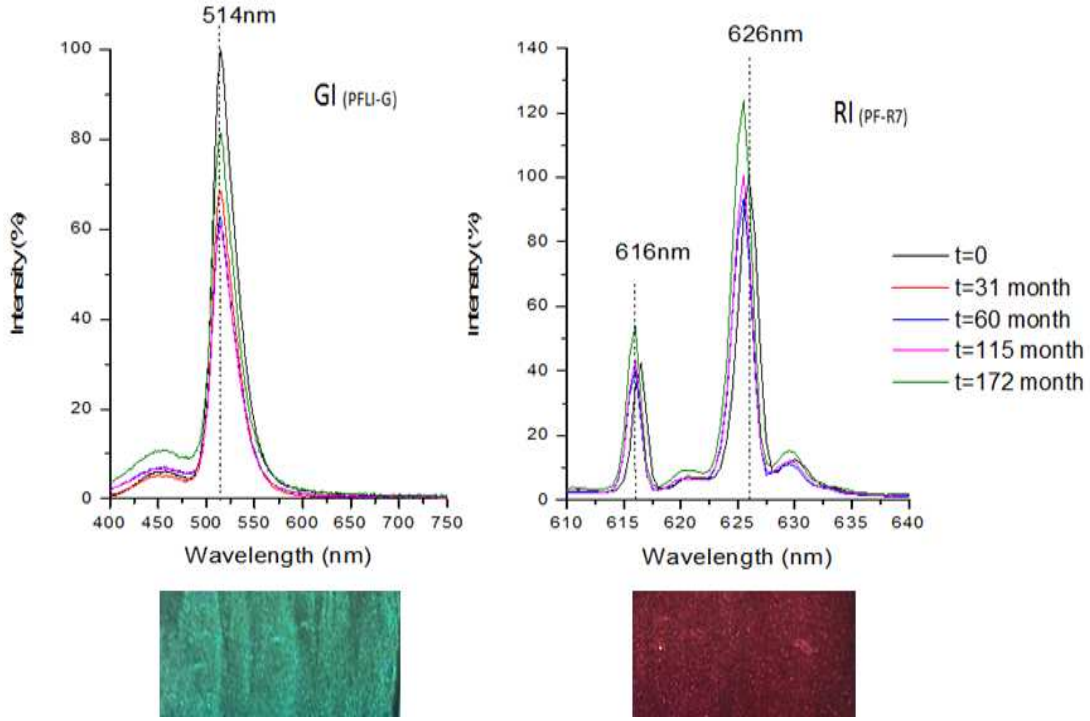

Figure 6.11 – PFLI-G and PF-R7 PL spectra showing the percentage loss (or gain) of intensity after different ageing periods (simulated irradiation times in months) and coating fluorescence image.

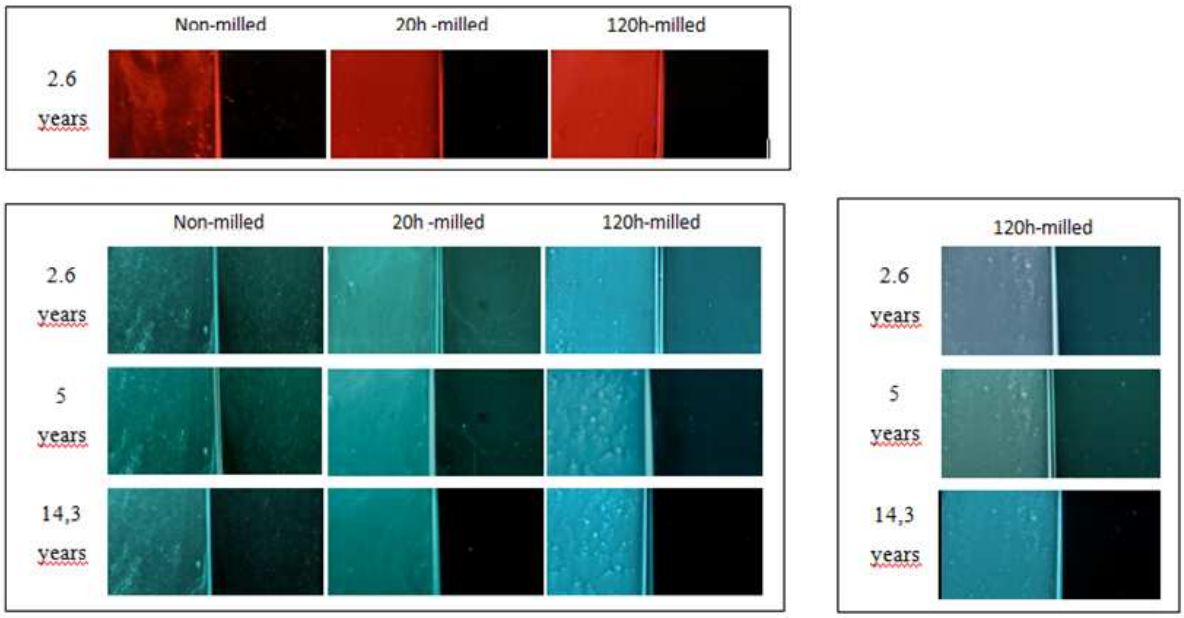

Figure 6.12 – Organic samples fluorescence decay for coatings under UV- light source (365nm) before ageing and after different ageing times: PFLO-R (top), PFLO-G (right), mixture (left)

6.5.2 – COATING YELLOWING

Yellowness (Yi) and Yellowing index (ΔYi)

The "Yellowness index" per se, does not give information on the additives influence on the coating aspect, therefore the data are shown in comparison to the relative aged blank sample (ΔYi, on BD for the pigments and on BA for the dye). The Yi of the blank samples along the artificial ageing (Fig.6.13) is noteworthy, though. The yellowness increases linearly with the ageing time for the BA sample ("only filming agent") but not for the other, especially BC ("filming agent and thickener"). Moreover the samples containing other additives than the filming matrix are yellower than BA.

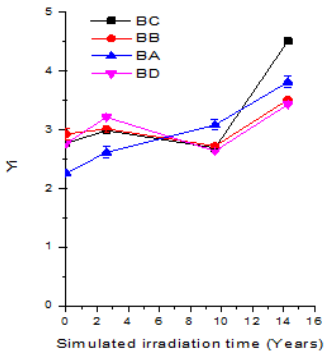

Figure 6.13 – Blank samples Yellowness index

The PFLO-G samples are quite yellower than the blank samples (value “0”) already before ageing, especially sample milled for 120h. Although increasing along the ageing, the final yellowing compared to the blank sample remains the same as before ageing (or is lowered, in the case of GO5d), while being a little bit higher for the PFLO-R samples. When the dye is present instead of a pigment, although being the initial yellowness higher than the blank sample, the final aspect is even bluer (independently on the dye concentration).

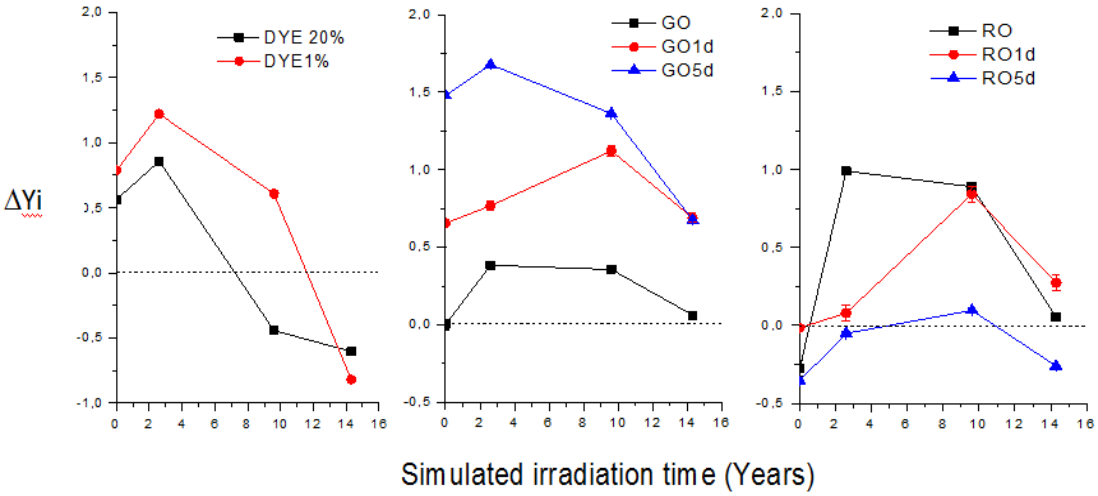

Figure 6.14 – Organic pigments and dye yellowness difference from the blank sample along the ageing time.

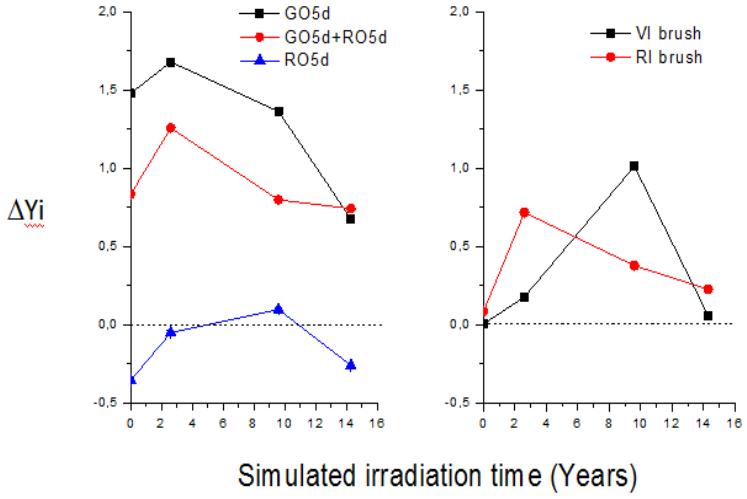

Figure 6.15 - Organic pigments mixture and inorganic pigments yellowing index

The organic pigments mixture (Fig.6.15) present an average yellowing index between the two, beside, after ageing corresponds to that of its green part.
The presence of inorganic pigments does not influence the matrix yellowing after 14.3 years ageing, although the curve trend and the previous observation about the matrix deterioration need to be considered.

Brightness and colour changes

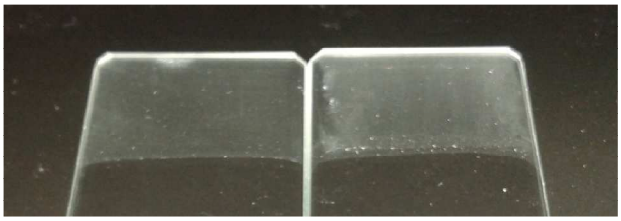

Figure 6.16 – coating aspect for 1 (right) and 3 (left) dipcoating deposition of GO

As shown in Fig.6.16, the opacity of a non-completely transparent coating is related to its thickness. This was clearly visible in the first screening tests in chapter 2. Having coated all the samples to the same thickness the additive comparison problem was avoided, although the ΔL* and ΔE* values reported here are completely dependent on the employed thickness: the 10µm coatings of the selected pigments evaluated in chapter 2 had, relatively to their aged blank sample, ΔE* values up to 4,2 (for PFLO-G) and ΔL* values up to 10,5 (for PF-R7) already after 1 month of natural ageing.
For all the samples (blanks included) the L* chromatic value decreased trough the time and the coating transparency was visibly increased. The presented ΔL* curves for the pigmented coatings, related to the loss of brightness of the blank samples (aged BD) themselves, presents an exponential decay trend (Fig. 6.17). The smaller the particle size of the organic pigments (GO5d and RO1d), the less opaque appears the coating owing to the presence of pigments particles (Fig.6.17). For a better evaluation of the transparency gain after 14.3 years of simulated ageing in Fig. 6.18 a column plot of the difference of the samples L* before and after ageing is presented.
In Fig. 6.19 a column plot of the difference in the samples colour before and after ageing is presented (note that the calculation does not take into account the colour change in the matrix itself). As shown in figure 6.20, the major colour variation through the ageing happens in different ways for different particle sizes of the same sample; for

example, the colour change is maximum after 9.6 years for the PFLO-G sample with smaller particle size but already after 2.5 years for the other. The PFLO-R samples behave in the opposite way. As for the mixture, also in the colour values its curve is an average of the curves of the two organic pigments from which it is composed. The dye presence, differently from the pigments, does not influence badly the coating; if possible, it enhances its transparency (Fig. 6.18)

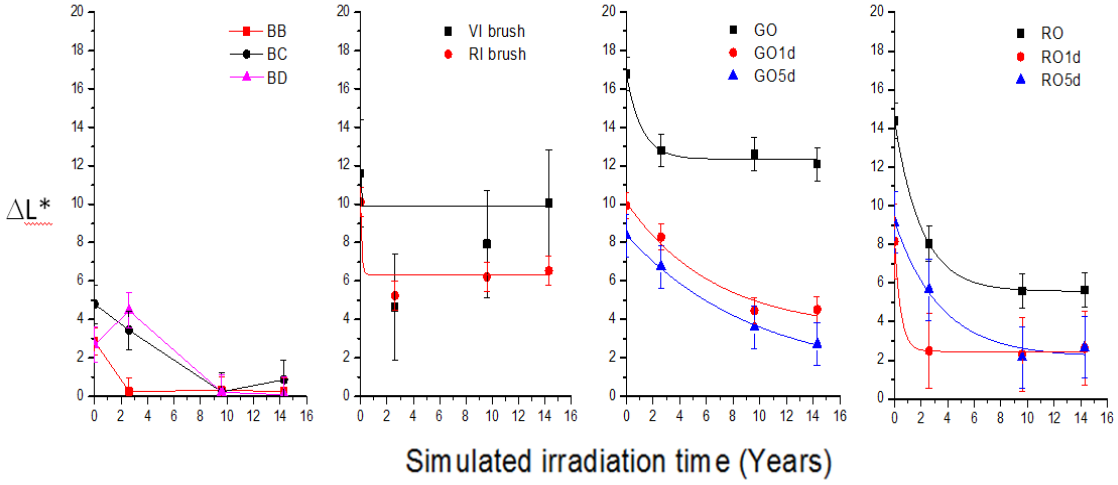

Figure 6.17 – Brightness difference from the blank sample through the years: for the non-pigmented coatings (right, referring to the BA sample) and the pigmented ones (referring to BD).

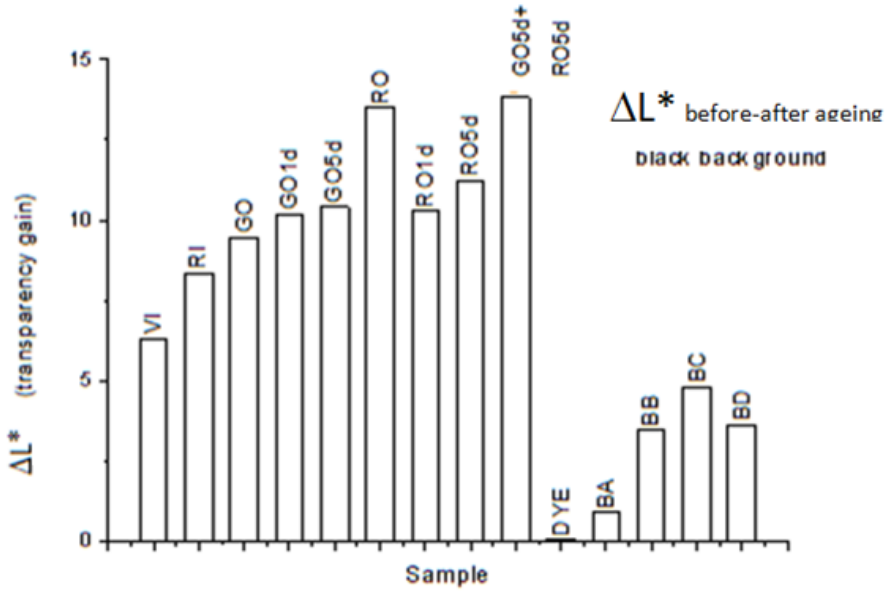

Figure 6.18 – Transparency gain in terms of L* value difference from 0 to 14.3 ageing years for the different coatings. The differences are intended as negative delta values.

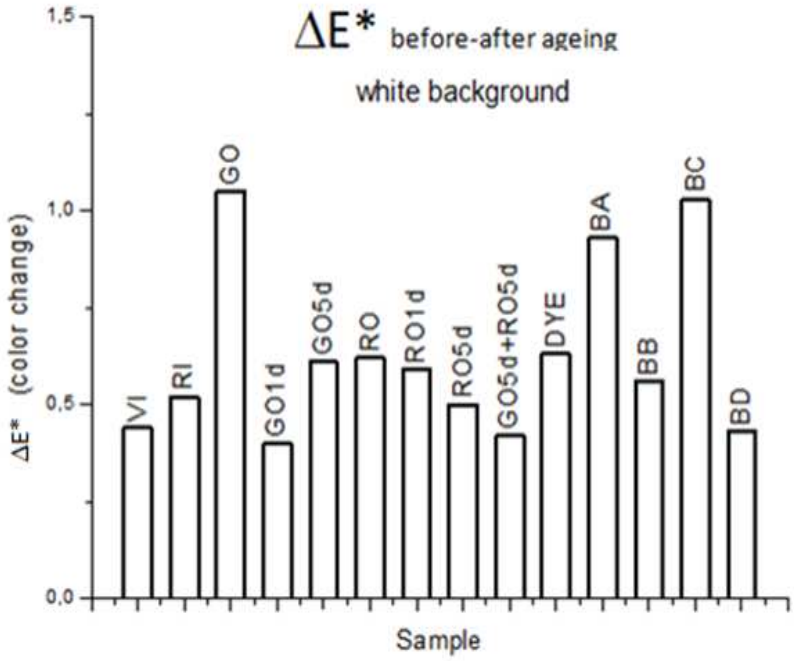

Figure 6.19 – Comparison of the colour parameters L*a*b* from 0 to 14.3 simulated ageing years for the different coatings

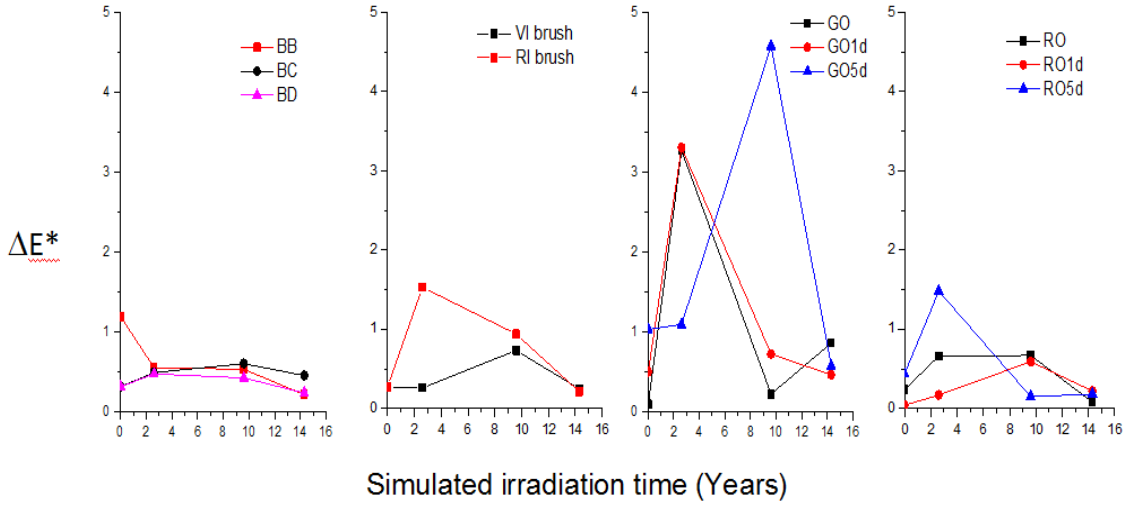

Figure 6.20 – colourimetric deviation from the blank sample (BA for the non-pigmented coatings and BD for the pigmented ones)

The low ΔL* and ΔE* values (Fig. 6.18 and 6.19) calculated for the inorganic pigment do not correspond to good optical properties, since the particles are big enough to be visually perceived. The different values obtained for the four blank samples also shows the importance of the presence of certain additives (e.g. the dispersant, absent in the bad-looking BC sample) on the final coating appearance.

Among the organic pigments, RO1d (PFLO-R 20h milled) is the one showing the best optical and ageing behaviour for what concerns colour and transparency. The same applies for RI (PF-R7) among the inorganic pigments. It has to be noted, though, the influence on the colourimetric measurements of the fluorescent emission, covering a wide portion of the spectra for what concerns the two green glowing samples.

6.5.3 – COATING REMOVABILITY

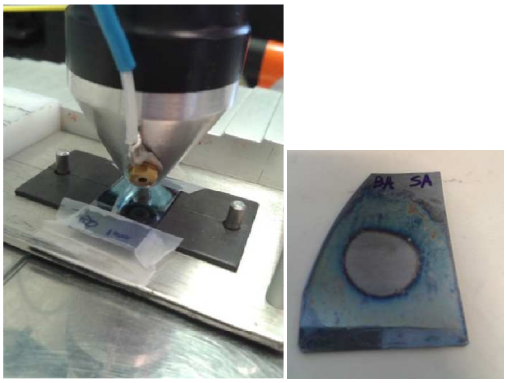

Figure 6.21 – Plasma treating and a sample dip-coated with BA formulation (diluted Acryl33) after 50s of plasma treating

The removal area, for all the pigmented samples and the blank BD, has a diameter of 8mm. The area interested by the plasma streamers action has a diameter of 11mm after 20s of treatment and of 13mm after 50s. The presence of a deposition nebulizer (coaxial to the plasma channel) and the nearness of the torch to the sample (2mm) cause a plasma plume widening, with a consequent minor action on the central part of the sample (non-removal zone), which position is influenced by the perpendicularity of the plume on the sample as can be observed in Fig. 6.26.

Concerning the IR measurements, through the ageing, a 1732cm^{-1} peak widening and new absorption bands between 1780cm^{-1} and 1665cm^{-1} are shown; bands at 1760 cm^{-1} and 1707 cm^{-1} , in particular, are observed already after 2,6 simulated ageing years for the samples without thickener. Moreover, the smaller the particle size of the organic pigments, the lower the absorption peak at 1107cm^{-1} (aliphatic CH_2 bending).

The removal rate curves presented an exponential decay trend as expected.

Organic pigments

The dye samples (1% and 20%) presented a good removability (more than 90%, Fig 6.22), even better than the relative blank sample BA when the concentration is 20%, that did not change through ageing. The organic samples coatings removability is influenced partially by the particle size, being more difficult for the smaller particles (Fig 6.22): after 50seconds of treatment the percentage removed for GO was 92%, for GO5d 45%, for RO 69% and for RO5d 83%. Visual assessment, on the other hand, showed how the bigger particles are actually more difficult to remove from the surface (Fig.6.27). That said, after the ageing period the removability of all the organic samples approaches to the same value, around 80% for PFLO-G and 70% for PFLO-R (Fig. 6.23). The mixture removability is the average value of the singular pigments removability.

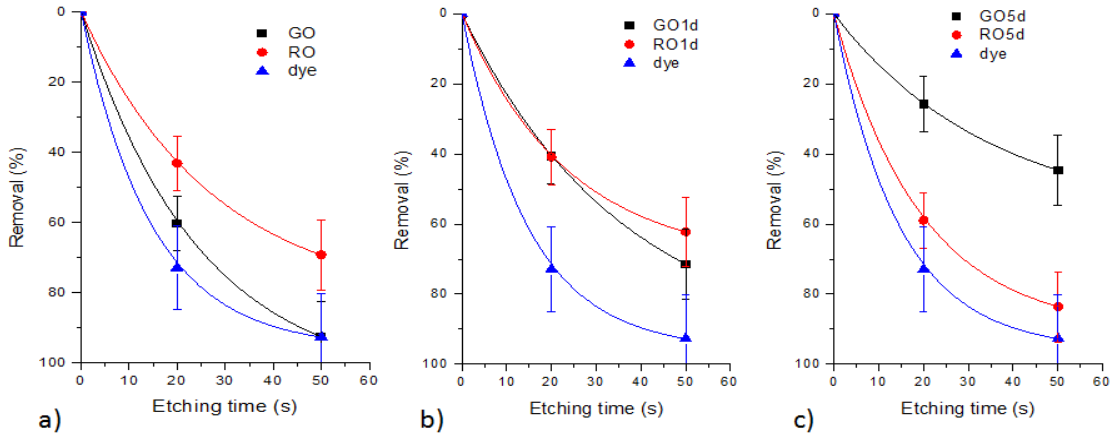

Figure 6.22 – Un-aged organic samples removal (% on sample not treated): a) un-milled; b) 20h milled; c) 120h milled

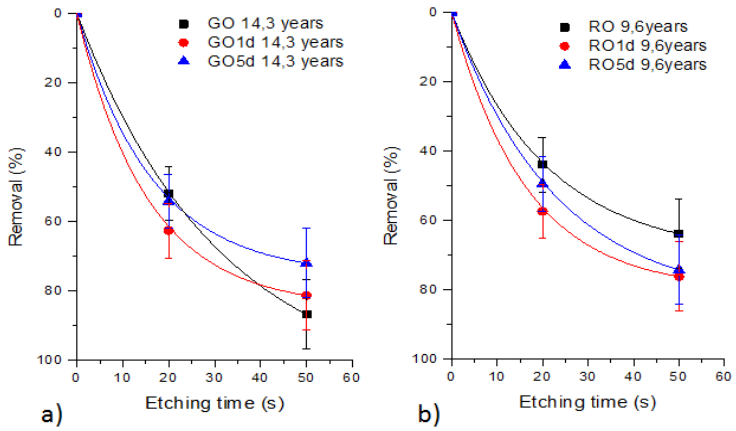

Figure 6.23 – Organic samples removal after 14.3 simulated ageing years, for different particle sizes: a) PFLO-G; b)PFLO-R

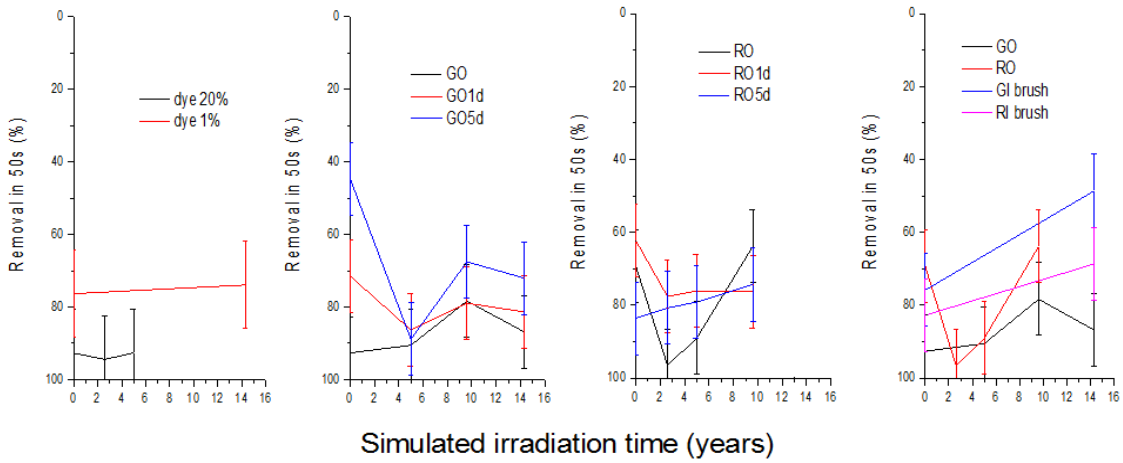

Figure 6.24 – Removal trend through the simulated ageing years for a 50s treatment for all the pigmented samples and the dye.

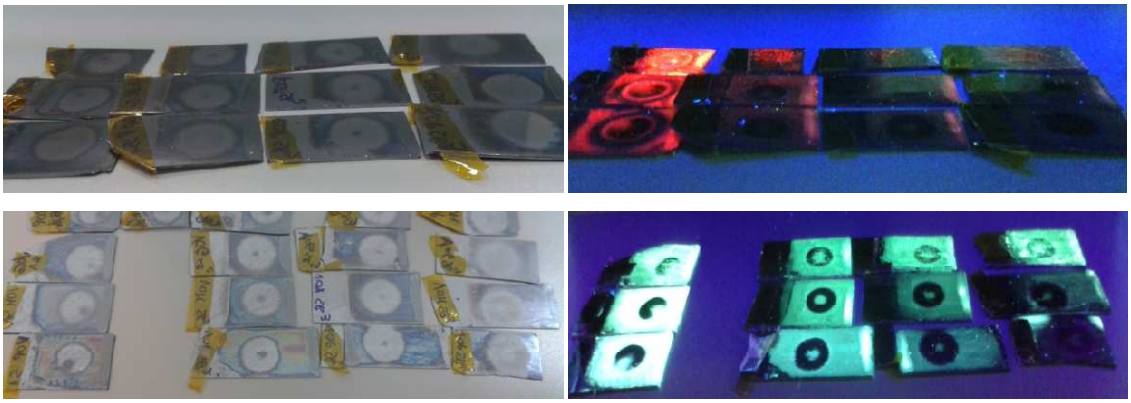

Figure 6.25 – PFLO-R (top) and PFLO-G (bottom) 50s treated samples under visible light (left) and under UV light (right). Samples of different ageing times from the left to the right (PFLO-R= 0,2.5,5,9.6 years; PFLO-G = 0,5,9.6,14.3 years) and different particle size from the top to the bottom (un-milled, milled 20h, milled 120h respectively)

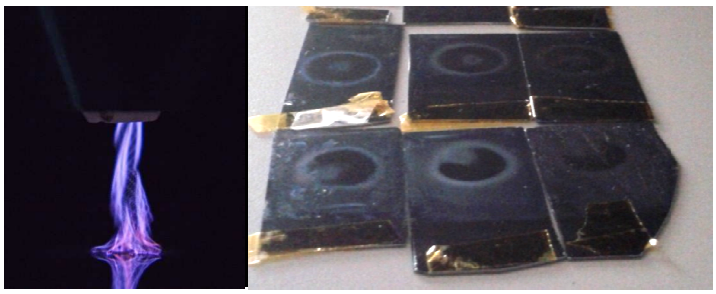

Figure 6.26 – plasma streamers and areas implied by their action for PFLO-G samples with different particle size: smaller particles on the right, bigger particles on the left

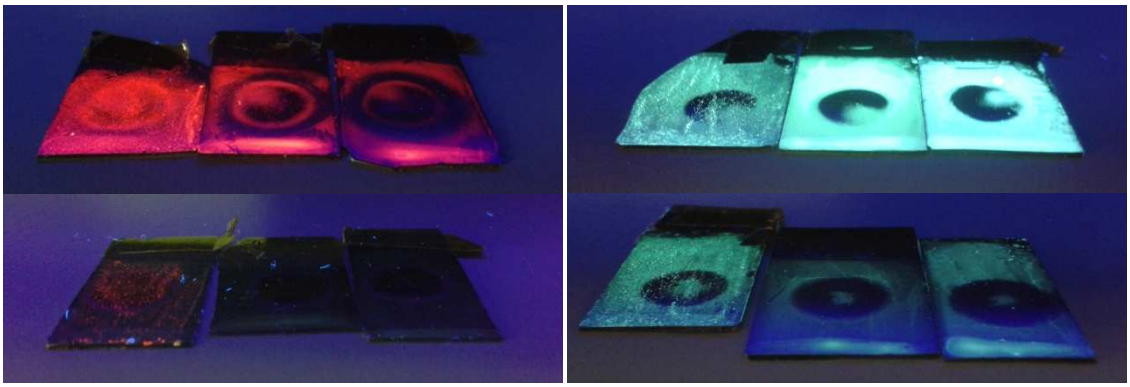

Figure 6.27 – Organic samples removal spots before (top) and after (bottom) ageing. Particle size decreasing from the left to the right

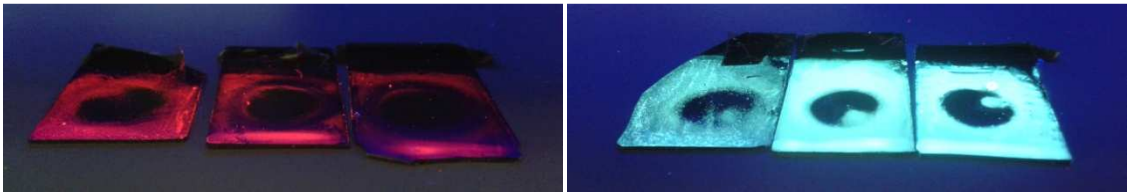

Figure 6.28 – Organic sample removal crater before ageing (cfr. Fig.6.27) after dry cleaning with cotton stick

Although the plasma cleaning per se did not remove the bigger particle from the surfaces, a simple cotton dry cleaning is sufficient for the removal as shown in Fig. 6.28.

Inorganic pigments

The inorganic particles were not removable from the surface, although this did not imply the matrix un-removability. On the other hand the removability was decreased after ageing: for example, the green glowing sample (GI) removability was reduced from 76% to 48% in 14.3 simulated ageing years. More than in the case of the organic pigments, thanks to this pigment's particle size, a cotton dry cleaning is sufficient to eliminate the pigment particles. The coating removal was in any case more difficult than for the coating made with organic pigment.

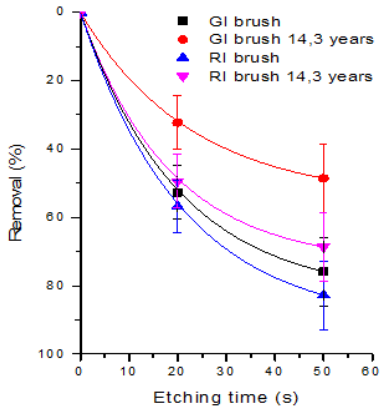

Figure 6.29 – Inorganic samples removal before and after 14.3 simulated ageing years

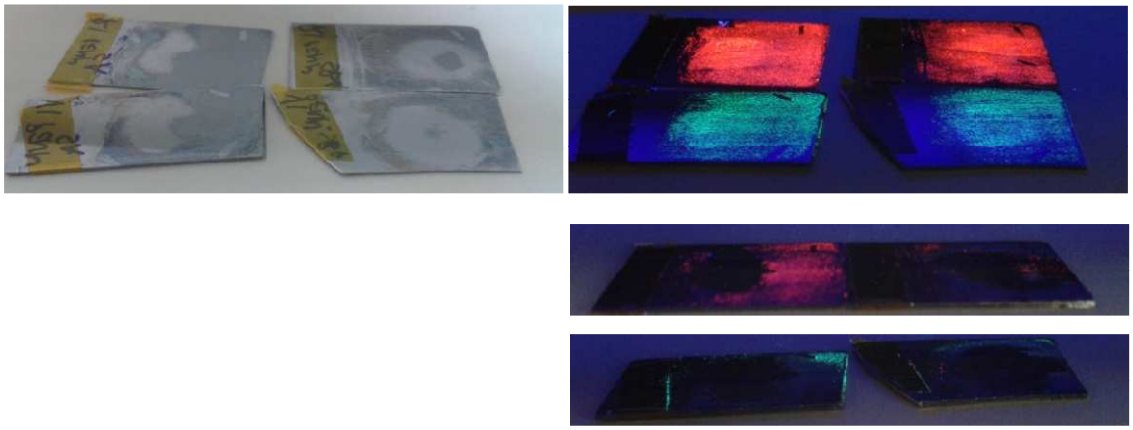

Figure 6.30 – PF-R7 and PFLI-G 50s treated samples under visible light (left) and under UV light (right). Samples of different ageing times from the left to the right (top): 0 and 14.3 years. Samples after cotton dry cleaning (bottom)

6.6 – CONCLUSIONS

The decay processes suffered by the pigments and the coating itself caused by a prolonged UV-light exposure have been studied in order to correlate the fluorescence output with the coatings health status using the formulations coated on glass slides and silicon wafer in chapter 5. The matrix composition is shown to influence the fluorescent decay behaviour of the samples and to be influenced in its yellowing and removability by the presence of additives. The presence of different pigments, and their different particle sizes, impacts differently on the coating aspect (e.g. colour and brightness) and removability by means of cold atmospheric plasma.

Fluorescence

The organic dye (TINOPAL SFP) and red glowing pigment (PFLO-R) undergo a substantially faster decay than the green glowing pigment (PFLO-G), while the inorganic pigments present an intermediate decay constant, but at the same time the percentage of intensity loss is irrelevant for display purposes. The decay of PFLO-G is not influenced by the pigment concentration in the coating but is strongly influenced by the presence of the thickener; PFLO-R decay constant, instead, remains unchanged. On the contrary, for what concerns the inorganic pigment, PFLI-G, its decay rate appears to be proportional to the concentration, although the film deterioration, causing the particles “un-covering”, impairs the decay evaluation. After ageing, the un-milled sample decay constant decreases for the organic samples and the fluorescent decay followed by smaller sized organic pigment particles is much faster. The particle size influences the PLE spectra and, therefore, the emission intensity at a certain wavelength. Regarding the un-aged samples, the highest excitation intensity was noticed for the 20h milled samples, for both the PFLO-G and PFLO-R, while after ageing the highest intensity is observed for the un-milled PFLO-G pigment. The UV-light exposure substantially impairs the excitability of the Europium complex, while the PLE intensity of the green glowing HPQ is uniformly reduced within the spectra, but in a higher degree for the 20h milled sample. While the inorganic pigments’ lifetime remained unchanged, the coating containing HPQ showed a lifetime shortening dependent on the additive processing time (i.e. particle size). The lifetime values were

not calculable, owing to the low fluorescent signal, for the samples containing the Europium complex and dye.

For what concerns the organic pigments mixture, proportionally to the pigment concentration in the coating, the Eu complex excitation curve remains unchanged both before and after ageing, while HPQ excitation is decreased after ageing. The fluorescence decay constant remains fixed for the former pigment, while increasing for the latter.

Appearance

All the samples containing other additives than just the filming matrix, dye excluded, appear yellower than the blank coating BA. The PFLO-G samples are quite yellower than the relative blank samples (BD, Yi value “0”) already before ageing, especially the sample milled for 120h. Although increasing along the ageing, the final yellowing compared to the blank sample remains the same as before ageing (or is lowered, in the case of PFLO-G 120h milled), while being a little bit higher for the PFLO-R samples. Besides corresponding to that of its green part after ageing, the organic pigments mixture present average yellowing index, transparency gain and colour change between the two components. When the dye is present instead of a pigment, the final aspect is even less yellow and more transparent, independently on the dye concentration. The presence of inorganic pigments does not influence the matrix yellowness after ageing, although the curve trend and the previous observation about the matrix deterioration need to be considered.

For all the samples the coating transparency increases through the ageing process. The ΔL^* curves for the pigmented coatings, related to the loss of brightness of the blank samples themselves, presents an exponential decay trend. The smaller the particle size of the organic pigments, the less opaque appears the coating. The major colour variation through the ageing happens in different ways for different particle sizes of the same sample: a longer exposure is needed for a visible colour change for the PFLO-G sample with smaller particle size, while PFLO-R samples behave in the opposite way. The low ΔL^* and ΔE^* values obtained for the inorganic pigment do not symbolizes good optic properties, since the particles are big enough to be visually perceived. The different values obtained for the four blank samples also shows the importance of the presence of

certain additives (e.g. the dispersant, absent in the bad-looking sample BC) on the final coating appearance.

For what concerns colour and transparency, among the organic pigments the 20h milled PFLO-R is the one showing the best optical and ageing behaviour. The same applies to PF-R7 among the inorganic pigments. It has to be noted, though, the possible influence on the colourimetric measurements of the fluorescent emission, covering a wide portion of the spectra for what concerns the two green glowing samples.

Removability

The etching curves present an exponential decay trend as expected. More than 90% of the coating containing the dye is removed, when at 20% it is even better removed than the relative blank sample; the etching efficiency do not change in relation to UV-ageing. The organic pigments' coatings removability is partially influenced by the particle size, being more difficult for the smaller particles. Visual assessment, on the other hand, showed how the bigger particles are actually more difficult to be removed from the surface. After ageing, however, the removability of all the organic samples approaches the same value, around 80% for PFLO-G and 70% for PFLO-R. Again the mixture removability is the average value of the singular pigments removability. The inorganic particles were not removable from the surface, although this did not imply the matrix un-removability. On the other hand the removability decreases after ageing: for example, the green glowing sample removability was reduced from 76% to 48%. Although the plasma cleaning per se did not remove the bigger particle from the surfaces, a simple cotton dry cleaning is sufficient for their removal.

REFERENCES

[1] *Colourimetry Part 6 -CIEDE2000 Colour difference formula*, CE-SO14-6/E, International standards, 2013

[2] *Standard practice for calculating yellowness and whiteness indices from instrumentally measured colour coordinates*, ASTM-E313-00, American Society for Testing and Materials, 2000

[3] *www.byk.com* – BYK-Gardner Additives and Instruments GmbH

[4] *www.specialchem4coatings.com/tc/colour-handbook* - SpecialChem coating and inks formulations

[5] *Colour iQC and Colour iMatch colour calculations guide*, X-Rite Manual, 2007

[6] *Lightness, Brightness and Transparency*, A. L. Gilchrist, Gilchrist ed, 1994

[7] *Paints and varnishes – exposure of coatings to artificial weathering – exposure to fluorescent UV lamps and water*, ISO-11507, International standards, 2007

[8] *Studio della rimozione mediante plasma atmosferico di prodotti polimerici di sintesi da superfici lapidee*, E.Verga Falzacappa, Tesi di laurea, Università Ca' Foscari Venezia, 2011

[9] *Characterization of cold atmospheric plasma*, K. C. Joerres, Milwaukee School of Engineering, 2014

[10] *www.nadir-tech.it* – NADIR Ricerca, consulenza, nuove tecnologie

[11] *www.panna-project.eu* – Plasma and Nano for new age soft conservation

[12] *Water dispersed polymers for textile conservation: a molecular, thermal, structural, mechanical and optical characterization*, M.Cocca, L.D'Arienzo, L.D'Orazio, G.Gentile, C.Mancarella, E.Marusticelli, C.Polcaro, Journal of C. H. Vol 7, 2007

Chapter – 7 –

CONCLUSIONS

AND FUTURE WORK

CONCLUSIONS

The aim was to exploit the visualization potentiality, specifically in the Cultural Heritage conservation field, of commercially available fluorescent compounds embedded in protective coatings. Spectral response of such coatings can promptly offer a practical tool for in-situ evaluations. Fluorescent additives will allow the restorer to effectively map the health status (e.g. the erosion) of the coating without the need for expensive monitoring devices, using the spectroscopic response as a measure of a coating's thickness, allowing also the evaluation of its uniformity. In order to do that, the additive behaviour through time must be known.

Therefore, after having selected and characterized some commercial fluorescent products, their water-based dispersions have been formulated and applied in order to be tested. Namely the selected products were PFLO-G for the organic pigments and PFLI-G for the inorganic pigments, both fluorescent in green; two other additives for each category, both fluorescent in red, PFLO-R and PF-R7, were selected as complementary pigments for an eventual mixture. Although not being embedded and tested as the other four, the grinding process has been applied in order to evaluate the effects of a bland milling on the pigment PFLI-Y, identified as a mixture of two inorganic sulphides: $(Zn^{2+}Cd^{2+})S$ and $Y_2O_2S:Eu^{3+}$. Both organic samples are identified by the manufacturer as pigmented melamine-formaldehyde copolymers, flushed as a sub-micron dispersion into a high quality printing ink varnish. The four selected emitting substances are all pigments, identified as HPQ (2-2'hydroxyphenyl-4(3H)quinazolinone), $BaMgA_{l1}0O_{17}:Mn^{2+}Eu^{2+}$, $Eu^{3+}(TTA)_3(TPPO)_2$ (Eu-tris(2-thenoyltrifluoroacetonate)-(bis-triphenylphosphinoxide)) and $Y_2O_2S:Eu^{2+}$.

In order to assess their performances in relation to the particle's size, the pigments have also been ground to nanometric size. In particular, the influence of external conditions on the emission response, such as the inclusion in an acrylic matrix and a prolonged UV- irradiation, has been investigated for three different milling times, i.e. particle size distributions. Also the influence of the additives on the photo-oxidative degradation and plasma removability of an acrylic coating have been evaluated. The plasma jet cleaning technique allowed performing a controlled non-contact removal.

Acryl33 was selected as film-forming agent and combined with a dispersing agent Joncryl HPD 96-E and a polysaccharide thickener for the dispersions stabilization

(Xanthan gum). The addition of surface tension modifiers, one anti-foamer and one hydrophobing agent was tested, though not successfully. The selected formulation had a 1,5% of solid resin content on water and a 20% concentration of pigment on dry resin, dip-coated with a ~190nm thickness. Despite its negative effects on the inorganic pigments particle size, the organic-dedicated dispersant was used in all the mixtures owing to the need of comparison between the different coatings formulations.

It is now possible to answer the questions proposed in introduction:

- *Is fluorescence affected by the matrix?*

Yes. When the pigments were embedded in the matrix all the PLE spectra showed the same drastic intensity decrease for wavelength longer than 350nm and all the samples lifetimes were reduced. A fluorescence output enhancement was observed for the green glowing organic pigment PFLO-G (HPQ) when in the presence of thickener (increased viscosity). The fluorescence output of PFLO-G was known to be sensitive to its particle size and the matrix polarity, pH and viscosity. In the case of PFLO-R environmental parameters as humidity and the strength of the complex-polymer interaction in the coating were important.
For the selected pigments, the solvent polarity is shown not to have a strong influence on the emission characteristics, although the samples fluorescent output is more intense when the solvent is water.

- *Does the pigments' particles grinding influence the fluorescent output?*

Yes. After several pre-tests, the organic pigments milling was performed for 20h and 120h, with the so-called "mixed beads" condition, in order to obtain different particle size distributions, which showed to be correspondent to different fluorescent intensities. In particular, for PFLO-G, the fluorescence slightly decreased with the particles' size when in dispersion while it increased when applied in coating (and the same happened for PFLO-R). The samples with the smallest fluorescent particles have a faster lifetime decay compared to the other samples embedded in the same concentration (20%), while for lower concentrations the lifetimes are even longer than the samples with bigger particle sizes.

In the inorganic samples, PFLI-G and PF-R7, thermal and mechanical stresses caused the Eu^{2+} oxidation, giving rise to degradation of colour quality. This has to be considered not only when testing the properties before and after ageing, but also during the grinding process, in order to avoid unwanted degradations.

The milling of inorganic pigments was shown to be ineffective; therefore their fluorescent properties were not further studied in relation to particle size. Moreover, severe grinding tests as ultrasounds treatment damage the samples, causing them to turn black. The mechanical dispersion with Ultra-Turrax is shown to be as effective as the bead-milling in reducing the pigments particle size; on the other hand, it seems to be a less controllable method (in terms of particle size) compared to the bead-milling.

- *Does the particle size influence the fluorescence decay of the organic samples?*

Yes. Different processing time greatly influenced the fluorescent output of the samples, in particular PFLO-R. After ageing, the decay constant of the un-milled sample decay constant decreases for the organic pigments. The fluorescent decay observed for smaller sized organic pigment particles is much faster.

Regarding the un-aged samples, the highest excitation intensity was noticed for the 20h milled samples, for both the PFLO-G and PFLO-R, while after ageing the highest intensity is observed for the un-milled PFLO-G pigment.

- *Is there a correlation between thickness, concentration and fluorescence giving the chance to the restorer to easily acquire information on the coating health status*?

Yes. For what concerns the inorganic pigments, an exponential trend is detectable both in the thickness/intensity plots and in the concentration/intensity plots. A linear correlation is observed between coating thickness and fluorescence output only at high concentrations for what concerns PFLO-R, and for all the concentrations (1-20%) for what concerns PFLO-G. The intensity of the HPQ sample (PFLO-G) presents an exponential trend, rapidly increasing and approaching a plateau for high concentration. The Europium complex (PFLO-R) exhibts concentration quenching phenomena, therefore being described by a peak function.

- *Do the pigments presence and/or particle size influence the properties of a waterborne coating or vice-versa?*

Yes. Slight variation in the particle size affects the physical appearance of the pigment and its compatibility towards the application. As for the appearance, the smaller the particle size of the organic pigments, the less opaque appears the coating. Moreover, the matrix composition is shown to influence the fluorescent decay behaviour of the samples. Yellowing and removability of the matrix are influenced by the presence of additives. All the samples containing other additives than just the filming matrix, dye excluded, appear yellower than the blank. The PFLO-G samples are quite yellower than the relative blanks, especially the one milled for 120h.

The removability of the coating with organic pigments is partially influenced by the particle size, being more difficult for the smaller particles. Visual assessment, on the other hand, showed how the bigger particles are actually more difficult to be removed from the surface.

- *Do the pigments presence and/or particle size influence the properties of the aged coating?*

Yes. The presence of different pigments, and their different particle sizes, impacts differently on the coating aspect (e.g. colour and brightness) and plasma removability.

After a long ageing period the pigments presence seemed not to cause yellowing, although an increase of the yellowing indexes through the ageing was noticed. When the dye is present instead of a pigment, the final aspect is even less yellow and more transparent, independently on the dye concentration. The presence of inorganic pigments does not influence the matrix yellowness after ageing. For all the samples the coating transparency increases through the ageing process with an exponential decay trend. The major colour variation through the ageing happens at different times for different particle sizes of the same pigment: a longer exposure is needed for a visible colour change of the PFLO-G sample with smaller particle size, while PFLO-R samples behave in the opposite way. The low ΔL^* and ΔE^* values obtained for the inorganic pigment do not correspond to good optics properties, since the particles are big enough to be visually perceived.

After ageing, the removability of all the organic samples approaches the same value, around 80% for PFLO-G and 70% for PFLO-R. For what concerns the dye, the removal

efficiency is really good and do not change in relation to UV-ageing. The inorganic particles were not removable by plasma torch from the surface, and removability decreases after ageing.

- *Does the exposure to UV light influence the pigments luminescence?*

Yes. As a consequence of a prolonged UV exposure the fluorescent emission intensity progressively decrease for the fixed excitation wavelength. A comparison of the respective decay of inorganic versus organic pigments shows some fundamentally important differences between the two families. The organic dye and red glowing pigment undergo a substantially faster decay than the green glowing pigment, while the inorganic pigments present an intermediate decay constant, but at the same time the percentage of intensity loss is irrelevant for display purposes.
For what concerns the organic pigments mixture, the Eu^{3+} complex excitation curve remains unchanged both before and after ageing, while HPQ excitation is decreased after ageing. The fluorescence decay constant remains fixed for the former pigment, while increasing for the latter. The inorganic pigments' lifetime remained unchanged, while the coating containing HPQ showed a lifetime shortening dependent on the additive processing time (i.e. particle size).

- *Are the pigments usable in tandem?*

Yes. No interaction in the fluorescence mechanisms of the two organic luminescent materials is detected for the "mixture" sample. No interaction is envisaged also between the inorganic powders. The obtained results and their chemical and physical differences allow to declare the two organic samples as complementary fluorescent additives, combinable and suitable for various applications in the field of conservation dedicated coatings.

- *Do the pigments have advantages on the dyes?*

Yes. Although dyes are easier to work with and no optical (yellowing/transparency) or mechanical (removability) disadvantages were reported, the pigments advantage consists in their light-fastness and their superior thermal stability.

Nevertheless, also fluorophores with a fast decay can find application in the coating's homogeneity check right after application. If the coating production comprises temperature or pH variations, this feature can be difficultly achieved by using dyes; furthermore the common water-dedicated dyes fluoresce in the blue spectral range, difficultly eye-perceivable on common substrates or even revealable by a portable spectrometer. Nowadays nanocrystals are commonly, and quite easily, synthesized obviating the need of grind large particles and permitting to obtain more transparent coatings; this will allow the use of fluorescent pigments with fast UV-decay as the identified metal-organic complex on which the product PFLO-R fluorescence is based, instead of the dyes.

FUTURE WORK

The fluorescence being influenced by the matrix effect, all the investigated properties (fluorescence decay and influence on matrix stability, yellowing and removability) will need to be related to a particular coating formulation. The formulation of a completely removable high performances waterborne coating for cultural heritage requirements is still a challenging open field. In the case of the presence of fluorescent additives, what is more, it would be necessary to tailor the formulation on each specific pigment's requirement in order not to impair the fluorescent properties and maintaining the coating functionality at the same time.

The development of formulations of more than one component requires research efforts aimed to the definition of the correlations between composition, phases' structure, application method, storing characteristics, compatibility, miscibility, viscosity, penetration depth and protection and consolidation functionality modulated in correspondence with the characteristics of the substrate to be treated. In particular, the penetration depth has to be considered when evaluating the removability of the coating and of the pigment's particles residues. Furthermore, the plasma-removability parameters and actability would be strongly influenced by the physical properties (e.g. conductivity) of the substrate.

For what concern the coating detection, the colour and the intrinsic fluorescence of the substrate have to be evaluated, not to mention the characteristics of detecting instrument used (e.g. repeatability). Moreover, the fluorescence decay in time will be strictly related to the weathering conditions.

Dispersion by means of mechanical disperser Ultra-Turrax T8 is shown to be a valid alternative to the bead milling of the organic pigments, especially if the purpose is to grind the pigments to the minimum particle size reachable while sparing time. Therefore further studies have to be done regarding the setup characteristics and the correlation time-particle size distribution for each specific pigment.

Acknowledgements

Foremost, I would like to express my sincere gratitude to Dr. Alessandro Patelli and Dr. Frank De Voeght, for offering me the international traineeship opportunity at VenetoNanotech and ChemStream.

My sincere thanks goes to my supervisor Prof. Alvise Benedetti for the confidence in my abilities and the strong motivation given when I needed it most.

Besides my supervisor, I would also like to thank my advisors Dr. Veerle Goossens and Dr. Stefano Voltolina for their encouragement, pertinent criticism, pragmatic suggestions and for having bravely endured my disquietude throughout the last year.

I am extremely thankful to Dr. Francesco Enrichi (VenetoNanotech) for his continuous support throughout my research, his patience, enthusiasm, and immense knowledge.

I express profound gratitude also to Dr. Monica Favaro (National Research Council), Prof. Marco Bortoluzzi (Ca'Foscari University of Venice) and Prof. Mirella Zancato (University of Padua) for providing me adequate facilities and valuable suggestions to conduct my research work and, in particular, to Dr. Laura Sperni (Ca'Foscari University of Venice) and Emanuele Verga Falzacappa (Nadir S.r.l.) for the wholehearted support.

Grateful thanks to my lab-mates Dr.Els Mannekens and Enrico Pontoglio for their sincere co-operation and for providing a friendly atmosphere during the course of my work.

I sincerely appreciate the excellent hospitality extended to me during the last year and the valuable help rendered by the whole staff of VenetoNanotech and UBCA, in particular Mrs. Chris De Ceulaerde.

Last but not the least, I would like to thank my parents for supporting me spiritually and economically throughout my studies.